



**HAL**  
open science

## Joint Europa Mission (JEM) a multi-scale study of Europa to characterize its habitability and search for extant life

Michel Blanc, Nicolas André, Olga Prieto-Ballesteros, Javier Gómez-Elvira, Geraint D. Jones, Veerle Sterken, William Desprats, Leonid Gurvits, Krishan Khurana, Aljona Blöcker, et al.

### ► To cite this version:

Michel Blanc, Nicolas André, Olga Prieto-Ballesteros, Javier Gómez-Elvira, Geraint D. Jones, et al.. Joint Europa Mission (JEM) a multi-scale study of Europa to characterize its habitability and search for extant life. *Planetary and Space Science*, 2020, 193, pp.104960. 10.1016/j.pss.2020.104960 . insu-02883533

**HAL Id: insu-02883533**

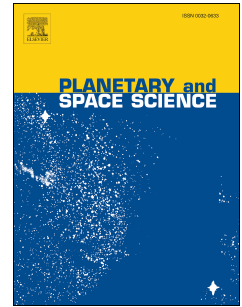
**<https://insu.hal.science/insu-02883533>**

Submitted on 30 Jun 2020

**HAL** is a multi-disciplinary open access archive for the deposit and dissemination of scientific research documents, whether they are published or not. The documents may come from teaching and research institutions in France or abroad, or from public or private research centers.

L'archive ouverte pluridisciplinaire **HAL**, est destinée au dépôt et à la diffusion de documents scientifiques de niveau recherche, publiés ou non, émanant des établissements d'enseignement et de recherche français ou étrangers, des laboratoires publics ou privés.

# Journal Pre-proof



Joint Europa Mission (JEM) a multi-scale study of Europa to characterize its habitability and search for extant life

Michel Blanc, Nicolas André, Olga Prieto-Ballesteros, Javier Gomez-Elvira, Geraint Jones, Veerle Sterken, William Desprats, Leonid I. Gurvits, Krishan Khurana, Aljona Blöcker, Renaud Broquet, Emma Bunce, Cyril Cavel, Gaël Choblet, Geoffrey Colins, Marcello Coradini, John Cooper, Dominic Dirkx, Philippe Garnier, David Gaudin, Paul Hartogh, Luciano less, Adrian Jäggi, Sascha Kempf, Norbert Krupp, Luisa Lara, Jérémie Lasue, Valéry Lainey, François Leblanc, Jean-Pierre Lebreton, Andrea Longobardo, Ralph Lorenz, Philippe Martins, Zita Martins, Adam Masters, David Mimoun, Ernesto Palumba, Pascal Regnier, Joachim Saur, Adriaan Schutte, Edward C. Sittler, Tilman Spohn, Katrin Stephan, Károly Szegő, Federico Tosi, Steve Vance, Roland Wagner, Tim Van Hoolst, Martin Volwerk, Frances Westall

PII: S0032-0633(19)30501-X

DOI: <https://doi.org/10.1016/j.pss.2020.104960>

Reference: PSS 104960

To appear in: *Planetary and Space Science*

Received Date: 1 December 2019

Revised Date: 15 April 2020

Accepted Date: 25 April 2020

Please cite this article as: Blanc, M., André, N., Prieto-Ballesteros, O., Gomez-Elvira, J., Jones, G., Sterken, V., Desprats, W., Gurvits, L.I., Khurana, K., Blöcker, A., Broquet, R., Bunce, E., Cavel, C., Choblet, Gaë., Colins, G., Coradini, M., Cooper, J., Dirkx, D., Garnier, P., Gaudin, D., Hartogh, P., less, L., Jäggi, A., Kempf, S., Krupp, N., Lara, L., Lasue, Jéé., Lainey, Valé., Leblanc, Franç., Lebreton, J.-P., Longobardo, A., Lorenz, R., Martins, P., Martins, Z., Masters, A., Mimoun, D., Palumba, E., Regnier, P., Saur, J., Schutte, A., Sittler, E.C., Spohn, T., Stephan, K., Szegő, Ká., Tosi, F., Vance, S., Wagner, R., Van Hoolst, T., Volwerk, M., Westall, F., Joint Europa Mission (JEM) a multi-scale study of Europa to characterize its habitability and search for extant life, *Planetary and Space Science* (2020), doi: <https://doi.org/10.1016/j.pss.2020.104960>.

This is a PDF file of an article that has undergone enhancements after acceptance, such as the addition of a cover page and metadata, and formatting for readability, but it is not yet the definitive version of record. This version will undergo additional copyediting, typesetting and review before it is published in its final form, but we are providing this version to give early visibility of the article. Please note that, during the production process, errors may be discovered which could affect the content, and all legal disclaimers that apply to the journal pertain.

© 2020 Published by Elsevier Ltd.

**Credit to authors**

The objective of the research described in this paper is to share with the planetary science community and mission designers a preliminary concept study for a joint USA-Europe mission to search for life. The overall coordination of this research was done by Michel Blanc, Olga Prieto-Ballesteros, Nicolas André and Javier Gomez-Elvira. The different authors all contributed to the elaborated contents on the basis of their specific expertise: scientific data analysis, modelling, instrument development, spacecraft architecture design, mission analysis, planetary protection, navigation, data downlink and radio astronomy. All co-authors equally contributed to the draft, which is the product of the collective expertise of the JEM team.

Journal Pre-proof



# 1 **Joint Europa Mission (JEM)**

## 2 **A multi-scale study of Europa to Characterize its Habitability**

### 3 **and Search for extant life**

4 Michel Blanc<sup>(1)</sup>, Nicolas Andre<sup>(1)</sup>, Olga Prieto-Ballesteros<sup>(2)</sup>, Javier Gomez-Elvira<sup>(2)</sup>, Geraint  
 5 Jones<sup>(3)</sup>, Veerle Sterken<sup>(4,5)</sup>, William Desprats<sup>(1,6)</sup>, Leonid I. Gurvits<sup>(7,16,38)</sup>, Krishan Khurana<sup>(8)</sup>,  
 6 Aljona Blöcker<sup>(9)</sup>, Renaud Broquet<sup>(10)</sup>, Emma Bunce<sup>(11)</sup>, Cyril Cavel<sup>(10)</sup>, Gaël Choblet<sup>(12)</sup>,  
 7 Geoffrey Colins<sup>(13)</sup>, Marcello Coradini<sup>(14)</sup>, John Cooper<sup>(15)</sup>, Dominic Dirkx<sup>(16)</sup>, Philippe Garnier<sup>(1)</sup>,  
 8 David Gaudin<sup>(6)</sup>, Paul Hartogh<sup>(17)</sup>, Luciano Iess<sup>(18)</sup>, Adrian Jäggi<sup>(4)</sup>, Sascha Kempf<sup>(19)</sup>, Norbert  
 9 Krupp<sup>(17)</sup>, Luisa Lara<sup>(20)</sup>, Jérémie Lasue<sup>(1)</sup>, Valéry Lainey<sup>(21)</sup>, François Leblanc<sup>(22)</sup>, Jean-Pierre  
 10 Lebreton<sup>(23)</sup>, Andrea Longobardo<sup>(24)</sup>, Ralph Lorenz<sup>(25)</sup>, Philippe Martins<sup>(26)</sup>, Zita Martins<sup>(27)</sup>,  
 11 Adam Masters<sup>(28)</sup>, David Mimoun<sup>(6)</sup>, Ernesto Palumba<sup>(33)</sup>, Pascal Regnier<sup>(10)</sup>, Joachim Saur<sup>(29)</sup>,  
 12 Adriaan Schutte<sup>(30)</sup>, Edward C. Sittler<sup>(15)</sup>, Tilman Spohn<sup>(31)</sup>, Katrin Stephan<sup>(31)</sup>, Károly Szegő<sup>(32)</sup>,  
 13 Federico Tosi<sup>(33)</sup>, Steve Vance<sup>(34)</sup>, Roland Wagner<sup>(31)</sup>, Tim Van Hoolst<sup>(35)</sup>, Martin Volwerk<sup>(36)</sup>,  
 14 Frances Westall<sup>(37)</sup>.

15 **Affiliations:** <sup>(1)</sup>IRAP, France ; <sup>(2)</sup>INTA-CAB, Spain; <sup>(3)</sup>MSSL/UCL, UK ; <sup>(4)</sup>University of Bern,  
 16 Switzerland; <sup>(5)</sup>ETH Zürich, Switzerland; <sup>(6)</sup>ISAE, France; <sup>(7)</sup>Joint Institute for VLBI ERIC,  
 17 Dwingeloo, The Netherlands; <sup>(8)</sup>UCLA, USA ; <sup>(9)</sup>Royal Institute of Technology KTH, Sweden,  
 18 <sup>(10)</sup>Airbus D&S, France, <sup>(11)</sup>Univ. Leicester, UK; <sup>(12)</sup>LPG, Univ. Nantes, France; <sup>(13)</sup>Wheaton  
 19 College, USA; <sup>(14)</sup>CSEO, USA; <sup>(15)</sup>GSFC, USA; <sup>(16)</sup>TU Delft, The Netherlands; <sup>(17)</sup>MPS, Germany;  
 20 <sup>(18)</sup>Univ. Roma La Sapienza, Italy; <sup>(19)</sup>LASP, Univ. Colorado, USA; <sup>(20)</sup>IAA, Spain; <sup>(21)</sup>IMCCE,  
 21 France; <sup>(22)</sup>LATMOS, France; <sup>(23)</sup>LPC2E, France; <sup>(24)</sup>IAPS, Italy; <sup>(25)</sup>APL/JHU, USA ;  
 22 <sup>(26)</sup>Télécom ParisTech, France ; <sup>(27)</sup>CQE, IST, Portugal  
 23 ; <sup>(28)</sup>Imperial College, UK; CBM, France; <sup>(29)</sup>University of Cologne, Germany; <sup>(30)</sup>SKA  
 24 Organisation, UK; <sup>(31)</sup>DLR, Germany; <sup>(32)</sup>WIGNER Institute, Hungary; <sup>(33)</sup>IAPS, Italy; <sup>(34)</sup>Jet  
 25 Propulsion Laboratory, USA; <sup>(35)</sup>ROB, Belgium; <sup>(36)</sup>IWF, Austria; <sup>(37)</sup>CBM-CNRS, France;  
 26 <sup>(38)</sup>CSIRO Astronomy and Space Science, Marsfield, NSW, Australia.

27

28 .

29

30

31  
32  
33  
34  
35  
36  
37  
38  
39  
40  
41  
42  
43  
44  
45  
46  
47  
48  
49  
50  
51  
52  
53  
54  
55  
56  
57  
58  
59  
60  
61

### ABSTRACT

Europa is the closest and probably the most promising target to search for extant life in the Solar System, based on complementary evidence that it may fulfil the key criteria for habitability: the Galileo discovery of a sub-surface ocean; the many indications that the ice shell is active and may be partly permeable to transfer of chemical species, biomolecules and elementary forms of life; the identification of candidate thermal and chemical energy sources necessary to drive a metabolic activity near the ocean floor.

In this article we are proposing that ESA collaborates with NASA to design and fly jointly an ambitious and exciting planetary mission, which we call the Joint Europa Mission (JEM), to reach two objectives: perform a full characterization of Europa's habitability with the capabilities of a Europa orbiter, and search for bio-signatures in the environment of Europa (surface, subsurface and exosphere) by the combination of an orbiter and a lander. JEM can build on the advanced understanding of this system which the missions preceding JEM will provide: Juno, JUICE and Europa Clipper, and on the Europa lander concept currently designed by NASA (Maize, report to OPAG, 2019).

We propose the following **overarching goals** for our proposed Joint Europa Mission (JEM): **Understand Europa as a complex system responding to Jupiter system forcing, characterise the habitability of its potential biosphere, and search for life at its surface and in its sub-surface and exosphere.** We address these goals by a combination of five Priority Scientific Objectives, each with focused measurement objectives providing detailed constraints on the science payloads and on the platforms used by the mission. The JEM observation strategy will combine three types of scientific measurement sequences: measurements on a high-latitude, low-altitude European orbit; in-situ measurements to be performed at the surface, using a soft lander; and measurements during the final descent to Europa's surface.

The implementation of these three observation sequences will rest on the combination of two science platforms: a soft lander to perform all scientific measurements at the surface and subsurface at a selected landing site, and an orbiter to perform the orbital survey and descent sequences. We describe a science payload for the lander and orbiter that will meet our science objectives.

62 We propose an innovative distribution of roles for NASA and ESA; while NASA would provide  
63 an SLS launcher, the lander stack and most of the mission operations, ESA would provide the  
64 carrier-orbiter-relay platform and a stand-alone astrobiology module for the characterization of  
65 life at Europa's surface: the Astrobiology Wet Laboratory (AWL). Following this approach, JEM  
66 will be a major exciting joint venture to the outer Solar System of NASA and ESA, working  
67 together toward one of the most exciting scientific endeavours of the 21st century: to search for  
68 life beyond our own planet.

69  
70 Key words: outer planets exploration; search for life; Jupiter system; ocean moon; habitability.

## 71 **1. Scientific goals of JEM**

### 72 **1.1. Searching for extraterrestrial life in the Solar System.**

73 Astrobiologists agree today that the conditions for habitability are directly related to the  
74 definition of life we can formulate on the basis of the only model of life we know, namely  
75 terrestrial life. From this standpoint, habitable environments must meet three basic requirements  
76 symbolically represented by the "Triangle of Habitability" (cf. Westall and Brack, 2018): 1) The  
77 presence of liquid water, which is the best solvent known for inorganic and many small organic  
78 substances. The H<sub>2</sub>O molecule has unique properties that are specifically useful for life, e.g.  
79 latent heat due to the chemical bonds, potential for high salt content due to its density, broad  
80 range of temperature and pressure stability, etc. 2) The availability of life-essential chemical  
81 elements, such as H, N, C, O, S, P, as well as transition metals that help provide structure to the  
82 biomolecules and provide nutrients to the organisms. Transition metals are made available  
83 through the dissolution of the minerals. 3) Energy sources available for life to maintain  
84 metabolism. In the absence of light, energy accessible for life is usually provided by chemical  
85 disequilibria sourced either by radiation, reactions activated by temperature, or redox reactions.  
86 An additional key dimension to planetary habitability is time. We do not know how quickly life  
87 appeared on Earth. The process must have been sufficiently fast at the beginning to impede  
88 backward reaction, but the emergence of forms of increasing complexity likely needed longer  
89 time scales, thus, implying the maintenance of habitability conditions over very long times.

90 Based on these considerations, Lammer et al. (2009) explored the variety of known  
91 configurations of planets and satellites to derive four classes of “habitable worlds”, or Habitats,  
92 as being the ones that meet partly the habitability conditions. Classes I and II relate to our  
93 terrestrial planets (Earth, Mars, Venus), and to the past or present existence of liquid water at  
94 their surface. Classes III and IV correspond to objects where liquid water can be found, not at the  
95 surface, but in sub-surface oceans, which are found among the icy satellites of Jupiter and  
96 Saturn: they are the “Ocean worlds”. Among them, Europa stands out as one of the most  
97 promising destinations, and certainly the most promising one in the Jupiter System. To  
98 understand why, let us first examine how the coupling of Europa to the Jupiter system may have  
99 maintained it “inside the triangle of habitability”.

## 100 **1.2. Searching for life in the Jupiter system.**

### 101 *The Galilean satellites.*

102 In our search for life in the Jupiter System, the four Galilean satellites, sketched in figure 1,  
103 immediately capture our attention. What we know of these moons today is essentially the legacy  
104 of the exploration of the Jupiter System by the Galileo mission. First, we recognize three likely  
105 “ocean worlds”: Europa, Ganymede and Callisto, whose sub-surface oceans, if confirmed, meet  
106 the first and most important condition for habitability. If we then turn to their internal structure,  
107 the two innermost moons, Io and Europa, are essentially “rocky moons”. Thus, Europa’s possible  
108 ocean must be in direct contact with the thick silicate mantle which occupies most of its volume.  
109 A third important characteristics is that Io, Europa and Ganymede are trapped in a 4:2:1 mean  
110 motion resonance, the so-called “Laplace resonance”, which provides them with a continuous  
111 source of internal heating due to the dissipation of tidal motions. Finally, both Io and Europa are  
112 recognized as “active moons”. While this is straightforward for volcanic Io, the permanent  
113 resurfacing processes of Europa’s terrains places it as well in this category. Even more  
114 importantly, a few repeated though still tentative observations by the Hubble Space Telescope  
115 (Roth et al. 2014) of plumes rising hundreds of kilometers above Europa’s surface indicate that  
116 Europa might be the subject of geyser-like activity like Enceladus, though less intense. Evidence  
117 of plumes of water by these marginal detections has been recently reinforced by two new  
118 observations, one from space and one from the ground: first, a re-examination of in situ low  
119 European altitude magnetic field and plasma wave data from Galileo, provided strong evidence

120 that at least on one occasion this spacecraft flew through a dense plume rising to at least 200 km  
121 above the surface (Jia et al., 2018); and secondly, direct searches for water vapor on Europa  
122 spanning dates from February 2016 to May 2017 with the Keck Observatory resulted in non-  
123 detections on 16 out of 17 dates, with upper limits below the water abundances inferred from  
124 previous estimates. But on one date (26 April 2016) water vapor corresponding to a total amount  
125 of about 2000 tons was clearly detected on Europa's leading hemisphere (Paganini, 2019). Taken  
126 together, available observations support the idea that Europa plumes are real, though sporadic  
127 and perhaps rare events.

128 Examined altogether, these four macroscopic properties point to Europa as the unique Galilean  
129 moon likely bearing a subsurface ocean in direct contact with the silicate mantle (the very  
130 definition of a Class III habitat), subject to tidal heating, and displaying signs of activity at its  
131 surface. Liquid water, a permanent energy source, and access to heavy elements at the sea-floor:  
132 even a very superficial inspection of the "triangle of habitability", to be refined in detail later,  
133 provides a strong indication that Europa likely stands "within the triangle". For all these reasons  
134 we are now going to focus on a "systemic" understanding of how this "Ocean world" is coupled  
135 to the Jupiter System, and on how the dynamics of the coupled Europa/Jupiter-System may  
136 maintain habitability conditions at Europa.

### 137 *Europa as a "Complex System" responding to Jupiter system forcing.*

138 One can describe Europa as a system of concentric and coupled layers, from the core to the  
139 exosphere and the plasma envelope, responding globally to Jupiter system forcing. This forcing  
140 is essentially of two types: gravitational (tidal) forcing, exerted mainly on the solid layers of  
141 Europa, and the electrodynamic interaction of Jupiter's corotating plasma, magnetic field and  
142 energetic particles with Europa's exosphere/ionosphere, surface and subsurface ocean.

### 143 **Tidal forcing.**

144 With a typical radius of 1500-2500 km, the four Galilean moons are large bodies inducing strong  
145 gravitational perturbation to their environments throughout their orbital motions. Figure 2  
146 illustrates the Laplace resonance linking the mean motions of Io, Europa and Ganymede and  
147 shows the temporal spectrum of the gravitational perturbations exerted on Europa (derived from

148 Lainey et al., 2006). Because of this orbital resonance, a dynamical equilibrium and continuous  
149 energy exchange are maintained between the three innermost Galilean moons.

150 Tides are a major actor for heating the interior of the moons, with a heat flow up to 70 times the  
151 radiogenic heating at Io (Hussmann et al. 2010). They affect both Jupiter and its moons. Because  
152 the moons are synchronous, orbital eccentricity is the most evident way to allow for tidal forcing  
153 inside the moons. Without the Laplace resonance, the eccentricity of the orbits would have been  
154 lost for long. But the Laplace resonance forces the eccentricities of Io and Europa to substantial  
155 values while the orbits are secularly evolving under tides.

156 In addition to the eccentricity of their orbits, the existence of an obliquity and large physical  
157 librations may allow for tidal friction inside the moons too. For the Galilean system, the  
158 obliquities are believed to be small, even though never measured so far (Bills & Ray 2000). The  
159 magnitude of physical librations depends on the moment of inertia of the moons. The presence of  
160 an internal ocean may allow a decoupling between the interior and the crust. Like for the  
161 obliquities, the physical librations of the Galilean moons remain unmeasured. A clear  
162 measurement of the obliquities and physical librations will allow a more accurate estimation of  
163 heating inside the bodies (Wisdom 2004).

164 On long time scales, the evolution of the Galilean system links the moons internal evolution with  
165 their orbital one. While the moons are heating up (cooling down) their viscosity may decrease  
166 (increase), allowing for significant feedback on the orbits. Studying such coupling, periodic  
167 solutions for Io's heating were pointed out by Ojakangas & Stevenson (1986) and Hussmann &  
168 Spohn (2004). More generally, the origin of friction inside the moons remains to be  
169 discriminated. In icy bodies, significant tidal dissipation may arise inside the silicate core, the  
170 ocean and the icy crust. While strong dissipation within the ocean remains unlikely (Tyler 2008;  
171 Chen et al. 2014), tidal heating may play an important role within the mantle (Moore (2003),  
172 Hussmann and Spohn (2004), Tobie et al. (2005)) and the icy crust (Cassen et al. (1979), Tobie  
173 et al. (2005), Nimmo et al. (2002)).

174 This resonant coupling mechanism has important consequences for all moons. In the case of  
175 Europa, it provides a permanent source of heating to the ice shell and mantle. But the temporal  
176 variation of total tidal heating and its vertical distribution between mantle and ice shell are

177 poorly constrained by observations. Figure 3 shows a simulation result from Tobie et al. (2003)  
178 predicting that most of the tidal heating goes into the ice shell, but this prediction has to be  
179 validated by adequate observations.

### 180 **Magnetospheric forcing.**

181 At the Jovicentric radial distance of Europa, the dynamics of the magnetosphere is dominated by  
182 three phenomena: (a) Jupiter's field lines host the strongest radiation belts in the Solar System,  
183 whose harshest region extends slightly beyond Europa's orbit ; (b) Jupiter's magnetic field lines  
184 corotate with the planet ; (c) the dominant source of plasma is Io's volcanic activity, which  
185 results in the injection of about one ton/s of fresh Iogenic ions into the corotating magnetic flux  
186 tubes. The centrifugal force acting on these flux tubes drives an outward diffusion of this Iogenic  
187 plasma, which dominates all other plasma sources throughout the inner and middle  
188 magnetosphere. At its radial distance, Europa is still imbedded inside the Jovian radiation belts,  
189 and it opposes two types of obstacles to the Jovian corotating magnetic flux tubes and plasma  
190 (Figure 4).

191 The first obstacle is the European surface. While the thermal plasma flow is deviated around this  
192 obstacle, energetic particles bombard the surface, producing space weathering, particle  
193 absorption and desorption, induced chemical reactions, and desorption of surface molecules.  
194 Some neutral exospheric particles experience charge exchange with the incident magnetospheric  
195 flow. Charged particles freshly implanted into the flow via pick-up are accelerated to tens of keV  
196 energies by Jupiter's strong corotation electric field. In this way the European interaction adds  
197 ions of European origin coming from its exosphere or from its surface, including ions of  
198 astrobiological interest, to the Jovian ion population.

199 In the sub-Alfvenic regime of this interaction, magnetic field lines first bend around this obstacle  
200 and pile up, before being diverted around it. The velocity difference between this magnetized  
201 flow and the European conductor induces a large potential drop, on the order of 200 kV, between  
202 the Jupiter-looking side of Europa and the opposite side. This potential drop in turn drives a  
203 current system which flows inside the tenuous ionosphere of Europa, before closing partly within  
204 the far-field Alfven wings generated by the obstacle, and partly through Jupiter's upper  
205 atmosphere. To understand the exchange of angular momentum and of energy between Europa



206 and the surrounding magnetospheric flow produced by this interaction, one must be able to  
 207 characterize the different components of this electrical circuit.

208 The second obstacle is the conducting ocean, which opposes the penetration of time-varying  
 209 magnetic field. The depth to which a signal is able to penetrate the conductor is given by the  
 210 parameter:

$$211 \quad S = (\omega_{is}\mu\sigma_{is}/2)^{-1/2}$$

212 called the skin depth where  $\omega_{is}$  is the frequency of the signal and  $\sigma_{is}$  the conductivity of the  
 213 obstacle. Galileo magnetometer data using Jupiter's rotating field as an 11-hour periodic signal  
 214 unambiguously confirmed the presence of a liquid water ocean but were not robust enough to  
 215 place reliable constraints on ice thickness, ocean thickness and ocean salinity. With its multiple  
 216 flybys, the Europa Clipper mission should be able to provide estimates of the inductive response  
 217 of Europa's ocean at both the 11-hr and 85-hour periods, and even of ocean thickness and  
 218 conductivity within a certain domain of these parameters. But a Europa Orbiter can provide  
 219 estimates of signal strength and response over the much broader range of frequencies of  
 220 magnetic fluctuations experienced in the European environment (see fig. 4, insert) and thus  
 221 provide unique and accurate estimates of ice thickness, ocean thickness and ocean conductivity,  
 222 as will be shown in section 2.1.

### 223 *Europa as a potential habitat*

224 In the context of a combined Europa orbiter-lander mission, we propose to re-examine now the  
 225 relationship of Europa to the "triangle of habitability" in the light of the coupling mechanisms of  
 226 Europa to the Jupiter system, which a Europa orbiter will be able to examine in unprecedented  
 227 detail.

228 Based on the above reflections, there are several converging reasons for identifying the system  
 229 formed by the ice shell and internal ocean of Europa and their interfaces above (with the  
 230 exosphere and Jovian magnetosphere) and below (with the sea floor and silicate mantle),  
 231 illustrated in Figure 5, as a potential habitable world:

- 232 - Tidal interaction with Jupiter and the other Galilean satellites produces heat dissipation
- 233 inside the solid components of Europa, mantle and ice sheet, with a still unclear



234 distribution between these two sinks. This energy complements radiogenic heating and  
235 may play an important controlling role in the maintenance of a liquid ocean, the activity of  
236 the rocky mantle and in the thickness of the ice shell. The huge amount of energy available  
237 is manifested as geological features that deform the icy crust around the globe. Some of  
238 them apparently are linked to aqueous reservoirs or the ocean. The geological  
239 interpretation of these features indicates the possible presence of giant shallow lakes in the  
240 subsurface, recent plume activity and diapirism, showing that the ice shell can mix  
241 vigorously:

242 - Europa's subsurface ocean is likely in direct contact with a silicate seafloor, possibly similar  
243 in composition to the terrestrial ocean crust. It is an open question whether the rocky  
244 mantle is geologically active, but if it is it may release essential elements for life: we know  
245 from terrestrial analogues that catalytic reactions associated with hydrothermalism at the  
246 seafloor alter rocks, making them porous, by favouring oxidation of minerals; they also  
247 produce oxidized and reduced fluids, as well as organic compounds and hydrogen. Mg-  
248 sulfates that are observed on the icy surface could be abundant in the ocean, forming from  
249 the oxidation of sulfides. Carbon species such as carbonates, methane or other  
250 hydrocarbons can form from carbon dioxide or primordial organics depending on the  
251 hydrogen fugacity or decomposition temperature.

252 - Apart from those produced during hydrothermal alteration of the rocks, other chemical  
253 gradients are produced on the surface. The moon orbits well inside the Jovian radiation  
254 belts, whose particles have direct access to its surface where they induce a host of  
255 radiolytic processes on the surface material, including the synthesis of oxidizers, again a  
256 source of free energy. Europa thus has the potential of displaying a redox couple between  
257 its sea floor and its surface, which can be a source of chemical energy if the oxidized  
258 species can be transported through the ice shell by endogenous processes, such as  
259 subduction as proposed by Kattenhorn and Prockter (2014). Galileo/NIMS first detected  
260 distortions in the water ice absorption bands occurring between 1 and 3  $\mu\text{m}$  reveal the  
261 existence of non-ice material mixed with water ice at specific locations on the surface of  
262 Europa. They have been identified as hydrated salt minerals like Mg-, Na-, Ca- sulphates,  
263 chlorides, perchlorates and carbonates (endogenous), hydrated sulphuric acid and hydrogen

264 peroxide ( $\text{H}_2\text{O}_2 \cdot 2\text{H}_2\text{O}$ ) (exogenous), or a combination of these three classes of compounds  
265 in varying proportions across the surface (McCord et al., 1999; Dalton et al., 2005; Dalton  
266 et al., 2010; Carlson et al., 2005; Loeffler and Baragiola, 2005; Brown and Hand 2013;  
267 Hanley et al., 2014). Many of these chemical elements may be related to catalysis of  
268 prebiotic molecules. In particular, magnesium may play a major role in stabilizing prebiotic  
269 molecules and catalysing more complex molecules (Russell et al. 2014). On the other hand,  
270 other compounds would also have an exogenous origin, such as silicates from impact  
271 materials (Zahnle et al. 2008) and sulphur species from Io and elsewhere that take part in a  
272 radiolytic S cycle on the surface (Carlson et al., 1999).

273 Provided that the ice shell is “partly permeable” to the transfer of chemical species between  
274 the liquid ocean and the icy surface, two key cycling processes may co-exist there:

275 - a net transport of radiolytically produced oxidizing species from surface to the liquid mass  
276 of the ocean;

277 - conversely, the possibility of transfer of biomolecules and even of specific forms of life from  
278 the deep ocean to the surface (more likely, to the sub-surface because of the radiation  
279 conditions there), or even to erupting plumes, as will be discussed later.

280 Under these assumptions, the sub-system of Europa extending from the ocean silicate floor to the  
281 ice shell surface, which corresponds exactly to the region of overlap between the domains of  
282 influence of tidal and magnetospheric forcing, constitutes a candidate “European biosphere”  
283 worth characterizing by means of quantitative measurements.

#### 284 **The potential dark biosphere of Europa.**

285 How could life possibly emerge in this putative European biosphere? Of all existing scenarios,  
286 abiogenesis at hydrothermal vents, with their highly reactive surfaces and protective porous  
287 niches, is favored by many (e.g. Baross and Hofmann 1985; Russell and Hall, 1997). In  
288 terrestrial hydrothermal vents, the building blocks of life were concentrated in the pores of the  
289 rocks, stabilized and assembled with the aid of mineral surfaces. The process had to be  
290 kinetically fast and in one direction with estimates of the time necessary ranging from some  
291 tens/hundreds of thousands to a few million years (Westall and Brack, 2018). The living cells

292 that emerged from this process were very simple, even compared to the simplest of living cells  
293 today. They consisted of hydrophilic molecules (long chain lipids) forming membranes that  
294 separated the molecules (proteins) undertaking the process of living reactions (metabolism), i.e.  
295 obtaining nutrients from the external environment and transforming them into energy and other  
296 molecular components of cells, as well as molecules capable of encoding and transmitting  
297 information (e.g. RNA, DNA and their as yet unknown predecessors). These first cells were  
298 fuelled on Earth by ingredients provided by simple organic molecules, as well as hydrogen,  
299 produced by Fischer-Tropsch alteration of the hot crust by circulating seawater and hydrothermal  
300 fluids, or released from organic rich fluid inclusions in ultramafic rocks. Their carbon source was  
301 either inorganic CO<sub>2</sub> dissolved in the seawater (degassed by differentiation and dissolved from  
302 the early CO<sub>2</sub> atmospheres), or the simple organic molecules provided by hydrothermal activity  
303 or dissolved from the relatively abundant organic matter raining down on the various bodies in  
304 the early Solar System in the form of carbonaceous meteorites, and comets. Such chemotrophic  
305 cells would have formed colonies, possibly even biofilms on the surfaces of rocks and minerals  
306 bathed in the hydrothermal fluids. Their abundance and distribution would have been strictly  
307 controlled by access to nutrients, as was the case on the early Earth.

308 If there is continued hydrothermal activity on the seafloor of Europa, the most likely forms of  
309 life to have lived possibly in the past and at present would be chemotrophs. These are surface  
310 specific life forms whose biomass development and distribution is controlled by access to  
311 hydrothermal fluids and chemical gradients. For possible traces of life on Europa to be detected  
312 today, either extant or extinct, it will be necessary for the traces to be transported up to the base  
313 of the ice shell and through it towards the surface. Under this restricting assumption, how can we  
314 design a “winning strategy” for our quest for life there?

### 315 **1.3. Searching for life at Europa.**

316 An efficient strategy to search for life at Europa must encompass three main types of contexts:  
317 the biological, the chemical, and the geological/geophysical contexts. Traces of extant or extinct  
318 life could be found potentially at the surface and near-surface environment of the ice,  
319 incorporated through reworking (impact gardening, mass wasting and internal dynamics) of  
320 material brought up from aqueous reservoirs, or in plumes of oceanic water spewed up into the  
321 exosphere: those are the places to look for. But bio-signatures, if they exist, will be strongly

322 influenced by the extreme environmental conditions reigning on the surface of the ice and in the  
323 exosphere – high radiation, production of corrosive oxidizing species and radicals, tenuous  
324 atmosphere and low water activity. This would lead to rapid death of living cells and rapid  
325 degradation of the organic components of life. The remnant organic molecules are likely to be  
326 refractory, particularly if they have been exposed to the surface for long periods of time.  
327 Therefore, the search for signs of life needs access to fresh endogenic materials, which should be  
328 coming from the habitable environment in the case of extant life, and must be performed with a  
329 specific instrumentation and in the appropriate layers:

330 - Subsurface sampling, a must in our strategy, must search for better protected samples that could  
331 be analysed in different physical states (solid/liquid). Analysis of samples in the aqueous phase  
332 will be obtained by melting near-surface ice samples, while chemical disequilibria will be  
333 simultaneously characterized during the search for biosignatures. The choice of performing our  
334 biomolecule characterization measurements in liquid rather than in solid phase depends on the  
335 type of biosignature and on the analytical procedure of identification, as will be explained in  
336 section 2.3.

337 - Capturing compounds in a plume, if and when it occurs, is another indirect way to access to  
338 material emerging from the sub-surface. Evidences of water plumes erupting from the surface up  
339 to 200 km around the southern hemisphere have been reported by Hubble Space Telescope  
340 images (Roth et al. 2014, NASA report 26/09/2016). Ejecting materials would be coming from  
341 the interior of Europa, potentially from liquid layers, so they could include important information  
342 about the habitable environments or even evidences of life, as will be discussed further in section  
343 2.2 and 2.3. This discovery offers a unique opportunity to access the interior materials. Details of  
344 how this phenomenon occurs in Europa are still unknown. Several mechanisms of plume  
345 production have been proposed for Enceladus, and the same might work on Europa (Porco et al.,  
346 2006; Kiefer et al., 2006; Schmidt et al., 2008). Not all of them involve liquid water: some of them are  
347 based on pressure changes in ice layers. The example of Enceladus shows that an oceanic origin  
348 can be considered if salt or other specific mineral grains are detected by future observations.

349

350 **1.4. JEM: the next logical step in NASA and ESA strategies for Jupiter System exploration.**

351 The design and planning of JEM will be able to rest on the unique asset of several missions to  
352 the Jupiter System to be flown by ESA and NASA in the coming decade: Juno (NASA), JUICE  
353 (ESA) and most importantly Europa Clipper. The host of data on Europa this mission will return  
354 from its 45 fly-bys will provide the necessary basis for the design of a lander mission, which is  
355 already under study by NASA. The overarching goal of JEM, complementary to its predecessors  
356 at Jupiter, can be formulated as follows:

357 **Understand Europa as a complex system responding to Jupiter system forcing,**  
358 **characterize the habitability of its potential biosphere and search for life at its surface and**  
359 **in its sub-surface and exosphere.**

360 To address this goal, the science plan of JEM, schematically represented in figure 6, will study  
361 Europa as a system of coupled layers at three scales: the global scale (European radius), a medium  
362 scale (the thickness of Europa's potential biosphere), on the basis of five priority science  
363 objectives.

## 364 **2. Detailed scientific objectives and measurement requirements.**

365 For each of our five science objectives, we describe now the corresponding measurement  
366 requirements and constraints on the mission profile, which are summarized in the Science  
367 Traceability Matrix of JEM (Annex I).

368 2.1. Global scale science investigations: Understand Europa as a system of coupled layers  
369 responding to Jupiter System forcing.

370 **PSO#1: Determine the global structure of the European magnetic field and plasma environment**  
371 **including potential plume characterization, and the associated response of Europa, including its**  
372 **ocean, to Jupiter System magnetospheric forcing.**

373 The interaction of Europa with the Jovian magnetospheric field and flow results in the complex  
374 distribution of plasmas, energetic particles, magnetic fields and electric currents illustrated in  
375 Figure 4. The resulting charged particle population is a complex mixture of ions of different  
376 origins: to the primary population of Iogenic ions, dominant in the Jovian plasma sheet, the  
377 European interaction adds ions of European origin coming from its exosphere, or even directly  
378 from its surface, or from its subsurface through potential plumes, into the magnetospheric flow.

379 Measuring its chemical composition bears a high astrobiological potential, since biomolecules  
380 present in Europa's surface layer may have made their way to the European charged particle  
381 environment as ionospheric and pick-up ions. JEM composition measurements must be able to  
382 find endogenic materials amidst the background of magnetospheric species constantly raining  
383 down on the surface. JEM magnetic field measurements will have to retrieve the 3-D picture of  
384 the four contributions to magnetic field configuration produced by the European magnetospheric  
385 interaction: (1) the background undisturbed Jovian magnetic field, which is on the order of 450  
386 nT; (2) a never detected hypothetical intrinsic European magnetic field generated by a core  
387 dynamo mechanism, of which we know only an upper limit (Schilling et al., 2004). Continuous  
388 low-altitude measurements by JEM will decrease its detection threshold by at least an order or  
389 magnitude; (3) the magnetic fields produced in the European environment by the European  
390 magnetospheric interactions; (4) the magnetic effects of the electric currents induced into  
391 Europa's conducting ocean by the varying Jovian magnetic field, on the order of 50-100 nT,  
392 which constitute a natural magnetic sounding of the ocean. To achieve a good accuracy in this  
393 magnetic sounding of Europa's ocean, one must separate the Jovian source (1) and the oceanic  
394 response to its variations (4) from the other two components. This goal can be achieved using  
395 models of various levels of complexity, such as the MHD model by Blöcker et al. (2016),  
396 illustrated in Figure 7. For the analysis of JEM magnetic field and plasma data, a comprehensive  
397 model separating the four contributions and simultaneously constraining ocean thickness,  
398 conductivity, and atmospheric densities will be developed, based on the data assimilation  
399 techniques currently used in meteorology and related research areas. This inversion process will  
400 take advantage of the two-point magnetic field measurements, on the orbiter and during the 22  
401 days of operation of the lander at the surface.

402 Figure 7, which shows the current systems, the global distribution of ionospheric densities  
403 around Europa, and the corresponding ionospheric currents, suggests that an orbit around 100 to  
404 200 km altitude will provide a good access to the current system near its intensity maximum.

405 Finally, the JEM orbiter would collect more useful data in two days of operation than what will  
406 be obtained from Europa Clipper in 40 flybys spread over three years. If a continuous time series  
407 is available from an orbiter for a period of 3 months or longer, one can use not only the main  
408 prime frequencies with large amplitudes, but also the broadband spectrum of much weaker lower

409 frequencies to sound the ocean under the ice sheet. As shown in Figure 8, adapted from Khurana  
410 et al. (2009), these frequencies, materialized by pink, green and yellow curves, allow a much  
411 better coverage of the (ocean thickness vs. amplitude of the magnetic response) parameter space  
412 than the sole dominant frequencies at the 11.1 hr (Jovian synodic) and European orbital (85.2 hrs)  
413 periods.

414 In addition, if the lander carries a magnetometer, simultaneous measurements with the orbiter  
415 will facilitate the decomposition of the internal and external fields directly in time domain. The  
416 decomposed internal and external field time series can then be Fourier decomposed into the  
417 primary field and Europa's response at not only the two prime frequencies but also the weaker  
418 non-harmonic frequencies. A strong advantage of two-point measurements is that even relatively  
419 short time series can be inverted into their constituent primary and secondary fields.

420 In conclusion, JEM will perform the following investigations to address the PSO#1:

- 421 - Determine the global structure of magnetic fields, electric currents, plasma and energetic  
422 populations in the European environment;
- 423 - Separate the four contributions to European magnetic fields and current systems;
- 424 - Use the natural fluctuations of the Jovian magnetic field to perform a broad-band magnetic  
425 sounding of the European sub-surface ocean;
- 426 - Determine the composition/flux of plume material to characterize the properties of any  
427 subsurface water.

428 **PSO#2: Determine the global structure of the solid body and potential biosphere of Europa, and**  
429 **their response to Jupiter System tidal forcing.**

430 To achieve the measurement objectives of PSO#2, JEM will combine altimetry, gravimetry, the  
431 characterization of rotation and magnetic measurements, using the geophysical investigations  
432 available on the orbiter and on the lander geophysical station, with the additional support of  
433 astrometry measurements. The following parameters will be determined in priority: (1) the  
434 harmonic expansion of the static gravity field and of the topography up to degree 30-40, (2) the  
435 amplitude (precision  $< 10^{-2}$ ) and phase (precision  $< 1^\circ$ ) of the gravity variations ( $k_2$  Love



436 number) and topographic deformation ( $h_2$  Love number) of the European tides, from which an  
437 accurate estimator of the ice shell can be derived, (3) the libration and rotation properties of  
438 Europa, from radio science (gravity field), altimeter data and surface lander positioning, (4) the  
439 instantaneous orbital characteristics of Europa and its long-term evolution, using the PRIDE-E  
440 astrometry experiment analyzed in the context of previous astrometry measurements of the  
441 orbital dynamics of the Galilean satellites (space and ground-based).

442 By combining these measurements, a rich set of integrated information on Europa's internal  
443 structure, dynamics and energy budget will be produced, including: (1) detailed radial profiles of  
444 the key geophysical quantities, (2) an assessment of the assumed hydrostatic equilibrium, (3) a  
445 global description of the undulations of the critical interfaces: ice shell/ocean, ocean/rock mantle,  
446 rock mantle/core (if the latter is precisely defined); (4) an accurate description of tidal  
447 deformation and heating, possibly including constraints on its distribution between the different  
448 layers.

449 Figure 9 shows results of simulations we performed of the use of the gravity science  
450 investigation of JEM. These results show that the gravity field can be retrieved up to a degree  $l$   
451 of 30 and possibly 40 for the orbital parameters and mission duration foreseen for JEM  
452 (compared to  $l < 20$  for the 45 fly-bys of Europa Clipper). Furthermore, the expected uncertainty  
453 on the measurement of Love number  $k_2$  would be about 20 times smaller: while Europa Clipper  
454 will do an excellent job to go beyond Galileo, significantly augmented information about the  
455 interior of Europa will be provided by JEM.

456 Furthermore, the combination of the measured gravity and topography tidal waves will provide a  
457 direct evaluation of the total ice shell thickness at the 5-km precision and of some of its  
458 mechanical properties at the resolution necessary to provide key constraints for dynamic models  
459 of the ice shell, for instance to decide about its conductive or convective nature. The combination  
460 of gravity and surface deformation phase lags will further allow to discriminate between  
461 predominant tidal dissipation in the ice shell or in the rock mantle, an important ingredient to  
462 investigate the coupling between the orbital dynamics and the thermal evolution of Europa and  
463 better constrain the chemical coupling and mass transfer processes at work between ocean,  
464 silicate floor, ice shell and surface.



465 PSO's 1 and 2 combined will provide unique information on the internal structure, layering and  
466 dynamics of Europa, using the synergies between measurement techniques deployed on the  
467 orbiter and on the lander. Figure 10 illustrates this complementarity of techniques (rotation  
468 monitoring, electromagnetic sounding, gravimetry, seismic or acoustic sounding...) and shows  
469 how their combination will provide a comprehensive description of key characteristics of the  
470 different layers of Europa's interior.

471 **2.2. Medium scale study: Determine the characteristics of the potential habitable zone of**  
472 **Europa.**

473 **PSO#3: Understand the exchange and transformation processes at the interface between**  
474 **the ice-shell surface/subsurface and the exosphere/ionosphere including potential plume**  
475 **characterization**

476 Europa's surface and exosphere. Europa's surface is composed of an icy porous regolith (50 to  
477 100  $\mu\text{m}$  grains) permanently bombarded by Jovian magnetospheric energetic ions (essentially  
478 keV to MeV  $\text{S}^{\text{n}+}$  and  $\text{O}^{\text{n}+}$  coming from Io's torus) and electrons (equivalent of 100 to 1000 times  
479 the dose rate at the Moon) and by photons (Cooper et al. 2001). The radiolysis and photolysis  
480 induced by this bombardment alter the optical layer of the surface, from microns up to meter  
481 depth, on a time scale between 10 and  $10^9$  years. The typical yield of  $\text{S}^+$  and  $\text{O}^+$  at keV to MeV  
482 energy is around 1000, so that the ice resurfacing rate induced by sputtering should be of  $\sim 0.1$   
483 microns / year (or 100 m/Gyr), significantly lower than the resurfacing rate due to meteoroid. As  
484 a consequence, the regolith can be a substantial trap for radiation-altered material.

485 The incident magnetospheric particles and photons decompose Europa's icy surface into  $\text{H}_2$ ,  $\text{O}_2$   
486 and  $\text{H}_2\text{O}_2$ . Preferential loss of the volatile  $\text{H}_2$  leaves an oxidized surface, a gravitationally bound  
487  $\text{O}_2$  atmosphere and peroxide trapped in ice (see the right-hand side of figure 11 from  
488 Shematovich et al. 2005). This processing also determines the state of trace species such as S, C,  
489 Na, K and Mg. Sources and sinks of trace species in Europa's icy surface are: implantation from  
490 Io plasma torus, upwelling or venting from interior sources, and meteorite impacts. As a result of  
491 sputtering, Europa's exosphere is expected to display a composition closely related to the surface  
492 composition, thus providing a probe to understand how the surface composition is processed by  
493 radiolysis/photolysis, enriched by exogenic sources and eroded by sputtering. The ultimate goal

494 for JEM will be to estimate the respective role of these processes and their spatial and temporal  
495 variations, using three signatures for each of these processes: compositional, energetic and  
496 spatial.

497 European plumes. Based on Enceladus studies, European plumes might be stratified according to  
498 the density of materials, with dust grains of salt, silicate materials or heavy organics remaining in  
499 the lower parts of the plume, while light volatiles would reach higher altitudes. Thus, the  
500 compounds that could be analysed at different altitudes could provide information about the  
501 formation history and habitability of the moon.

502 In summary, JEM will perform the following investigations in the context of PSO#3:

- 503 - Determine the composition and spatial distribution of major and trace species of Europa's  
504 exosphere;
- 505 - Ascertain the roles of the surface/subsurface, magnetosphere, dust and possibly plumes as  
506 drivers of exosphere formation.

507 **PSO#4: Understand the exchange processes between the ice-shell surface/subsurface and the**  
508 **potential habitable zone.**

509 Exchange processes between the ice-shell surface/subsurface and deep aqueous layers constrain  
510 the possibility of finding signatures of the non-accessible habitable zone with JEM observations  
511 of surface and subsurface chemistry and geological features. The extreme diversity of these  
512 surface features is illustrated in Figure 12. In order to recognize which features are young and  
513 have endogenous origin, JEM will benefit from: a) Europa Clipper and JUICE mission  
514 measurements of remote imaging, spectroscopy and radar scanning of Europa, which will  
515 provide for the first time detailed information on geological features, activity and history at  
516 regional resolution; b) JEM global accurate geophysical measurements, particularly topography;  
517 c) JEM novel information at the local scale of the landing site.

518 Resurfacing by cryovolcanism, geyserism or tectonism could have effects on transportation of  
519 materials and cycling of the elements in the moon. In this regard, the study of the local  
520 geological features (e.g. morphology, grain sizes of surface materials, presence of boulders,  
521 presence of small craters, stratigraphic relationship between materials), the distribution of

522 materials, and the subsurface structure at the landing site will help to characterize the nearest  
523 aqueous layer at the lander spot. A relation between surface and subsurface features can reveal  
524 the depth of liquid reservoirs and their putative links to the surface.

525 Due to the extreme conditions on the surface, the relative abundances of key materials for  
526 habitability, such as organics, minerals and volatiles containing bio-essential chemical elements  
527 might differ according to their stratigraphy position, chemical state (redox state, degradation  
528 rate) and phase (e.g. water ice/clathrate hydrate). Deposition of radiation energy into materials is  
529 controlled by the chemical and physical properties of the regolith at the landing site (e.g. grain  
530 size, porosity mineral, crystallinity). These parameters determine the so-called “biosignature  
531 preservation potential” (BPP) at the surface/subsurface, which is especially significant for the  
532 search for biosignatures (see 2.3). Magnetic field intensity and radiation dose measurements at  
533 the landing site will be needed to determine the BPP. Selection of the landing site is critical to  
534 maximize the probability of finding fresh endogenous materials, which seems to be more  
535 frequent in the leading hemisphere according to previous studies (see Figure 13).

536 Availability of chemical elements that life needs depends on the physical and chemical  
537 properties of the solvent. This novel investigation can be performed by JEM by characterizing  
538 the melt endogenous materials in the liquid state: a) pH, since it influences the stability,  
539 reactivity and mobility of elements, inorganic and polar organic compounds; b) Redox potential,  
540 which affects the behavior of many elements and chemical constituents in aqueous media and in  
541 the living organisms and is the main energy source for chemotroph organisms; c) conductivity,  
542 which is affected by salinity. Dissolved inorganic ions such as  $Mg^{2+}$ ,  $Ca^{2+}$ ,  $K^+$ ,  $Na^+$ ,  $Cl^-$ ,  $SO_4^{2-}$ ,  
543  $HCO_3^-$  and  $CO_3^{2-}$  can constitute redox couples that could provide energy for chemosynthetic life;  
544 d) volatiles (e.g.  $CH_4$ ,  $NH_3$ ,  $O_2$ ,  $H_2$ ) that are sources of nutrients and potential biosignatures.

545 In summary, the investigations that JEM will perform to address PSO #4 are:

- 546 - Detect any geological feature which involves exchange processes between surface/interior at  
547 the landing site and determine whether any activity exists today;
- 548 - Determine the proximity to liquid water reservoirs in the landing site area;

549 - Characterize the biosignature preservation potential of accessible surface materials at the  
550 landing site;

551 - Characterize the physical properties at the landing site;

552 - Characterize the key compounds associated with habitability near the surface;

553 - Characterize the wet context of surface materials.

### 554 2.3. Local scale study:

#### 555 **PSO#5. Search for bio-signatures at the surface / subsurface.**

556 At present, space exploration considers distinct categories of biosignatures requiring different analytical  
557 techniques with different detection limits:

558 1) General biomarkers (molecular bio-signatures) are indisputable evidence of life. They are  
559 biological polymers like polysaccharides, lipids, proteins or some form of information-  
560 transmitting molecule similar to DNA. Of particular interest are conservative biomolecules that  
561 are deeply and ubiquitously rooted in the tree of life, proteins that are involved in deeply rooted  
562 and widespread metabolic pathways, structural components of cell walls of broad prokaryotic  
563 groups, and phylogenetically conserved structural proteins and storage compounds of broad  
564 prokaryotic groups conserved under stress, e.g. with limited water availability. These different  
565 groups are presented in Figure 14.

566 2) Organic indicators of past or present life. Since high radiation conditions on the European  
567 surface may degrade any material if it is exposed for any length of time, biomolecules will likely  
568 break up and react, producing degraded organic compounds that can also be symptomatic of the  
569 presence of life. It is critical to validate the biological origin of those degraded compounds.

570 3) Inorganic indicators of past and present life: biogenic stable isotope patterns in minerals and  
571 organic compounds, biogenic minerals, or certain atmospheric gases produced by metabolism.

572 4) Morphological and textural indicators of life, e.g. any object or pattern indicating bio-organic  
573 molecular structures, cellular and extracellular morphologies, or biogenic fabric on rocks.

574 Discerning the origin of the bio-signatures is mandatory, specifically for the simpler organics  
575 since they may as well come from meteorites or from ejecta produced by plume activity.  
576 Organics may form by interaction of surface materials with the radiation environment if CO<sub>2</sub> is  
577 originally present in the ice matrix (Hand et al., 2007). Detection of formamide (CH<sub>3</sub>NO) is  
578 particularly crucial, since it is a key compound for the formation of nucleic acids. However, an  
579 exogenous origin of some organics (e.g. PAH) cannot be ruled out.

580 The JEM search for biosignatures will primarily focus on local scale studies on a landing site  
581 where fresh and young material will be expected, coming from the near surface or even from  
582 putative plumes. In near-surface investigations, direct sampling and contact analysis instruments  
583 are absolutely necessary since the concentration of bio-signatures is assumed to be very low.  
584 Sampling materials at depths below 5-10 cm from the leading hemisphere is required for access  
585 to unaltered molecules. Measurements may require the sample to be in the solid or liquid phase  
586 for analysis, depending on the biosignature typology and the technique used for its recognition.  
587 Simple molecules of categories 2 and 3 can be detected and identified directly by vibrational  
588 spectroscopy if they are present in the solid matrix of ice. For isotopic ratios and some more  
589 complex organics (e.g. amino acids, lipids), their unambiguous identification can be performed  
590 by mass spectrometry after sample volatilization, which is a step of the GC/MS procedure. To  
591 unambiguously identify macromolecules of category 1 (e.g. polysaccharides, proteins or  
592 DNA/RNA) a biochemical analytical technique is necessary, such as antibody microarrays  
593 immunoassays. This technique can identify macromolecules because they bind to their particular  
594 3D structures in a liquid medium, which is needed to transport the antibodies and to allow  
595 binding to the specific antigens/target molecules. In JEM, the liquid medium will be obtained by  
596 melting the ice sample of the near surface. Antibodies can also recognize and identify small but  
597 still complex molecules such as aromatic amino acids (Phe, Tyr, Trp) and PAHs such as benzo-  
598 a-pyrene.

599 Besides near-surface science, JEM will also search for bio-signatures of extant life in the  
600 exosphere and in plumes if their existence is confirmed. Traces of life there could include  
601 organic and inorganic biosignatures expelled from the habitable zone, even cells, cellular  
602 material, or biomolecules. Closer to the “vent” exit points, deposits containing rock fragments

603 hosting either extant (or recently dead) life forms or the fossilized remains of life might be  
604 found.

605 In conclusion, PSO #5 will include a set of investigations which are unique in the Solar System  
606 exploration, such as:

607 - identifying general biomarkers;

608 - detecting and characterizing any organic indicator of past or present life;

609 - identifying morphological and textural indicators of life;

610 - detecting and characterizing any inorganic indicator of past and present life;

611 - determining the origin of sampled material;

612 - determining if living organisms persist in sampled materials.

### 613 **3. Proposed scientific instruments:**

614 The implementation of the JEM science plan is based on the joint operation of scientific  
615 investigations on two complementary platforms: a lander (currently under study by NASA) and a  
616 carrier/orbiter, each including a baseline main element and an optional small detachable  
617 platform. We describe now the instrument suite required on each of these platforms to meet our  
618 measurement requirements.

#### 619 3.1. The Orbiter instrument suite.

620 To meet our measurements requirements, we propose that the Orbiter carries the instruments listed in  
621 Table 1, some of them to be operated during a minimum of 22 days simultaneously with lander data relay,  
622 then all of them during the subsequent 3 months of nominal orbital science, and again some of them  
623 during the final descent to Europa's surface. The added complexity of the extreme radiation environment  
624 at Jupiter drives the orbiter instrument architecture. We make the choice of decoupling the sensor heads  
625 from their part of their electronics. This allows flexibility in their accommodation, easier radiation  
626 mitigation, full integration of the scientific capabilities of each of them and ensures optimum science  
627 return while keeping the total resources low.

628 The gravity field, the tidal deformations (both gravitational and physical) and the rotational state  
629 (obliquity and physical librations in longitude) will be determined by means of Doppler and  
630 range measurements carried out both on the orbiter-to-ground, two-way, coherent link, and on  
631 the orbiter-to-lander proximity link. The two-way link to ground, enabled by an onboard  
632 transponder (Integrated Deep Space Transponder or IDST) operating at X or Ka-band, will  
633 provide radiometric observables to estimate a  $> 20 \times 20$  gravity field,  $k_2$  Love number, and global  
634 obliquity and physical librations of the moon.

635 The magnetometer (MAG) instrument will measure the magnetic field in the vicinity of the  
636 spacecraft. This is crucial for a) resolving the interaction of Europa with Jupiter's magnetosphere  
637 with multipoint measurements, b) constraining the extent of Europa's intrinsic magnetization,  
638 and c) searching for evidence of induced electric currents in Europa's subsurface ocean. The  
639 typical range, resolution, and noise-level of this instrument are  $\pm 10 \mu\text{T}$ , up to 50 pT (dependent  
640 on range), and  $< 100 \text{ pT}/\sqrt{\text{Hz}}$  (at 1 Hz) respectively. The range is more than adequate to measure  
641 expected magnetic fields at Europa.

642 The Laser Altimeter (LA) will investigate the surface and interior of Europa. By measuring the  
643 time-of-flight of a laser pulse transmitted from the instrument, backscattered at the moon's  
644 surface and detected in the instrument's receiver telescope, height profiles can be obtained in  
645 along-track direction. Combining many of these tracks, the local, regional, and global  
646 topography of Europa can be obtained. From the pulse-spreading of the returned pulse the  
647 surface roughness on the scale of the laser footprint (order of a few tens of meters) can be  
648 measured. Information on the albedo at the laser wavelength (1064 nm) can be gained from the  
649 intensities of the transmitted and returned pulses. By obtaining not only good spatial coverage  
650 but also temporal coverage with laser ground-tracks, the tidal deformation of Europa's ice shell  
651 along its orbit around Jupiter will be measured. From the tidal signal (expressed in terms of the  
652 radial tidal Love number  $h_2$ ), the extension of Europa's ice shell can be constrained, especially  
653 when combined with measurements of the tidal potential by the radio science experiment. By  
654 measuring the phase-lag of tidal deformation LA will provide constraints on the internal heat  
655 production of Europa. Combined with phase-lag measurements of the tidal potential a highly  
656 dissipative silicate interior could be detected. The instrument is composed of a transceiver unit



657 and two electronic units. The transceiver unit contains the complete laser subsystem and the  
658 optical chain of the receiver.

659 The Ion Mass Spectrometer and Electron Spectrometer (IMS/ELS) suite will provide the most  
660 comprehensive and critically needed thermal and suprathermal plasma measurements to achieve  
661 the following science objectives: (1) reliably characterize plasma ion and electron currents  
662 constituting major backgrounds for magnetometer detection of the oceanic source of induced  
663 magnetic field; (2) characterize Europa's environment, its composition, structure and dynamics  
664 and Europa's interaction with the Jovian magnetosphere; and (3) unveil and quantify the key  
665 processes of erosion and exchange of elements at Europa surface, including presence of expelled  
666 minor/trace elements, possibly representative of sub-surface layers.

667 The ELS sensor is an electrostatic analyzer that will provide fast 3D measurements in the energy  
668 range 1 eV-30 keV and will be customized for the energy range as well as the dynamic range  
669 encompassing magnetospheric suprathermal and thermal plasma originating from Io, cold  
670 ionospheric species including photoelectrons and ram negative ions from Europa, as well as  
671 pick-up negative ions likely to be observed around Europa.

672 The Ion Mass Spectrometer (IMS) sensor is a 3D mass spectrometer that will measure positive  
673 ion fluxes and provide detailed composition measurements at Europa. A major feature of IMS is  
674 its Time Of Flight (TOF) section. which includes two MCP detectors, one with high-count  
675 measurements to ensure a good time resolution, and a second one, based on the reflectron  
676 technique, to provide an enhanced mass resolution. This double detection allows a detailed  
677 composition analysis capable of measuring multiply charged ions and separating ions of the  
678 same mass / charge ratio (e.g. S<sup>++</sup> and O<sup>+</sup>).

679 The Ion and Neutral Mass Spectrometer (INMS) is a time-of-flight mass spectrometer using an  
680 ion mirror (reflectron) for performance optimization. A TOF mass spectrometer has inherent  
681 advantages with respect to other mass spectrometer concepts since it allows recording of a  
682 complete mass spectrum at once without the necessity of scanning over the mass range of  
683 interest. INMS is a time of flight (TOF) mass spectrometer with  $M/\Delta M \approx 1100$  resolution over a  
684 mass range of  $M/q = 1-1000$  u/e.



685 The Dust Analyzer (DA) is a TOF impact mass spectrometer that uses the technology of the  
686 successful Cosmic Dust Analyzer (CDA) operating on Cassini and employs advanced reflectron-  
687 type ion optics optimized for the combination of high mass resolution, large target area, and  
688 large Field-of-View (FOV). For unambiguous recognition of valid dust impacts, a coincident  
689 detection method will be implemented with all analog signals being continuously monitored with  
690 threshold detection.

691 The additional Langmuir Probe (LP) (if resources allow it) will consist of one boom with a  
692 spherical sensor at the tip. The LP will monitor the cold plasma parameters (electron and ion  
693 number densities, the electron temperature and the plasma drift velocity), as well as signals from  
694 micrometeorite impacts on the S/C. The derived LP parameters will provide the basis to a)  
695 characterize the European ionosphere and its dynamics; b) characterize the plume dust and plasma  
696 properties; c) characterize the ambient size/mass distribution of mm-sized dust around Europa  
697 and in the Europa torus; and d) monitor the spacecraft potential for use by the particle  
698 spectrometers and for the determination of the integrated EUV flux.

699 In addition, the Planetary Radio Interferometry and Doppler Experiment for JEM (PRIDE-E) is an  
700 instrument with zero demand on the science payload mass, and only ad hoc demand on other S/C  
701 resources (the onboard power, commands, telemetry). This experiment is designed as an enhancement of  
702 the science output of the mission using the JEM radio links and the extensive infrastructure of Earth-  
703 based radio astronomy facilities. PRIDE-E is a repetition of PRIDE-JUICE, one of the experiments of the  
704 JUICE mission (Witasse et al. 2015). PRIDE is based on the use of Very Long Baseline Interferometry  
705 (VLBI) instrumentation available and operational on more than 40 Earth-based radio telescopes. The  
706 applicability of the VLBI technique for ad hoc experiments with planetary probes has been demonstrated  
707 for the Huygens probe (Pogrebenko et al. 2004, Lebreton et al. 2005, Bird et al. 2005), Venus Express  
708 (Duev et al. 2012., Bocanegra Bahamón et al. 2018) and Mars Express (Duev et al. 2016, Bocanegra  
709 Bahamón et al. 2019) missions. The prime scientific objective of PRIDE-E is to provide inputs into  
710 improvement of the ephemerides of the Jovian system. PRIDE-E will also provide complementary  
711 measurements of the S/C lateral coordinates and radial velocity in the interests of other science  
712 applications. Various applications of PRIDE-E measurements for improvements of Jovian system  
713 ephemerides and related parameters are discussed in detail by Dirkx et al. (2016, 2017, 2018).

714 To accommodate and operate this instrument suite on the Orbiter Science Platform will take the estimated  
715 resources shown in Table 2.

716 3.2. The Lander instrument suite.

717

718 On the NASA side the instrumentation for the lander will be selected based on a future AO to which  
719 European institutes may contribute under the umbrella of their national funding agencies. In this section  
720 we focus on the sensors to be delivered by ESA to the lander through the proposed standalone  
721 Astrobiological Wet Laboratory (described in section 4.3.3) augmented by two geophysical sensors. To  
722 meet our measurements requirements, the Lander should carry the instrument suite presented in Table 3,  
723 to be operated during a minimum of 22 days.

724 Multi-probe immunoassay-based (MPAS) instruments have been proposed for planetary  
725 exploration: the Life Marker Chip (LMC) (Sims et al, 2012) and the Signs Of Life Detector  
726 (SOLID) (Parro et al., 2005; 2008; 2011), but neither LMC nor SOLID can be implemented in  
727 the AWL because of mass and volume restrictions. We are therefore proposing a different  
728 approach adapted to AWL constraints.

729 The MPAS instrument must be based on simplicity and robustness. It minimizes the use of  
730 electronic devices, mechanical actuators and power consumption. The most promising concept is  
731 something well known on biomedical laboratories: the lateral flow assay (LFA) or  
732 immunocapillary test, as it is also called. The first immunoassay based on lateral flow was  
733 reported in 1978 and it has been extensively used on pregnancy tests (Mark, 2010). In the LFA  
734 developed for MPAS, the *Sample Pad* is in contact with the fluid deposit and it is flooded with  
735 the water sample coming from the ice fusion. The sample moves forward by capillarity to the  
736 *Conjugate Pad*, preloaded with a set of antibodies (Ab) labeled with colloidal gold or colored  
737 latex spheres. At this step the target molecules (organics, biomarkers, or antigen-Ag) bind to  
738 their corresponding Ab's and the sample movement continues through the *Detection Pad*. Once  
739 the labeled sample gets the multi-probe *Detection Array*, the couple Ag-Ab binds again to the  
740 immobilized Ag-conjugate (in a competitive immunoassay) or immobilized capturing Ab  
741 (sandwich assay), and dark spots corresponding to the trimeric complexes Ag-AuAb-ConAg or  
742 Ag-AuAb-capAb are visualized by illuminating (visible) the array and image capturing with a  
743 small camera.

744 The Multiparametric probe (MPP) will have heritage from the MECA package onboard the  
745 Phoenix mission which was the unique probe with capability to perform chemical analysis of a

746 water sample. The MECA package (Kounaves, 2003) was a wet chemistry lab with sensors to  
747 measure:  $H^+$ , dissolved  $O_2$ , redox potential, oxidants and reductants, and several ions and  
748 cations. The MECA package was designed as a multi-sample instrument with a mass, volume  
749 and power consumption out of the scope of the instrumentation for this mission. From the  
750 different alternatives available in the environmental monitoring market, the most attractive by its  
751 miniaturization capabilities are those sensors based on ChemFET technology (Jimenez-Jorquera,  
752 2010). Oxygen dissolved, pH, conductivity,  $NH_4^+$ ,  $NO_3^-$ ,  $Ca^{2+}$ ,  $K^+$ ,  $Cl^-$ ,  $NO_3^-$  are parameter with  
753 sensors developed to measure it.

754 The VISTA (Volatiles In Situ Thermogravimetric Analyzer) sensor is a miniaturized  
755 thermogravimetry analyzer that will perform measurements of the Europa volatile compounds  
756 (Palomba et al. 2016). The instrument is based on thermogravimetric analysis (TGA) and its core  
757 is a Quartz Crystal Microbalance (QCM), oscillating at a resonant frequency linearly related to  
758 the mass deposited on its sensible area. The technique measures the change in mass of a sample  
759 as a function of temperature and time. VISTA measurement goals are: a) to discriminate  
760 between water ice and clathrate hydrates, by heating the QCM up to the decomposition  
761 temperature of clathrate hydrates at 120-160 K (Lunine and Shevchenko 1985) and to the  
762 sublimation temperature of water ice (200 K at a depth of 3 meters, Handbook of Chemistry and  
763 Physics 1980), and by recording the temperature at which mass loss due to heating occurs; b) to  
764 measure the composition of non-ice materials, by heating the PCM up to the dehydration  
765 temperatures of possible Europa components, ranging in the interval 220-320 K (McCord et al.  
766 2001), by recording the temperature where mass loss due to heating occurs and by measuring the  
767 volatile/refractory abundance ratio (this measurement which is fundamental to characterize the  
768 non-ice material is not performed by other instrumentation onboard the lander); c) to detect and  
769 measure the relative abundance of organics, by heating the PCM up to organics desorption at  
770 about 230 K and measuring the mass difference before and after desorption.

771 The magnetometer can provide magnetic field measurements at a rate of up to 128 Hz and an  
772 accuracy of 0.1 nT. One on the lander itself, and one on a short (0.5m) boom will ideally be  
773 needed. The laser retroreflector has the property to reflect light back to its source with a  
774 minimum of scattering. A laser onboard the orbiter could target the device from a distance of  
775 tens to hundreds of thousands of km (for instance from the halo orbit). Attached to the lander it  
776 would allow to determine the exact landing site with a precision of a few meters and the

777 measurement of tides and of the rotational state already during the relay phase (like a control  
778 point). The device is fully passive (no power or data consumption). A good example is the  
779 ExoMars 2016 Schiaparelli retroreflector ([http://exploration.esa.int/mars/57466-](http://exploration.esa.int/mars/57466-retroreflector--)  
780 [retroreflector--](http://exploration.esa.int/mars/57466-retroreflector--)  
[for-exomars-schiaparelli/](http://exploration.esa.int/mars/57466-retroreflector--)). It has a size of 54 mm in diameter and a total mass of 25 g.  
781 Our estimate of the resources needed to operate this instrument suite on the Surface Science  
782 Platform is shown in Table 4.

#### 783 **4. Proposed mission configuration and profile**

##### 784 **4.1. JEM orbits and science operations.**

785 The implementation of the science plan of JEM will rest upon instruments deployed  
786 synergistically on two space platforms: a carrier/relay/orbiter platform (hereafter referred to as  
787 orbiter), and a soft lander platform, both described in section 4.2. These 2 platforms will be used  
788 to perform the 3 sequences of scientific observations, or **science sequences**, illustrated in Figure  
789 15:

790 **A. A surface science sequence** involving the lander instruments, planned to last about 22  
791 days on a selected site;

792 **B. An orbital science sequence** involving the orbiter instruments. This sequence will first  
793 overlap in time with the surface science sequence, while the orbiter platform will reside on  
794 a halo orbit of the Jupiter-Europa system to relay the orbiter data to Earth, before  
795 continuing in low European orbit for a planned duration of three months;

796 **C. A descent science sequence** will correspond to an additional period, after the end of  
797 sequence B, during which the orbiter will explore regions of the exosphere/ionosphere very  
798 close to the surface, below the lowest altitude to be covered by Europa Clipper, to search  
799 for biomolecules in the lowest layers of the exosphere.

800 Our astrometry experiment PRIDE-E (section 3.4), will support and complement these three  
801 sequences from Earth using the world-wide VLBI network of radio telescopes.

802 The determination of the landing site (sequence A) and of the B and C orbits must be the result  
803 of a detailed optimization aimed at fulfilling our measurement requirements. For sequence B, we  
804 have chosen a scenario fulfilling different requirements on two different successive orbits. For  
805 sequence C, the requirement of measuring exospheric species in the near-surface exosphere  
806 could be implemented by de-orbiting the orbiter platform and taking data from its initial orbit  
807 until final impact, or by letting the working orbit of sequence B evolve naturally until final  
808 impact. A detailed mission analysis will be needed to identify the most promising approach.

809 The spatial/temporal coverage provided by our JEM orbiter will nicely complement the coverage  
810 and the scientific information to be provided by Europa Clipper, which will have flown 45 times  
811 by Europa a few years before JEM, providing data both much closer to the surface, and at much  
812 larger distances from it, than the high-inclination orbits of JEM will allow. JEM will provide a  
813 three-months continuous coverage of European planetary fields and plasma populations on a high-  
814 inclination orbit, after an initial sequence on a halo orbit which will provide a detailed insight  
815 into the structure of the European Alfvén wings. To reach these orbits, starting from Earth with a  
816 SLS launch, the JEM flight complement will have to go through a succession of mission  
817 sequences (S-1 to S-9) listed in Table 5, first on heliocentric orbits and then on Jovicentric orbits  
818 before reaching its first European orbit.

819 The choice of the sequence of orbits will be the result of a trade-off in a 3D parameter space  
820 described by:

- 821 - the Total Ionizing Dose (TID) accumulated along the spacecraft trajectory, which gives the  
822 maximum operation time our platforms will be able to live through;
- 823 - the shielding thickness used to protect the equipment and mitigate radiation dose effects,  
824 which has a direct incidence on the weight of the platform and instruments;
- 825 - the total Delta V provided by the propulsion system, with direct impact on spacecraft total  
826 wet mass.

827 The JEM spacecraft will first cruise on a DV-EGA trajectory to Jupiter (Figure 16, sequence S-  
828 1). We choose this trajectory to bring the maximum mass possible into Jovian orbit and

829 accommodate a significant science payload on each platform, at the expense of a larger travel  
830 time.

831 After a Jupiter Orbit Insertion (JOI) immediately followed by a PeriJove Raise Manoeuvre  
832 (PRM) to minimize exposition to the inner parts of the Jovian radiation belt (sequence S-2), the  
833 JEM spacecraft will execute a tour in Jovicentric orbits to reach Europa (sequence S-3 and figure  
834 17). Here we choose the 12-L1 tour with only flybys of two Galilean satellites (Ganymede and  
835 Callisto) to reach Europa in a short time and minimize the dose accumulated (Campagnola et al,  
836 2014), in order to enable a lifetime in European orbit significantly above 4 months, at the expense  
837 of a significant Delta V. At the end of sequence S-3, the JEM flight complement is injected on an  
838 eccentric European orbit from which the lander stack is released, de-orbits and executes its  
839 landing sequence.

840 Immediately after lander release, the JEM orbiter will be transferred to a halo orbit to fulfil its  
841 relay function. At that point, the lander and the orbiter will start their science operations.

842 The geometry of the science orbits has been the object of a mission analysis summarized in  
843 Annex III. It is shown in Figure 18. During the 35-day surface science sequence, the orbiter is  
844 primarily used to study the Alfven wings produced by the European magnetospheric interaction  
845 (sequence S-5). At the end of surface science operations, it is transferred to a low altitude 200-  
846 km high-inclination orbit to perform a global mapping of gravity and magnetic fields and of the  
847 European plasma populations (sequence S-7). After 3 months of science operations, the orbiter  
848 leaves its 200-km circular orbit to explore the very low latitude exosphere in the final descent  
849 sequence (S-8).

## 850 **4.2 Environmental constraints on the JEM mission**

### 851 Planetary protection:

852 As the interest in icy Solar System's bodies is increasing with exciting new findings, new  
853 missions are proposed and particularly towards Jupiter's moon Europa. On the basis of  
854 deliberations of the dedicated Task Working Group on the Forward Contamination of Europa  
855 (NRC, 2000) and of the studies of new international experts working groups such as the  
856 "Planetary Protection for the Outer Solar System" (PPOSS) working group commissioned by the

857 European Science Foundation, a conservative approach has been defined to be required to protect  
858 the European environment: Indeed since Europa may have a global ocean possibly connected with  
859 the surface, viable extremophile microorganisms such as cold and radiation tolerant organisms  
860 may survive a migration to the sub-surface of the ocean and multiply there. According to the  
861 COSPAR Planetary Protection policy, a general requirement for every lander mission to Europa,  
862 categorized as IV, has to be applied in order to reduce the probability of inadvertent  
863 contamination of a subsurface ocean by viable terrestrial microorganisms or their spores to less  
864 than  $\sim 10^{-4}$  per mission (1 viable microorganism / 10,000 missions).

865 COSPAR Planetary protection policy of Icy moons missions is under revision. In the context of  
866 future missions to these moons, some concepts require an updated definition such as: the  
867 environmental conditions potentially allowing terrestrial organisms to replicate; the specific  
868 problematic species that might easily adapt to such extreme environments; the period of  
869 biological exploration of 1000 years already discussed for Europa Clipper; and even a definition  
870 and characterization of "Enhanced Downward Transport zones" at the surface of icy moons that  
871 require special care (Coustenis et al., 2019).

872 In the case of the Europa lander, there is a consensus that planetary protection requirements must  
873 be even more stringent than for Mars. The NASA Europa Lander team, following the previous  
874 requirements defined for Europa Clipper, proposes changes in the entry parameters used to  
875 calculate the probability of contamination of the European surface/subsurface. As examples of  
876 this severity, all species in the bioburden should be included, not just bacterial spores, and the  
877 probability of contaminating a liquid reservoir with less than 1 living organism should be  
878 estimated. To achieve that, new approaches and technologies must be implemented, such as  
879 terminal sterilization systems and lethality modelling including bio-reduction due to spaceflight.

880 In order to comply with these significantly more stringent International Regulations and to meet  
881 the maximum allowed bioburden levels, a strict planetary protection strategy will be set up for  
882 JEM. It will integrate the lessons learnt from the past, current and planned missions to the outer  
883 Solar System, including those regarding the limitation on crash probability for orbiters, the  
884 sterility requirements on landers, penetrators and orbiters that do not meet the non-crash  
885 probability, and an ultra-cleanliness level for all life detection instruments and those which are  
886 not exposed to the sterilising radiation during the spaceflight.

887



888 Radiations:

889 The inner magnetosphere of Jupiter where Europa orbits is the most severe radiation  
890 environment in the Solar System. This presents significant challenges for operating a spacecraft  
891 and its science instruments at Europa. The phases when the mission elements are in orbit around  
892 Europa are by far the most constraining ones in terms of radiation doses. Low-altitudes orbits  
893 around Europa however have a clear advantage in terms of reduced radiation doses when one  
894 takes into account the complex trajectories traced by charged particles in the combined Jovian  
895 and European magnetic fields (Truscott et al., 2011). Figure 19 shows the results of our radiation  
896 analysis for these phases using SPENVIS, the JOSE model, as well as various assumptions  
897 described in the caption. The sensitive parts and electronics will need to be shielded to reduce the  
898 effects of the total ionizing dose (TID), which is equivalent to 50 kRad inside a 22 mm Al  
899 sphere. Table 6 presents the total ionizing doses received during the different phases of the  
900 Europa science mission as a function of the thickness of the aluminium shield. A number of  
901 mitigation measures in subsystems designs, shielding of critical elements, and use of radiation  
902 hardened parts are discussed in sections 3 and 4.3.

903 Europa is within a hard radiation environment, with particle fluxes >20 times larger than at  
904 Ganymede. The instantaneous background flux due to radiation in low-altitude Europa orbits  
905 presents significant challenges for the science instruments but is slightly lower than the JUICE  
906 worst case. The flux is on the order of up to  $10^5$ - $10^6$   $\text{cm}^{-2} \text{sr}^{-1} \text{s}^{-1}$  behind 10-20 mm Al. This  
907 higher background may have a significant impact on the SNR of certain detectors. Sophisticated  
908 background suppression techniques will need to be implemented together with shielding  
909 optimizations in order to ensure maximal science return as discussed in section 3.

910 **4.2. The JEM flight system.**911 *Global architecture.*

912 In its baseline configuration, illustrated in Figure 20, the JEM flight system is composed of two  
913 platforms, possibly augmented by an additional CubeSat element (Gaudin, 2016), not described  
914 in this article:

915 - **A soft lander platform:**



916 Given the heritage and expertise gained from previous studies, this platform, with 26 kg payload  
917 mass class (including a 32% margin) operating 22 days on surface, should most likely be  
918 delivered by NASA with possible contributions of European national agencies at the  
919 investigation level. It will perform investigations in astrobiology, ice characterization and  
920 geophysics (Hand et al. 2017).

921 As an essential component of the JEM concept, we propose that ESA studies and discusses with  
922 NASA the procurement of a small sub-platform, the «Astrobiology Wet Laboratory » (AWL), to  
923 conduct original astrobiology investigations specialising in the analysis of wet samples (see  
924 4.3.3).

925 - **A carrier/orbiter/relay platform:**

926 This platform will fulfil the key functions of injecting the lander stack into an European orbit just  
927 prior to

928 its de-orbitation, and of relaying the lander data to Earth. It will also carry a focused instrument  
929 suite

930 (section 3.1) to perform global high-resolution measurements of the gravity, magnetic field and  
931 topography fields and of the plasma/neutral environment along European orbits.

932 **Optional augmentation:** a mission that is likely to fly beyond 2030 should include a small  
933 platform that could be released from the main orbiter in European orbit to perform focused  
934 scientific measurements. Following an open call to the academic community for cubesat ideas, it  
935 could be selected on the basis of scientific merit, either as a science contribution to one of the  
936 JEM PSO's, or as an opening to a new research theme. One particularly appealing option has  
937 been studied by the authors of this article: using a cubesat for a targeted flyby through a Europa  
938 plume that would have been previously identified during the beginning of the Europa science  
939 orbits (Gaudin et al., 2016).

940 **4.2.1. The JEM Orbiter complement.**

941 **4.2.1.1. The carrier / orbiter / relay platform**

942 The JEM carrier/orbiter platform will serve two objectives: (1) deliver the NASA lander to an  
943 orbit around Europa, and relay its scientific data to Earth; (2) perform global high-resolution  
944 measurements of the gravity, magnetic field and topography fields and of the plasma/neutral  
945 environment. The proposed JEM orbiter concept, presented in Annex II, is inherited from two  
946 platforms currently developed by ESA:

947 1- the European Service Module (ESM) of the Orion Multi-Purpose Crew Vehicle (MPCV), from  
948 which the mechanical and propulsion bus is adapted for JEM. The ESM serves as primary power and  
949 propulsion component of the Orion spacecraft. It presents several advantages for the JEM mission: it can  
950 carry a very heavy payload (the Orion Crew Vehicle is in the 10 tons class), it can be launched on SLS,  
951 and it is developed in a NASA / ESA collaboration framework. Many key systems proposed to be reused  
952 for JEM will be flight-proven at the time of JEM mission adoption.

953 2- the Jupiter Icy Moons Explorer (JUICE) platform, which provides a relevant basis for the  
954 avionics of an interplanetary mission to Jupiter. The JUICE spacecraft, to be launched in May  
955 2022, provides key assets for the other components of the JEM orbiter: a rad-hard avionics  
956 adapted to the specific constraints of an interplanetary mission and protected within a lead-  
957 shielded vault, and a power subsystem designed for LILT (Low Intensity Low Temperature)  
958 conditions.

959 Figure 21 shows the general configuration of the carrier/orbiter and its interface with the lander  
960 stack, before deployment (left) and just after lander stack release (right).

#### 961 **4.2.2. The JEM Lander complement.**

##### 962 **4.2.2.1. The Soft Lander platform.**

963 For the purpose of this work we assumed that the soft lander platform will be delivered by  
964 NASA and benefit from the heritage of several previous studies of its concept. Figure 22 shows  
965 its architecture in the 2017 SDT report (Hand et al., 2017), a concept still under review. The soft  
966 lander will be the final element of the “lander stack” which also includes a propulsion stage and  
967 a sky crane following a concept similar to the Mars Science Laboratory sky-crane. A gimbaled  
968 high gain antenna, co-aligned with the panoramic camera and mounted on the same articulated  
969 mast, will be used for the communications with the carrier-orbiter. The lander will be equipped,  
970 in addition to the payload, with a robotic arm with collection tools.

971 In line with the JEM science plan, we propose the functional structure presented in figure 23 for  
972 the surface science platform carried by this soft lander. The analysis of samples of  
973 astrobiological interest will be performed by two complementary sample analysis facilities, one  
974 devoted to the analysis of solid samples, and another one dealing with liquid samples. The  
975 interest in the wet chemistry measurements is testified by the recent selection in the ICEE-2  
976 program for instrument development of two technologies incorporating microfluidic systems  
977 (MICA: Microfluidic Icy world Chemistry Analyzer ; MOAB: Microfluidic Organic Analyzer  
978 for Biosignatures). The two facilities will be served by a common articulated arm shown in  
979 figure 22. In addition to astrobiology investigations, the lander will also operate a geophysics  
980 station for the study of the planetary fields, the sounding of the sub-surface and the study of the  
981 properties of the surface ice.

982 We propose that the liquid sample analysis facility, called AWL for Astrobiology Wet  
983 Laboratory, be developed by ESA with sensor provided by its member states.

#### 984 4.2.2.2. The Astrobiology Wet Laboratory (AWL)

985 We envisage two accommodation options for the AWL: on the lander (AWL/L), or deployable  
986 as a separate element at the surface (AWL/S). The latter option requires that the arm holds the  
987 instrument and deposits it on the surface. The reason for selecting one of other option could be  
988 based on the arm design constrains but also on the biochemical cleanliness conditions. AWL  
989 detects large organics molecules (proteins, lipids, etc.) and to avoid false positives the level of  
990 biochemical cleanliness of the arm solid sampler should be stricter than if it only supplies  
991 samples to an organic analyser or a vibrational spectrometer. If the AWL works at the surface it  
992 has its own sampler; if it is inside the lander it only has a module to liquefy the sample. From an  
993 engineering point of view, it is more efficient to have the AWL inside the lander. The AWL  
994 could also host the magnetometer with a small increase of mass (deployment boom, sensor head  
995 and electronic) and if it is on the lander it could also include the thermogravimeter. In this case,  
996 the ESA contribution is a totally independent package, with clear interfaces with the lander.

997 **AWL/S description:** the block diagram of the Astrobiology Wet Laboratory (AWL) is shown in  
998 Figure 24. In the AWL/S option it is composed of: i) a Sample Acquisition Module in charge of  
999 making a 10 cm hole to take a liquid sample, ii) the Data Processing Unit which controls the

1000 instrumentation and the communication with the lander; iii) a Power Unit composed by the  
1001 batteries and circuit to regulate the power and distribute it to the other units; iv) a  
1002 Communication Unit to establish the connections with the lander via an umbilical cable. An  
1003 external structure support allows one to deploy the AWL with the lander manipulator. For the  
1004 Sample Acquisition Module (SAM), we have evaluated different alternatives for drilling  
1005 (Ulamec 2007, Biele 2011, Weiss 2011, Sakurai 2016), taking into account the limitations on  
1006 resources and trying to reduce as much as possible the use of any mechanism. The most  
1007 promising option is the use of a drilling system based on laser. Sakurai (2016) has demonstrated  
1008 the capabilities of this concept. Some of the characteristics of SAM are summarized in Table 7:

1009 Figure 25 shows a sketch of the concept proposed. The water sample is taken in two steps: i) the  
1010 first 5 cm of ice (degraded by the radiation) are sublimated by the laser and ii) the tube is moved  
1011 down by a pneumatic actuator and once in contact penetrates by 5 cm in the ice. The tube is  
1012 pressurized and heated to provide conditions in which the water is stable. At this moment the  
1013 sample is sucked by a syringe (controlled by a spring) to fill the sample deposit. From this  
1014 deposit the instruments are filled. A single pressurized deposit (nitrogen TBC) is used for tube  
1015 movement and pressurization. The most critical components of the AWL/S are the batteries.  
1016 They are the heaviest element and need to be controlled above a determined temperature to  
1017 maintain their performances. For radiation protection, the Warm and Shielding Box has a  
1018 thickness of 18 mm Al to allow the use of space standard components. Figure 26 shows the  
1019 AWL mechanical configuration. A warm and shielding box (WSB) is used to maintain the  
1020 operational temperature and protect all the electronics for radiation. The WSB will guarantee by  
1021 design bio-cleanliness after integration. The SAM will have an isolation lid that will be closed  
1022 once at the end of the integration to maintain biological cleanliness. An opening protected with  
1023 an EPA filter will help the decompression during launch. The external structure supports the  
1024 magnetometer boom and allows hanging to the lander articulated arm.

1025 This configuration allows ejection from the lander if for some scientific reason it was  
1026 recommended to explore some site far from it. The AWL side could be equipped with small  
1027 airbags following a similar concept implemented in the Pathfinder lander. A set of petals could  
1028 guarantee its vertical orientation.

1029 **AWL/L description:** The main difference with the AWL/S is the SAM, which in this case is  
1030 reduced to a module to liquefy the sample and has no batteries, making the Power Unit much  
1031 simpler. The process for obtaining the liquid sample is similar to the one proposed for the  
1032 AWL/S.

#### 1033 **4.2.3. Exploring the potential of the Square Kilometre Array for enhanced data downlink** 1034 **capabilities.**

1035

1036 The Square Kilometre Array (SKA)<sup>1</sup> is an international project aiming to eventual construction  
1037 of the radio telescope with the collecting area of the order of one square kilometer. Its physical  
1038 construction is to start in 2021 in two locations, in Western Australia and South Africa, with the  
1039 full operational deployment well before the realistic launch date of the mission described in this  
1040 paper. The SKA part located in South Africa, the so-called SKA-Mid, will cover the standard  
1041 deep space communications radio bands at 2.3 and, importantly, 8.4 GHz, the latter being one of  
1042 the main operational data downlink bands for the JEM mission. The SKA1-Mid, the first  
1043 implementation part of the complete SKA project, is presented in detail in Annex IV.

1044

1045 The SKA's high sensitivity warranted by its unprecedented collecting area has been considered  
1046 as an important asset for potential deep space communication applications early in the SKA  
1047 project development stage (e.g., Bij de Vaate et al. 2004, Fridman et al. 2010). The use of SKA1-  
1048 Mid for deep space communication has also been considered during the detail design phase  
1049 (Schutte 2016). A preliminary discussion between the JEM proposing team and the SKA  
1050 Organization has identified a significant mutual interest in using the SKA to enhance the data  
1051 downlink capability of JEM for short periods during each of the three generic science sequences:  
1052 (Sequence B) SKA will be able to increase the data volume returned to Earth from the carrier-  
1053 orbiter by about an order of magnitude; (Sequence A) SKA might be able to receive data directly  
1054 from the lander or from the JEM cubesat, without a relay by the orbiter; (Sequence C) finally,  
1055 SKA could directly receive data from the orbiter during the critical descent science phase, thus  
1056 solving the platform pointing conflicts between the high-gain antenna and the INMS instrument.  
1057 An in-depth investigation of engineering and operational issues of the SKA use as a JEM science

---

<sup>1</sup> <https://www.skatelescope.org>, accessed 2020.03.23.

1058 data reception station will be addressed at the appropriate phases of the JEM project. Some  
1059 preliminary engineering considerations are given in Annex IV. As it becomes clear from the  
1060 estimates presented there, SKA-Mid could increase deep space telemetry rates by more than an  
1061 order of magnitude for short communication sessions.

## 1062 **5. Proposed international collaboration schemes:**

1063 We propose the following share of responsibilities between ESA and NASA, to be discussed by  
1064 the two agencies: (1) The two baseline platforms would be operated by NASA with the support  
1065 of ESA; (2) NASA would build and operate the lander platform and study with ESA the  
1066 possibility of deploying from that platform a small ESA-provided « Astrobiology Wet  
1067 Laboratory (AWL)» as an option; (3) ESA would take a major responsibility in the delivery of  
1068 the carrier/orbiter/relay platform, ranging from the delivery of the full platform to the delivery of  
1069 an integrated « science investigation platform » and of critical subsystems; (4) The proposed  
1070 selection of scientific investigations on the different flight elements would be validated by ESA  
1071 for the carrier/orbiter and by NASA for the lander and will likely include contributions from the  
1072 two corresponding scientific communities. ESA would support the developments required to  
1073 reach TRL6 during the study phase for the AWL, the MPAS and the MPP sensors. ESA would  
1074 initiate early in the project the planetary protection plan and its implementation.

## 1075 **6. Summary and conclusions**

1076 In this article we described the design of an exciting planetary mission to search for bio-  
1077 signatures at Jupiter's ocean moon Europa and characterize it as a potential habitat. We started  
1078 from a more general question: what are the evolutionary properties of a habitable moon and of its  
1079 host circumplanetary system which make the development of life possible. By choosing the  
1080 Jupiter system as our destination, we can build on the advanced understanding of this system  
1081 which the missions preceding JEM, Juno, JUICE and Europa Clipper will provide. We propose  
1082 the following **overarching goals** for the JEM mission: **Understand Europa as a complex**  
1083 **system responding to Jupiter system forcing, characterise the habitability of its potential**  
1084 **biosphere, and search for life at its surface and in its sub-surface and exosphere.** These  
1085 goals can be addressed by a combination of five Priority Scientific Objectives providing detailed

1086 constraints on the science payloads, on the platforms that will carry them and on the mission  
1087 architecture.

1088 Scientific observations will be made during three sequences: 1- on a high-latitude, low-latitude  
1089 European orbit providing a global mapping of planetary fields (magnetic and gravity) and of the  
1090 neutral and charged environment; 2- in-situ measurements at the surface, using a soft lander  
1091 focusing on the search for bio-signatures at the surface and sub-surface using analytical  
1092 techniques in the solid and liquid phases, and a surface geophysical station; 3- measurements of  
1093 the very low exosphere in search for biomolecules originating from the surface or sub-surface  
1094 during the final descent phase.

1095 These observations will be done by two science platforms: a soft Europa lander and an orbiter. In  
1096 this concept, the carrier/orbiter will carry the lander stack from Earth to a European orbit from  
1097 which it will release the lander. It will then provide the data relay during the lander operations  
1098 and perform science operations during the relay phase on a halo orbit of the Europa-Jupiter  
1099 system, before moving to its final European science orbit for three months.

1100 Our orbiter payload includes seven well-proven instruments to characterize planetary fields and  
1101 the plasma, neutrals and dust environment. To efficiently address the radiation issue, we propose  
1102 to decouple the sensor heads from the other parts of the electronics and to group these parts in a  
1103 dedicated vault or a well-shielded location within the platform. Appropriate planetary protection  
1104 measures corresponding to at least Planetary Protection Category IVb will be applied to all  
1105 subsystems, including the payload and the spacecraft element.

1106 Our lander science platform is composed of a geophysical station and of two complementary  
1107 astrobiology facilities carrying biosignature characterization experiments operating respectively  
1108 in the solid and in the liquid phases. The development of the liquid phase laboratory, called  
1109 AWL for “Astrobiology Wet Laboratory”, could be a specific European contribution. The two  
1110 astrobiology facilities will be fed by a common articulating arm operating at the platform level  
1111 that will collect the samples at the surface or sub-surface. We are proposing two alternative  
1112 options for the deployment of AWL: inside the main platform, where it would benefit from all its  
1113 infrastructure and services, or outside of it as an independent sub-platform, to be deployed with  
1114 the help of the articulated arm.

1115 Given their investments and experience in the space exploration of the Jupiter system, NASA  
1116 and ESA are in the best position to collaborate on the implementation of JEM. To make JEM an



1117 affordable and appealing joint exploration venture for the two agencies, we propose an  
1118 innovative distribution of roles; ESA would design and provide the carrier-orbiter-relay platform  
1119 while NASA would provide an SLS launcher, the lander stack and most of the mission  
1120 operations. We showed in this article that this delivery is technically possible using a safe  
1121 technical approach, taking advantage of a double heritage of European developments for space  
1122 exploration: the Juice spacecraft for the JEM orbiter avionics, and an adaptation of the ORION  
1123 ESM bus for its structure. Following this approach, we believe JEM will be a very appealing  
1124 joint venture of NASA and ESA, working together towards one of the most exciting scientific  
1125 endeavours of the 21st century: search for life beyond our own planet.

1126

1127 Acknowledgements: The authors received support from the sponsors of their home institutions  
1128 during the development of their projects, particularly at the two institutes leading this effort: at  
1129 IRAP, Toulouse, MB and NA acknowledge the support of CNRS, University Toulouse III – Paul  
1130 Sabatier and CNES. At CAB, Madrid, OPB and JGE acknowledge the support of INTA and  
1131 Spanish MINECO project ESP2014-55811-C2-1-P and ESP2017-89053-C2-1-P and the AEI  
1132 project MDM-2017-0737 Unidad de Excelencia “María de Maeztu.”. We would also like to  
1133 extend special thanks to the PASO of CNES for its precious assistance and expertise in the  
1134 design of the mission scenario.

1135



1136 **ANNEX I: Summarized traceability matrix for JEM / OVERARCHING GOAL:**  
1137 **Understand Europa as a complex system responding to Jupiter system forcing,**  
1138 **characterize the habitability of its potential biosphere, and search for life at its surface.**

1139

#### 1140 **ANNEX II: JEM orbiter system design**

1141 The main design drivers of the carrier/orbiter are:

- 1142 - to accommodate a 2,8 tons lander stack, to sustain the lander during cruise and to eject it with the
- 1143 highest accuracy and reliability,
- 1144 - to accommodate a very large tank capacity to provide the required delta V (~ 3 km/s) for a ~13
- 1145 tons composite,
- 1146 - to accommodate large appendages (large solar generator to cope with low solar flux and high
- 1147 radiation degradation, high gain antenna, instruments boom to support the orbiter's instruments
- 1148 suite),
- 1149 - to maintain spacecraft resources and reliability in a very harsh environment (high radiation in
- 1150 European orbit, very cold temperature at Jupiter),
- 1151 - to provide a sound mechanical interface with the Space Launch System (SLS).

1152 The projected mass budget and ISP of the carrier and lander stack are shown in Table A2.1.

1153 Delta and propellant budget. The launch and transfer strategy (NASA design) features a large  
1154 Deep Space Maneuver (DSM) and an Earth Gravity Assist to reach Jupiter. This so-called  
1155 DVEGA scenario was also used by Juno. The SLS performance (Block 1 version) for this  
1156 scenario is 13,3 tons. The delta V budget during the Jupiter Tour (Table A2.2) is taken from the  
1157 JPL design known as the "12-L1" Tour ("Jovian tour design for orbiter and lander missions to  
1158 Europa", Campagnola et al, 2014). The total delta V budget amounts to 3050 m/s. Assuming an  
1159 orbiter dry mass of 2500 kg and a lander stack of 2800 kg, the propellant budget reaches 7900  
1160 kg. The composite wet mass (13,2 tons) is compatible with the launcher capability. The  
1161 maximum dry mass requirement put on the JEM orbiter is therefore 2500 kg, including 20%  
1162 system margin. Note that an additional gravity assist at Earth would allow to reduce the DSM  
1163 intensity, and provide very significant additional mass margin at the cost of one additional year  
1164 of transfer.

1165 As an alternative to the SLS, use of a Falcon Heavy launcher would significantly reduce the  
1166 mission cost, though likely at the expense of an additional Earth gravity assist: we did not study  
1167 this option in detail but it should be kept in mind.

1168 The delta budget is consistent with the JPL mission profile (DV-EGA transfer, 12-L1 Jupiter  
1169 Tour). The propellant budget fits within the Orion ESM capability (8600 kg) with margin. Based  
1170 on these key figures, it has been possible to perform a rough study of the JEM orbiter. Figure  
1171 A2.1 shows its baseline configuration, stacked and deployed.

1172 Radiation design: The radiation system design is a compromise between shielding mass and rad-  
1173 hard electronics development. The radiation analysis results in a TID of 50 kraal inside a 22 mm  
1174 Al sphere. This 50 kraal value is the design target considered for JUICE, and it is proposed to be  
1175 considered also for JEM to maximize the reuse of the JUICE electronics. Assuming a compact  
1176  $0,5 \text{ m}^3$  vault (half the JUICE volume), the 22 mm equivalent Al leads to 188 kg of lead shielding  
1177 (4.5 mm of lead thickness, assuming 15% of shielding efficiency thanks to use of a high Z  
1178 material).

1179 Power sizing: Power generation in LILT conditions ( $50\text{W}/\text{m}^2$ - $130^\circ\text{C}$ ) and under the very harsh  
1180 radiation environment at Europa is a challenge. Displacement damage is produced in the solar  
1181 cells under electrons and protons irradiation, significantly reducing the EOL power. To reduce  
1182 cost, mass and complexity, the JUICE solar generator ( $85 \text{ m}^2$ ) is downsized for JEM to  $78 \text{ m}^2$  (4  
1183 panels of the 5-panel JUICE wings are kept). The same design approach as currently used on  
1184 JUICE is proposed for JEM, with a  $300 \mu\text{m}$  thick cover glass protecting the solar cells.  
1185 Extrapolating the JUICE solar generator's performance on the JEM mission profile demonstrates  
1186 that a  $78 \text{ m}^2$  solar generator will provide around 650 W end of life. This value is used as power  
1187 requirement for JEM orbiter design.

1188 Mechanical, propulsion and thermal control: The Orion ESM mechanical bus is reused and  
1189 adapted for JEM. The primary structure is a cylindrical shape of 4 m in diameter and 3 m in  
1190 height, made of aluminum-lithium alloy. All equipment specific to the Orion mission (e.g. life  
1191 support systems) are removed from the central box to free space for the Lander Stack, that is  
1192 accommodated on the top face of the orbiter (as the Orion Crew Vehicle), with the Solid Rocket  
1193 Motor (SRM) fitted inside the inner rectangular cylinder. Guided rails are added within the inner  
1194 box to ease and secure the lander's ejection. The mechanical interface between the orbiter and  
1195 the lander is made with a skirt mounted on the SRM tank. A planetary protection back shell

1196 covers the entire lander stack to keep it clean. The lower part of the inner cylinder accommodates  
1197 the 0,5 m<sup>3</sup> lead-shielded electronics vault. The JEM bi-propellant propulsion system makes the  
1198 maximum reuse of the ESM design. The 27 kN main engine is removed, and only the 4 nominal  
1199 490 N (Aerojet R-4D) are kept. These 4 main engines provide a 2 kN thrust used in the nominal  
1200 case for the large Jupiter and Europa Insertion Manoeuvres (JOI, EOI). The Reaction Control  
1201 System (RCS) is downgraded, replacing the 220 N engines by 22 N thrusters (MOOG DST-12,  
1202 used on JUICE). 4 pods of 3 x 22 N thrusters provide attitude control during main engines boost  
1203 and a safe back-up in case of one 490 N failure. Two upper pods of 4 x 22 N provide attitude  
1204 control around Z. The 4 large propellant tanks (with a maximum capacity of 8600 kg of  
1205 propellant, compatible with JEM needs of 7900 kg) and the 2 pressurant tanks are kept. The  
1206 Orion ESM thermal control system (designed to reject 5 kW of heat) is considerably simplified  
1207 and downsized for a fully passive control system, using a network of surface heat pipes to  
1208 transport the heat to the radiators. The same MLI blankets (with external conductive layer) are  
1209 used as for JUICE, to ensure a clean EMC environment for the orbiter's plasma package.

1210 Power system: A two-wing 78 m<sup>2</sup> solar generator provides the required 650 W EOL power. The  
1211 JUICE PCDU is reused to condition the electrical power on a regulated 28 V bus. A 167 Ah  
1212 battery (JUICE battery downscaled to 3 modules) supplies the spacecraft during the 3 hours  
1213 eclipses in European orbit, and complements the solar generator in high power phases such as  
1214 insertion manoeuvres. The PCDU also provides the electronics of the Solar Array Drive  
1215 Mechanism (SADM), to optimize radiation shielding.

1216 Avionics: The JUICE avionics is reused for the JEM orbiter. The central computer, the science  
1217 mass memory and the Remote Interface Unit (RIU) are packaged into a single unit to improve  
1218 shielding efficiency. Attitude control is based on a gyro-stellar estimation filter, reaction wheels  
1219 for fine pointing (high gain antenna, laser altimeter) and RCS thrusters. The X-band  
1220 communication system is reused from JUICE and based on a Deep Space Transponder, a 2,5m  
1221 high gain antenna, and two low gain antennas for communication in LEOP and emergency TC  
1222 link at Jupiter. Two UHF antennas (reused from Mars Express) are used for lander TM recovery.

1223 Relay Operations: The concept of operations is driven on one side by the configuration of the  
1224 antennas and on the other side by the mission needs. The HGA (High Gain Antenna) is located  
1225 below the spacecraft and the large beam width UHF antenna is located on a lateral face of the  
1226 spacecraft. This ensures that there is, for any orbit around Europa and out of Jupiter eclipses, a

1227 significant section of the orbit where pointing HGA towards Earth is compatible with having  
1228 UHF antenna in visibility of the lander. The HGA allows a data rate towards earth of more than  
1229 15 kbps for a mission need that is below 150 Mb per day. Thus only a small fraction of the relay  
1230 orbit requires pointing of HGA towards Earth.

1231 Design for payload:

1232 A 5m magnetometer boom is used to provide a clean magnetic environment to the MAG sensors.  
1233 The possibility to accommodate the JUICE recurrent 10.6m MAG boom will be investigated in  
1234 Phase A. All design measures taken on JUICE to ensure the best EMC cleanliness performances  
1235 are reused for JEM: the electronics vault provides an efficient Faraday cage to contain E-field  
1236 radiation from electronics, a distributed single grounding point is implemented within the PCDU  
1237 to avoid common mode perturbation, external surfaces (solar generator, MLI) are covered with  
1238 an outer conductive coating to avoid charging, a magnetic shield is implemented on the most  
1239 perturbing units (reaction wheels, motor drives). Two monitoring cameras will provide pictures  
1240 of the lander's ejection. The overall resources allocation for the JEM orbiter is 50 kg and 100 W.  
1241 The launch mass budget fits within the SLS capability and includes a 20% system margin on the  
1242 carrier's dry mass.

1243

1244

1245 **ANNEX III: Orbitography for the JEM mission**

1246 Once the Carrier has released the Lander, it must act as a relay for the total duration of the  
 1247 Lander mission. Choosing a halo orbit around the Jupiter-Europa L1 Lagrangian point (JEL1)  
 1248 provides a great coverage of the landing site. The unstable nature of those orbits allows low-  
 1249 energy transfers, while the cost of orbit maintenance is very low.

1250 Halo orbits are families of unstable periodic orbits in the 3-body problem around collinear  
 1251 Lagrangian points [*Dynamical Systems, the Three-Body Problem ad Space Mission Design*  
 1252 (*Koon et al., 2006*)]. The choice of a specific halo orbit among its family is subject to a few  
 1253 constraints:

- 1254● The position of the landing site
- 1255● The science expected to be accomplished
- 1256● The  $\Delta V$  needed to reach and to leave this orbit
- 1257● The time of flight to reach and to leave this orbit.

1258 The variation of the radiation dose is negligible regarding the choice of a specific halo orbit.

1259 Because of the symmetry of the 3-body problem, the landing site is assumed to be on the  
 1260 northern hemisphere of Europa, and the halo orbits are chosen in the southern class for this  
 1261 study. The results would be the same with a landing site on the southern hemisphere and with  
 1262 northern halo orbits. In order to investigate the Europa-magnetosphere interaction, a halo orbit  
 1263 near Europa is preferred.

1264 Once a specific halo orbit is chosen, the transfer from this halo orbit to a low-altitude, near polar,  
 1265 circular orbit around Europa (LEO) is studied. The characteristics selected for this orbit are an  
 1266 inclination between  $80^\circ$  and  $90^\circ$ , and an altitude between 100m and 200km [*Europa Study 2012*  
 1267 (*NASA*)]. First, at each position on the halo orbit, a small burn (few m/s) in the unstable direction  
 1268 toward Europa is performed.

1269 Then, when one of those trajectories features an extremum of distance to Europa, the osculating  
 1270 orbital elements are calculated to see if they match the requirement of the LEO. A tangent burn  
 1271 to circularize around Europa is then applied. A set of halo orbits [*Global search for planar and*  
 1272 *three-dimensional periodic orbits near* (*Russell, 2006*)] labelled with ID's (Figure A3.1 and  
 1273 Table A3.1) was investigated in order to highlight the range of possibilities for a transfer from a  
 1274 halo orbit to a LEO. Figure A3.4 shows a subset of these couples of halo and transfer orbits.

1275 The results (Figures A3.2 and A3.3) indicate a  $\Delta V$  between 440m/s and 540 m/s, for a duration  
1276 of 1-7 days. Some halo orbits have more possibilities of transfer than others. Some of them don't  
1277 have any possibilities of transfer (ID = 275). The closer to Europa the halo orbit is, the higher the  
1278  $\Delta V$  is. If we take a look at the range of possibilities of LEO's for each halo orbit, choosing a  
1279 more specific LEO could limit the possibilities even more. Characteristics of some of the  
1280 reachable LEO orbits are shown in Table A3.2, and characteristics of the corresponding transfer  
1281 orbits in Table A3.3.

1282 If a specific LEO is necessary, one solution would be to pick the transfer to a LEO close to the  
1283 desired LEO, and then perform a change of altitude and a change of inclination. A change of  
1284 altitude from 200km to 100km is 40m/s while a change of inclination of  $10^\circ$  is 240m/s (which is  
1285 not negligible). However, we can expand the possibilities of transfer using a non-negligible burn  
1286 to leave the halo orbit. To limit the degree of freedom of this problem, a simple tangent burn is  
1287 used [*Connecting halo orbits to science orbit at planetary moons (Bokelmann and Russell,*  
1288 *2017)*].

1289 The number of possibilities is largely expanded. Even if the  $\Delta V$  tends to be higher, a transfer  
1290 with less than 530 m/s and a reasonable time of flight can always be found (less than 3 days).  
1291 Even more, the spectrum of reachable LEO is also wide. The last thing to be done is to select the  
1292 transfer best suited for the mission.

1293  
1294

#### 1295 **ANNEX IV: Square Kilometre Array as a data downlink reception station for JEM**

1296 This annex gives a preliminary overview of the potential capabilities of the advanced radio  
1297 astronomy facility, the Square Kilometre Array (SKA), and in particular its first  
1298 implementation phase for medium-range frequencies, SKA1-Mid as an Earth-based receiving  
1299 station for the JEM science data downlink. The primary mission of SKA is the advancement of  
1300 radio astronomy. However, exploratory discussions on a potential use of some fraction of the  
1301 SKA observing time enhancing science output of planetary missions are underway too. Basic  
1302 parameters of the SKA1-mid used in the estimates presented below are taken from the SKA  
1303 Info Sheets<sup>2</sup> and references therein.

---

<sup>2</sup> <https://www.skatelescope.org/technical/info-sheets/>, accessed 2020.03.23.

<sup>3</sup> <https://www.sarao.ac.za/media-releases/meerkat-joins-the-ranks-of-the-worlds-great-scientific-instruments-through-its-first-light-image/>, accessed 2020.03.25.

1304

**A4.1 Description of SKA1-Mid**

1306

1307 The SKA1-Mid instrument will be an array of 197 offset Gregorian dishes and associated  
1308 signal processing equipment (figure 4.1). The dishes will provide a total collecting area of  
1309 32,700 m<sup>2</sup>. Of these, 64 dishes have been constructed as part of the MeerKAT precursor  
1310 telescope, while an additional 133 dishes will be constructed for SKA1. MeerKAT is already  
1311 operational and early scientific results include the discovery of more than 1200 new galaxies in  
1312 its First Light image<sup>3</sup> and the highest resolution images yet of our galactic center<sup>4</sup>.

1313 SKA1-Mid will re-use much of the existing MeerKAT infrastructure, including the shielded  
1314 subterranean Karoo Array Processor Building and the electrical power system. SKA1-Mid is  
1315 being designed for 24/7 operation and an overall time efficiency greater than 0.9. Several  
1316 critical systems (power supply, core power distribution, processor cooling, etc.) are redundant.  
1317 The full SKA1-mid array will consist of a circular dense core and three spiral arms extending  
1318 to a distance of approximately 90 km from the core (figure 4.2). The instrument will be located  
1319 near Carnarvon in the Karoo region of South Africa, approximately centered on the following  
1320 coordinates: 30°42'46.37"S, 21°26'35.50"E.

1321 SKA1-Mid will cover the frequency range 0.35–13.8 GHz in 5 bands. The cryogenically  
1322 cooled Band 5 receivers of SKA1-mid will cover the frequency range from 4.6 to 13.8 GHz,  
1323 and will therefore include the X-band telemetry allocation around 8.4 GHz.

1324 The SKA1-Mid construction roll-out will progress through several array releases, with all  
1325 dishes (and MeerKAT) integrated and commissioned by 2027. It is likely that a series of  
1326 expansions and upgrades will be implemented following 2027, as part of the future SKA2  
1327 project.

1328

**A4.2 Summary of SKA1-Mid potential for the support to deep space missions**

1330

1331 The sensitivity of SKA1-Mid in terms of the ratio G/T (where G is the telescope gain and T is  
1332 the system noise temperature) will be about 25 times that of a generic modern X-band 35 m

---

<sup>4</sup> <https://www.sarao.ac.za/south-africas-meerkat-discovers-giant-radio-bubbles-at-centre-of-milky-way/>,  
accessed 2020.03.25.



1333 Earth-based deep space data reception station. This leads to three transformational capabilities  
 1334 for deep space missions. In particular,

1335 • SKA1-mid will be able to increase the data rate of science data downlink delivered to Earth  
 1336 comparing to the currently operational deep space communication assets.

1337 • SKA1-mid will be able to receive data directly from small descent and landing probes or from a  
 1338 mini-satellites (e.g., a JEM cubesat), without a relay spacecraft.

1339 • SKA1-mid could directly receive data from a mission spacecraft during critical phases of high  
 1340 scientific interest, like a descent to a planetary surface, radio occultation, etc.

1341 In many cases, the SKA1-mid facility will be the only instrument on Earth capable of providing  
 1342 these capabilities, and could therefore be an important resource for future deep space  
 1343 exploration.

1344 In order to evaluate the capacity of SKA1-mid for data reception, a model link budget has been  
 1345 analyzed under the following assumptions:

1346 • Spacecraft transmitter Power: 50 W

1347 • Onboard HGA gain: 44.8 dB

1348 • Pointing loss: 0.1 dB

1349 In the X-band, the SKA1-mid Band 5 receiver figure of merit (G/T) has been conservatively  
 1350 estimated as 67.22 dB. Assuming the following link parameters:

1351

1352 • Link margin: 3 dB;

1353 • Bit error rate (BER):  $10^{-5}$ ;

1354 • Ratio of the energy per transmitted bit,  $E_b$ , to the spectral noise density,  $N_0$ ,  
 1355  $E_b/N_0 = 0.3$ ;

1356 • Modulation: QPSK;

1357 • Forward error correction: turbo code with the code rate 0.25;

1358 • The distance between the spacecraft and Earth:  $8 \times 10^8$  km.

1359 These parameters result in the over-the-air data rate of 1.6 Mbps when using SKA1-mid as  
 1360 reception station, and up to 2.3 Mbps under ideal conditions. This calculation should be  
 1361 considered an initial estimation, and further study is required. The major underlying  
 1362 assumption is that 60% of the collecting area of the SKA1-mid array can be used for reception,  
 1363 due to the difficulty in correcting phase errors of the outer spiral arm dishes. Thus, a



1364 conservative working assumption is that dishes up to a radius of approximately 1.3 km (i.e.  
1365 most of the core) can be successfully phased up.

1366 For radio telescopes it is customary to express their instantaneous sensitivity performance in  
1367 terms of effective collecting area over system temperature ( $A_e/T_{\text{sys}}$ ). This parameter for SKA1-  
1368 mid at 8.4 GHz is  $A_e/T_{\text{sys}} = 890 \text{ m}^2/\text{K}$ . At a radius of 1.3 km, the total available sensitivity is  
1369 reduced to 60% of the total, giving  $A_e/T_{\text{sys}} = 534 \text{ m}^2/\text{K}$ .

1370

1371

Journal Pre-proof

1372 **BIBLIOGRAPHY**

- 1373 Baross, J.A. and S. E. Hoffman (1985). *Origins of Life and Evolution of the Biosphere* 15(4):  
1374 327-345.
- 1375 Bills, B., Ray, R. (2000). *J. Geophys. Res.*, 105 (E12), p. 29277-29282
- 1376 Biele J. et al. (2011). *Adv. Space Res.*48, 755-763
- 1377 Bij de Vaate J.G. et al. (2004), '*Spacecraft Tracking Applications of the Square Kilometre*  
1378 *Array*', 3rd International Workshop on Tracking, Telemetry and Command Systems for Space  
1379 Applications, TTC 2004, 93–100 (<https://arxiv.org/abs/2002.10024>)
- 1380 Bird M.K., Allison M., Asmar S.W., Atkinson D.H., Avruch I.M., Dutta-Roy R., Dzierma Y.,  
1381 Edenhofer P., Folkner W.M., Gurvits L.I., Johnston D.V., Plettemeier D., Pogrebenko S.V.,  
1382 Preston R.A., Tyler G.L., 2005, *Nature* 438, 800-802
- 1383 Blöcker A., J. Saur, and L. Roth (2016), *J. Geophys. Res.*., 121, doi: 10.1002/ 2016JA022479.
- 1384 Bocanegra Bahamón T.M., Molera Calvés G., Gurvits L.I., Duev D.A., Pogrebenko S.V., Cimò G., Dirx  
1385 D., and Rosenblatt P., 2018, *AA* 609, A59
- 1386 Bocanegra Bahamón T.M., Molera Calvés G., Gurvits L.I., Cimò G., Dirx D., Duev D.A., Pogrebenko  
1387 S.V., Rosenblatt P., Limaye S., Cui L., Li P., Kondo T., Sekido M, Mikhailov A.G., Kharinov M.A.,  
1388 Ipatov A.V., Wang W., Zheng W., Ma M., Lovell J.E.J., and McCallum J.N. 2019, *A&A*, 624, A59
- 1389 Bokelmann, K.A., Russell, R.P.: Halo orbit to science orbit captures at planetary moons. *Acta Astron.*  
1390 **134**, 141–151 (2017). <https://doi.org/10.1016/j.actaastro.2017.01.035>
- 1391 Brown M.E. and Hand K.P. (2013). *Astronomical J.* 145, 110
- 1392 Campagnola,S., Buffington,B. B., Petropoulos, A.E. (2014). *Acta Astronautica*, 100, 68-81
- 1393 Carlson R.W. et al. (1999). *Science* 286, 97-99
- 1394 Carlson et al., (2005). *Icarus* 177, 461-471

- 1395 Cassen, P., et al. (1979). *Geophys. Res. Lett.* 6(9): 731-734.
- 1396 Chen, E. M. A. et al. (2014). *Icarus*, Volume 229, p. 11-30
- 1397 Cooper, J. F., et al. (2009). *Planet Space Sci.*, Volume 57, Issue 13, p. 1607-1620
- 1398 Cooper J.F. et al. (2001). *Icarus* 149, 133-159
- 1399 Coustenis et al. (2019). The COSPAR Panel on Planetary Protection Role, Structure and  
1400 Activities. *Space Research Today* 205, 14-26
- 1401 Dalton et al., (2005). *Icarus* 177, 472-490
- 1402 Dalton, J. B. et al. (2010). EGU General Assembly Conference Abstracts.
- 1403 Dirx D., Gurvits L.I., Lainey V., Lari G., Milani A., Cimò G., Bocanegra-Bahamon T.M.,  
1404 Visser P.N.A.M., 2017, PSS 147, 14–27
- 1405 Dirx D., Lainey V., Gurvits L.I., Visser P.N.A.M. 2016, PSS 134, 82-95
- 1406 Dirx D., Prochazka I., Bauer S., Visser P.N.A.M., Noomen R., Gurvits L.I., Vermeersen L.L.A.  
1407 2018, *Journal of Geodesy*, p. 1-16
- 1408 Duev D.A., Molera Calvés G., Pogrebenko S.V., Gurvits L.I., Cimò G., Bocanegra Bahamon  
1409 T.M., 2012, *A&A* 541, A43
- 1410 Duev D.A., Pogrebenko S.V., Cimò G., Molera Calvés G., Bocanegra Bahamón T.M., Gurvits  
1411 L.I., Kettenis M.M., Kania J., Tudose V., Rosenblatt P., Marty J.-C., Lainey V., de Vicente P.,  
1412 Quick J., Nicola M., Neidhardt A., Kronschnabl G., Ploetz G., Haas R., Lindquist M., Orlatti A.,  
1413 Ipatov A.V., Kharinov M.A., Mikhailov A.G., Lovell J.E.J., McCallum J.N., Stevens J., Gulyaev  
1414 S.A., Natush T., Weston S., Wang W.H., Xia B., Yang W.J., Hao L.F., Kallunki J., and Witasse  
1415 O. 2016, *A&A* 593, A34
- 1416 Fridman P.A., Gurvits L.I., Pogrebenko S.V. (2010) *The SKA as a Direct-to-Earth Data*  
1417 *Acquisition Facility for Deep Space Science Missions*, in *Wide Field Science and Technology*  
1418 *for the Square Kilometre Array*, eds. S.A. Torchinsky, A. van Ardenne, T. van den Brink, A.J.J.  
1419 van Es, A.J. Faulkner, ISBN 978-90-805434-5-4, p. 43-50 [PoS(SKADS 2009)006]

- 1420 Gaudin, D., ISAE master study report, 2016.
- 1421 Hand K.P. et al. (2007). *Astrobiology* 7, 1006-1022
- 1422 Hand K. P. and Chyba, C.F. (2007) Empirical constraints on the salinity of the European ocean  
1423 and implications for a thin ice shell, *Icarus* 189, 424–438.
- 1424 Hand K.P., Murray, A. E., Garvin, J. B., Brinckerhoff, W. B., Christner, B.C., Edgett, K.S.,  
1425 Ehlmann, B.L., German, C.R., Hayes, A.G., Hoehler, T.M., Horst, S.M., Lunine, J.I., Nealson,  
1426 K.H., Paranicas, C., Schmidt, B.E., Smith, D.E., Rhoden, A.R., Russell, M.J., Templeton, A.S.,  
1427 Willis, P.A., Yingst, R.A., Phillips, C.B., Cable, M.L., Craft, K.L., Hofmann, A.E., Nordheim,  
1428 T.A., Pappalardo, R.P., and the Project Engineering Team (2017): Report of the Europa Lander  
1429 Science Definition Team.  
1430
- 1431 Hanley, J., et al. (2014). *J. Geophys. Res.-Planets* 119(11): 2370-2377.
- 1432 Hussmann, H., Spohn, T. (2004). *Icarus*, 171, 391-410
- 1433 Hussmann, H., et al. (2010). *Space Sci. Rev.* 153 (1-4): 317-348.
- 1434 Jia, X., Kivelson, M. G., Khurana, K., Kurth W. S. (2018), Evidence of a plume on Europa from  
1435 Galileo magnetic and plasma wave signatures, *Nature Astronomy*, 2, 459-464.
- 1436 Jimenez-Jorquera C. et al., (2010). *Sensors* 10.
- 1437 Kattenhorn S.A. Prockter L.M. (2014). *Nature Geoscience* 7, 762-767
- 1438 Khurana, K.K., Kivelson M.G., Hand K.P. and Russell, C.T., Electromagnetic induction from  
1439 Europa's ocean and deep interior, in *Europa*, Arizona University Press, 571-586 (2009).
- 1440 Khurana, K. K.; Jia, X.; Kivelson, M. G.; Nimmo, F.; Schubert, G.; Russell, C. T., Evidence of a  
1441 Global magma Ocean in Io's Interior, *Science*, **332**, 1186 (2011).
- 1442 Kiefer et al. (2006). *Science* 314, 1764-1766
- 1443 Koon, W. S., Lo, M. W., Marsden, J. E., & Ross, S. D. (2006). Dynamical systems, the three-body  
1444 problem and space mission design. *California Institute of Technology, Pasadena, CA, USA*.
- 1445 Kounaves, S.P. et al., (2003). *J. Geophys. Res.* 108, 10.1029/2002JE001978
- 1446 Lainey, V., et al. (2006). *Astronomy & Astrophysics*, 456, 783-788.

- 1447 Lammer et al. (2009). *Astros. Astrophys. Rev.* 17: 181-249
- 1448 Lebreton J.-P., Witasse O., Sollazzo C., Blancquaert T., Couzin P., Schipper A.-M., Jones J.B., Matson  
1449 D.L., Gurvits L.I., Atkinson D.H., Kazeminejad B., Pérez-Ayúcar M. 2005, *Nature* 438, 758-764
- 1450 Loeffler and Baragiola, (2005). *Geophys. Res. Lett.* 32, L17202
- 1451 Lunine, J. L. and Atkinson, D. J. (1985). Thermodynamics of clathrate hydrate and low and high  
1452 pressures with application to the outer solar system. *Ap. J. Supplement* 58-3; 493-531
- 1453 McCord et al., (1999). *J. Geophys. Res.-Planets* 104, 11827-11851
- 1454 McCord, T. B., et al. (2001). *J. Geophys. Res.-Planets* 106(E2): 3311-3319.
- 1455 Maize, E. Europa Lander and technology Update. Presentation to the August 2019 OPAG  
1456 Meeting. University of Colorado's Laboratory for Atmospheric and Space Physics (LASP)  
1457 Boulder, CO  
1458
- 1459 Mark D. et al., (2010). "Microfluidic lab-on-a-chip platforms: requirements, characteristics and  
1460 applications." *Chemical Society Reviews* 39.
- 1461 Moore, W., (2003). *J. Geophys. Res.*, 108, Issue E8, pp. 15-1
- 1462 Nimmo, F., et al. (2002). *Geophys. Res. Lett.* 29(7).
- 1463 NRC (Natl. Acad. Sci. Washington, DC). Task Group on the Forward Contamination of Europa,  
1464 Space Studies Board, National Research Council (U.S.) (2000) Preventing the Forward  
1465 Contamination of Europa
- 1466 Ojakangas, G.W., Stevenson D.J., (1986). *Icarus*, 66, 341-358
- 1467 Paganini, L., Villanueva, G. L., Roth, L., Mandell, A. M., Hurford, T., Retherford, K. D.,  
1468 Mumma, M. J. (2019) A measurement of water vapour amid a largely quiescent environment on  
1469 Europa, *Nature Astronomy* 2397-3366, doi.org/10.1038/s41550-019-0933-6
- 1470 Pappalardo R.T., W. B. McKinnon and K. K. Khurana, *Europa*, University of Arizona Press,  
1471 Tucson, (2009).
- 1472 Parro V. et al., (2005). *Planet. Space Sci.* 53, 729-737

- 1473 Parro, V. et al., (2008). *Astrobiology* 8, 987-999
- 1474 Parro, V. et al., (2011). *Astrobiology* 11, 969-996
- 1475 Patterson G.W. et al. (2012). *Icarus*, 220, 286-290
- 1476 Porco C.C. et al (2006). *Science*, 311, 1393-1401
- 1477 Pogrebenko S.V., Gurvits L.I., Campbell R.M., Avruch I.M., Lebreton J.P., van't Klooster  
1478 C.G.M., 2004, in *Planetary Probe Atmospheric Entry and Descent Trajectory Analysis and*  
1479 *Science*, A. Wilson (ed.), ESA SP-544, 197-204
- 1480 Roth L. et al. (2014). *Science* 343, 171-174
- 1481 Russell, M. J. and A. J. Hall (1997). *J. Geol. Soc.* 154: 377-402.
- 1482 Russell, M. J., et al. (2014). *Astrobiology* 14, 308-343.
- 1483 Russell, R.P. (2006) Global search for planar and three-dimensional periodic orbits near europa. *J. Astron.*  
1484 *Sci.* **54**, 199–226. <https://doi.org/10.1007/BF03256483>
- 1485 Sakurai T. et al., (2016). *Cold Regions Science and technology* 121.
- 1486 Schilling, N., et al. (2004). *J. Geophys. Res.-Planets* 109(E5).
- 1487 Schmidt J. et al. (2008). *Nature* 451, 685-688
- 1488 Schutte, A.N., 2016, 'The Square Kilometre Array Radio Telescope: Transformational  
1489 Capabilities for Deep Space Missions', 15<sup>th</sup> Reinventing Space Conference, 27 October 2016,  
1490 London
- 1491 Shematovich V.I. et al. (2005). *Icarus* 173, 480-498
- 1492 Sims M.R. et al., (2012). *Planet. Space Sci.* 72.
- 1493 Tobie, G., et al. (2003). *J. Geophys. Res.-Planets* 108(E11).
- 1494 Tobie, G., et al (2005). *Icarus*, Volume 177, Issue 2, p. 534-549

- 1495 Truscott, P. et al. (2011). IEEE TRANS. NUCL. Sci., 58(6), 2776 – 2784.
- 1496 Tyler R., (2008). Nature, 456, 770-772
- 1497 Ulamec S. et al., (2007). Rev. Environ Sci. Biotechnol. 6
- 1498 Weiss P. et al. (2011). Adv. Space Res. 48
- 1499 Westall, F, Brack, A. (2018) The Importance of Water for Life, Space Science Reviews 214(2). DOI:  
1500 [10.1007/s11214-018-0476-7](https://doi.org/10.1007/s11214-018-0476-7)
- 1501 Wisdom J., (2004). Astronom. J. 128, 484–491.
- 1502 Witasse, O., Altobelli, N., Barabash, S., Bruzzone, L., Dougherty, M., Erd, C., Fletcher, L.,  
1503 Gladstone, R., Grasset, O., Gurvits, L., Hartogh, P., Hussmann, H., Iess, L., Langevin, Y.,  
1504 Palumbo, P., Piccioni, G., Sarri, G., Titov, D., and Wahlund, J.E. 2015, JUICE: A European  
1505 Mission to Jupiter and its Icy Moons, in European Planetary Science Congress, pp. EPSC2015-  
1506 564.
- 1507 Zahnle K. et al. (2008). Icarus 194, 660-674

Table 1: Proposed list of orbiter platform instruments and their contribution to the different Priority Science Objectives (PSO's) presented in section 2.

Orbiter Science Platform - JEM (Orbiter-Carrier) ESA/NASA		
	Facility/Instrument	Reference PSO
<b>Core Payload</b>	Gravity Science Investigation (GSI)	PSO#2, PSO#4
	Magnetometer (MAG)	PSO#1, PSO#3, PSO#4
	Laser Altimeter (LA)	PSO#2, PSO#4
	Ion Mass Spectrometer + Electron Spectrometer (IMS/ELS)	PSO#1, PSO#3, PSO#5
	Ion and Neutral Mass Spectrometer (INMS)	PSO#3, PSO#5
	Dust Analyser (DA)	PSO#1, PSO#3, PSO#5
<b>Augmentation</b>	Langmuir Probe (LP)	PSO#1, PSO#3



Table 2: Projected resource requirements for the different orbiter platform instruments.

Orbital Science Platform projected required resources						
Facility/Instrument	Outside the vault	Inside the vault				
		Mass (kg)	Volume (m <sup>3</sup> )	Total (kg)	Power (W)	TRL
GSI	-	3.4	0.006	3.4	22	5
<u>MAG</u>	<u>0.1</u>	<u>0.1</u>	0.001	<u>0.2</u>	<u>0.4</u>	<u>8/9</u>
LA	11	9	0.08	20	40	5-6
IMS/ELS	7	3	0.006	10	11	5
<u>INMS</u>	3.2	3	0.006	6.2	16	5-6
<u>DA</u>	<u>7.5</u>	<u>2.6</u>	<u>0.003</u>	<u>10.1</u>	<u>9.7</u>	<u>5-6</u>
<u>Total for core payload</u>	28.8	21.1	0.102	49,9	99.1	
<u>Augmentation: LP</u>	<u>1.6</u>	<u>3</u>	<u>0.004</u>	4.6	<u>6</u>	5-6

Table 3: Proposed list of surface science platform instruments and their contribution to the different Priority Science Objectives (PSO's) presented in section 2.

Surface Science Platform - JEM (Lander) NASA	
Facility/Instrument	Reference PSO
<b>1. Solid Sample Analysis</b>	
Organic compound analyzer	PSO#4, PSO#5
Vibrational Spectrometer	
Microscope	
PanCam	
<b>2. Liquid Sample Analysis Astrobiological Wet Laboratory</b>	
Multiprobe Array Sensors (MPAS)	PSO#5
Multiparametric Probes (MPP)	PSO#5
<b>3. Geophysical Science</b>	
Geophone	PSO#2, PSO#4
Magnetometer	PSO#1
Laser reflector	PSO#2

Table 4: Projected resource requirements for the different instruments of the surface science platform.

Surface Science Platform projected required resources			
Facility/Instrument	Mass (kg)	Power (W)	TRL
AWL sensors MPAS	0.15	1.4	3-4
AWL sensors MPP			
AWL sensors VISTA			
	0.1	1	3-4
	0.09	0.24	5-6
Total for AWL (cf. 4.3.3.2)	11 (incl. 7 for shielding)	17.4 Whr	
MAG	0.6	0.8	8/9
Laser Reflector	0.0025	-	-

Table 5: approximate flight time  $\Delta V$  and TID (behind 2,5 mm finite Al slab shell)

Sequence	Sequence name		Flight time	$\Delta V$ (m/s)	TID @ 2.5mm Al
S-1	Launch + cruise	Reach Jupiter System	4,9 years	800	~
S-2	JOI + PRM maneuver	Insert into the Jovian system	6,5 months	1000	~
S-3	Jovian tour to Europa vicinity	Phase the spacecraft with Europa	9,5 months	100	125 krad
S-4	EOI +	Insert into Europa,		700	~

	Ejection to relay orbit	release the lander, reach relay orbit			
S-5	Lander relay	Relay and downlink lander data	35 days	~	370 krad
S-6	Relay to LEO	Reach low-altitude quasi-polar orbit	1-3 days	400 (TBC)	12 krad/day
S-7	LEO operations	Support orbiter science mission	3 months	50	930 krad
S-8	Descent to surface				
S-9	Impact	End of mission			
<u>Total</u>			6,6 years	<u>3,05 km/s</u>	1,5 Mrad

*Table 6: Total Ionizing Dose (TID, in krad) versus Aluminium thickness (in mm) for the relay phase, the transfer to Low-Europa Orbit (LEO), the science orbit as well as the total for these three phases. For the relay and transfer phases, the second column corresponds to the worst case scenario with a radiation design factor of 2; for the LEO the second column corresponds to the case where the reduced radiation environment at low-altitude around Europa is taken into account (factor 3 reduction), and the third column to the worst case scenario with a radiation design factor of 2. The values obtained are very similar to those reported in the 2012 NASA Europa Orbiter report.*

Al absorber thickness (mm)	S5 - Lander relay TID (krad)		S6 - Relay to LEO TID (krad)		S7 - LEO operations TID (krad)			S5 to S7 - Total TID (krad)		
	<i>no margin</i>	<i>margin x2</i>	<i>no margin</i>	<i>margin x2</i>	<i>no margin</i>	<i>Europa shield.</i>	<i>margin x2</i>	<i>no margin</i>	<i>Shield/no marg</i>	<i>margin x2</i>
2,5	369	738	12,3	24,6	930	310	620	1311	691	1382
3	299	598	9,98	20,0	753	251	502	1062	560	1120
4	207	414	6,91	13,8	521	174	347	735	388	775
5	152	304	5,07	10,1	382	127	254	539	284	568
6	117	233	3,89	7,77	293	97,6	195	413	218	436
7	92,61	185	3,09	6,18	233	77,5	155	328	173	346
8	75,6	151	2,52	5,04	190	63,2	126	268	141	283
9	62,9	126	2,10	4,19	158	52,6	105	223	118	235
10	53,2	106	1,77	3,54	133	44,5	88,9	188	99,4	199
11	45,5	91,0	1,52	3,03	114	38,0	76,1	161	85,1	170
12	39,3	78,6	1,31	2,62	98,6	32,9	65,8	139	73,5	147
13	34,2	68,5	1,14	2,28	85,9	28,6	57,2	121	64,0	128
14	30,0	60,0	1,00	2,00	75,3	25,1	50,2	106	56,1	112
15	26,5	53,0	0,88	1,76	66,4	22,1	44,3	93,8	49,5	99,0
16	23,5	46,9	0,78	1,56	58,8	19,6	39,2	83,1	43,9	87,7
17	20,9	41,8	0,70	1,39	52,4	17,5	34,9	74,0	39,1	78,1
18	18,7	37,4	0,62	1,24	46,8	15,6	31,2	66,1	34,9	69,8
19	16,7	33,5	0,56	1,12	42,0	14,0	28,0	59,3	31,3	62,6
20	15,1	30,1	0,50	1,00	37,7	12,6	25,2	53,3	28,1	56,3

22	12,3	24,6	0,41	0,82	30,8	10,3	20,5	43,5	23,0	45,9
25	9,23	18,5	0,31	0,61	23,1	7,70	15,4	32,6	17,2	34,5

Table 7: summarized characteristics of the Sample Analysis Module (SAM)

MAIN TECHNICAL CHARACTERISTICS OF SAM
Drilling activities consumption 10 W for 1 hour.
Additional sample processing 2.5 W for 3 hour.
Data processing & control core consumptions 5W.
Orbiter has the capacity to charge and monitor the battery (req. 85 W.hr)
Battery should be maintained warmed to $T > -20^{\circ}\text{C}$
No redundancy
Standard flight EEE components
Control based on a FPGA running a low frequency
S/W in coded C and small program size < 64 KB
Power conditioning based on COTS converter
Orbiter has the capacity to charge and monitor the battery (req. 145 W.hr including AWL self heating).
Battery configuration 5 series-cell & 5 parallel cells. Total weight < 1.5 kg.

Table A2.1: JEM projected mass budget and ISP.

Carrier dry mass	2 485 kg	
Lander Stack mass	2 800 kg	
ISP	315 s	R-4D 490 N

Table A2.2: JEM deltaV and propellant budget

	Delta V (m/s)	Propellant (kg)	Wet mass (kg)	Comment
<b>Cruise (DSM / EGA)</b>	800	3 002	13 163	4,9 years transfer (DVEGA)
<b>JOI + PRM</b>	1 000	2 809	10 160	840 JOI + 160 PRM
<b>Jupiter Tour</b>	100	234	7 351	Europa 2012 study
<b>EOI</b>	600	1 256	7 117	elliptical orbit 200×7000 km
<b>Ejection to relay</b>	100	187	5 861	allocation
<b>Relay to science</b>	400	349	2 875	200×200 km
<b>Orbit maintenance</b>	50	41	2 526	3 months in orbit
<b>Total</b>	<b>3 050</b>	<b>7 878</b>	<b>13 163</b>	

Table A3.1: Characteristics of the range of the reachable LEO

ID	Inclination (°)		Altitude (km)	
	min	max	min	max
100	82,8	89,8	116	198
150	83,4	89,8	103	200
200	80,2	82,9	104	199
225	88,1	89,7	109	196
250	80,5	87,8	101	199
275	-	-	-	-
284	81,1	88,7	102	185

Table A3.2: Characteristics of some of the reachable LEO

ID	Inclination (°)		Altitude (km)	
	min	max	min	max
100	80,0	89,9	100	190
150	80,2	90,0	102	199
200	80,1	90,0	103	199
225	80,1	89,9	102	199
250	80,0	90,0	101	200
275	80,0	89,9	100	200
284	80,0	90,0	100	200



Table A3.3: Characteristics associated to the set of transfers

	Halo orbit ID	$\Delta V_{\text{total}}$ (m/s)	Duration (days)	Altitude (km)	Inclination (°)
a)	100	488	1,6	118	84,8
b)	150	491	1,2	110	85,5
c)	200	512	1,3	104	82,6
d)	225	539	1,3	108	84,0
e)	250	534	3,7	104	87,6
f)	275	541	2,1	115	82,4
g)	284	551	1,8	119	84,3
h)	284	515	1,2	199	80,8

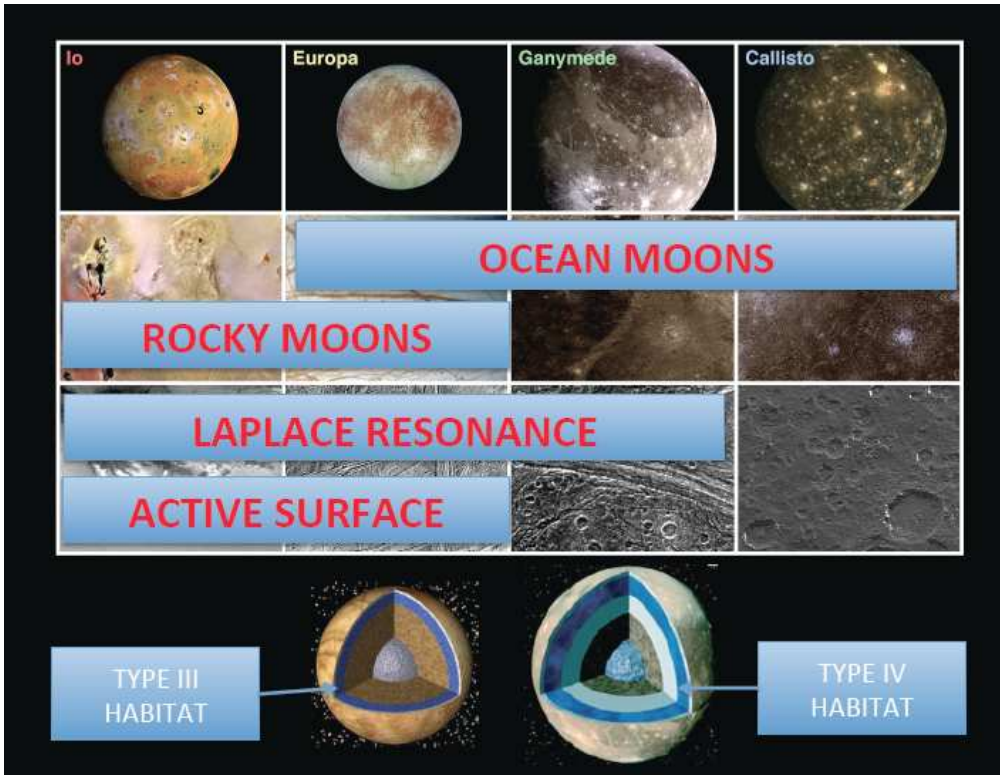


Figure 1: when the four Galilean moons are broadly characterized by the four properties shown, Europa stands out as the best possible candidate "habitable moon" (see text)

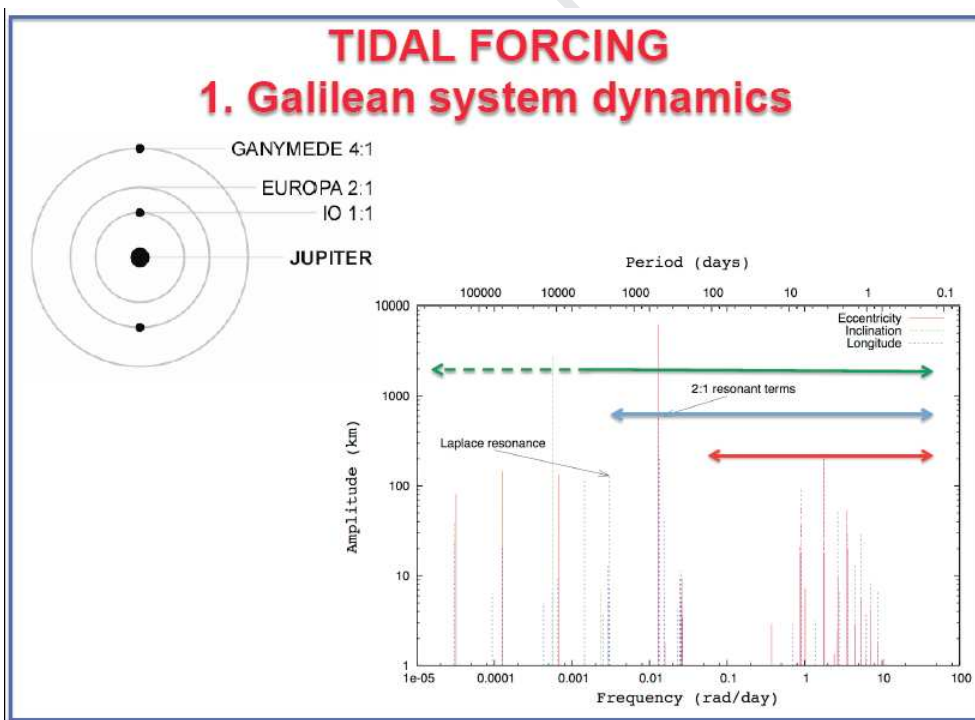


Figure 2: Tidal coupling of Europa to the Jupiter System is controlled by the dynamics of the Galilean system and its Laplace resonance (left). The figure shows the very broad spectrum of gravitational perturbations exerted on Europa's motion in its reference frame. The short periods, to the right, correspond to the orbital motions of the different satellites and their beats, which induce the most important tidal stresses. The long periods to the left correspond to all long-period oscillations of the system, and include the pendular motions in the Laplace resonance. The ranges of periods accessible respectively to JEM alone (red line), to the succession of missions to Jupiter (blue) and to the combinations of long series of astrometric measurements from the ground and from space (green) are also indicated (derived from Layné et al., 2006)

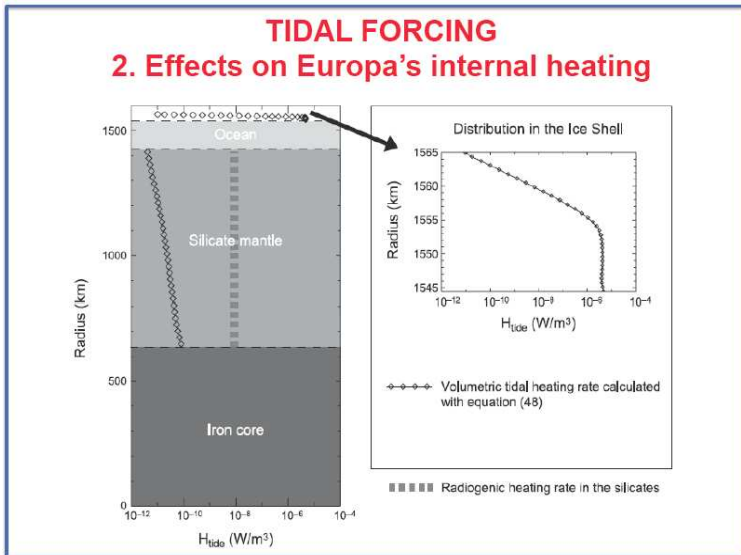


Figure 3: Tidal coupling between Io, Europa, Ganymede and Jupiter is responsible for a continuous transfer of angular momentum and energy between Jupiter and the three moons resulting in continuous heating of their interiors, ice shells, and oceans. The model of Tobie et al. (2003) shown here predicts that most of this heating goes to the ice shell in the case of Europa. Observations from an orbiter will be critical to solve this open question.

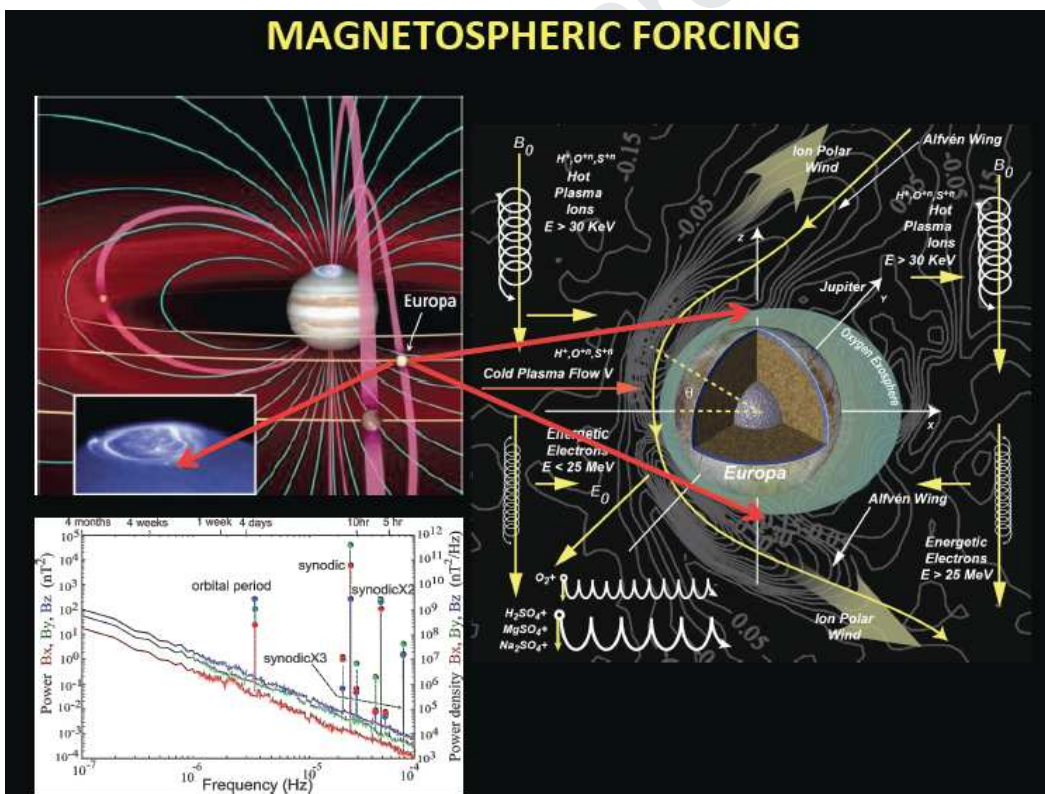


Figure 4: A simplified representation of Europa's interaction with the Jovian magnetosphere, which involves two obstacles: Europa's surface, and its subsurface ocean. This interaction generates effects from the planetary scale (a giant electrical current system coupling Europa's ionosphere to the Jovian ionosphere) to the very local European scales (the space weathering of Europa's icy surface by magnetospheric thermal and radiation belt particles). The broad-band spectrum of magnetic fluctuations associated with this interaction, seen in the European frame, allows an accurate magnetic sounding of Europa's ocean (diagram in white insert, courtesy K. Khurana).

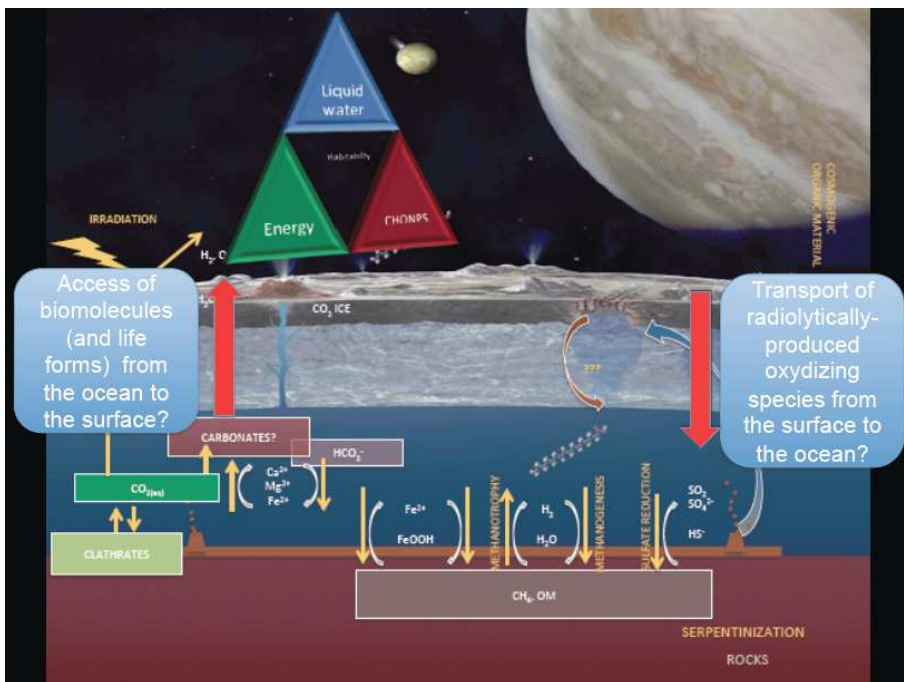


Figure 5: An examination of the properties of the layers of Europa extending from the silicate sea-floor to the ice shell surface and near-surface exosphere in the light of the "triangle of habitability" leads to the important conclusion that this aqueous internal region of Europa may be considered as a potential "dark biosphere" (see text).

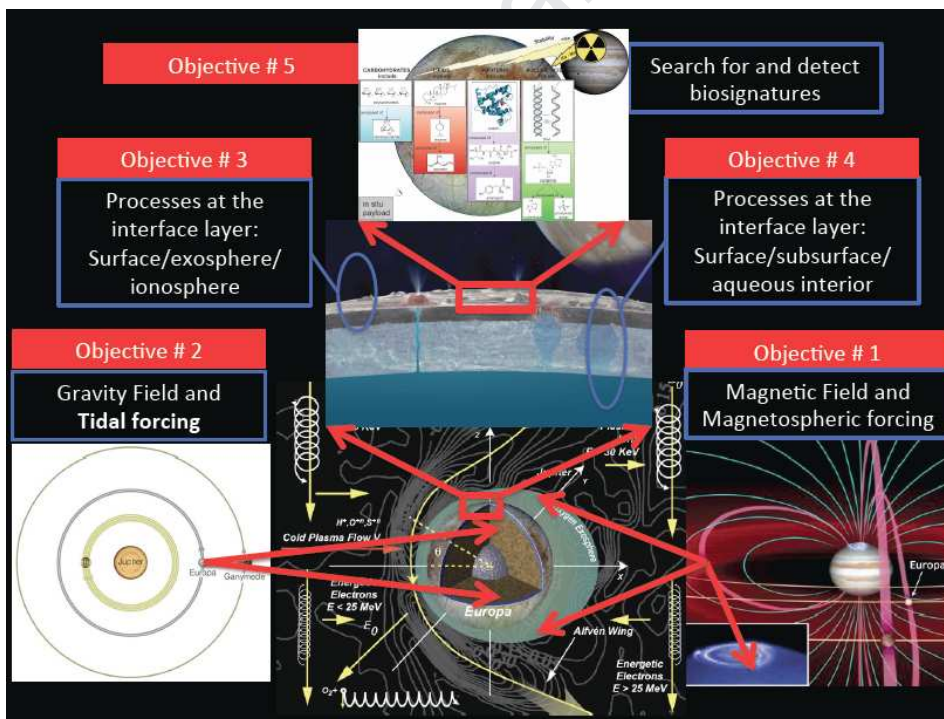




Figure 6: This logical chart of our Science Plan shows the three successive scales investigated by JEM, from bottom upwards: (1) the global Europa, a complex system responding to the two main types of Jovian forcing; (2) the scale of Europa's potential biosphere (median figure) and (3) finally the local scale at which we will perform life detection experiments.

The JEM science plan successively articulates five "Priority Science Objectives", culminating with PSO #5, the search for biosignatures of life at the surface, sub-surface and eventually in the exosphere, to reach its Overarching Goals.

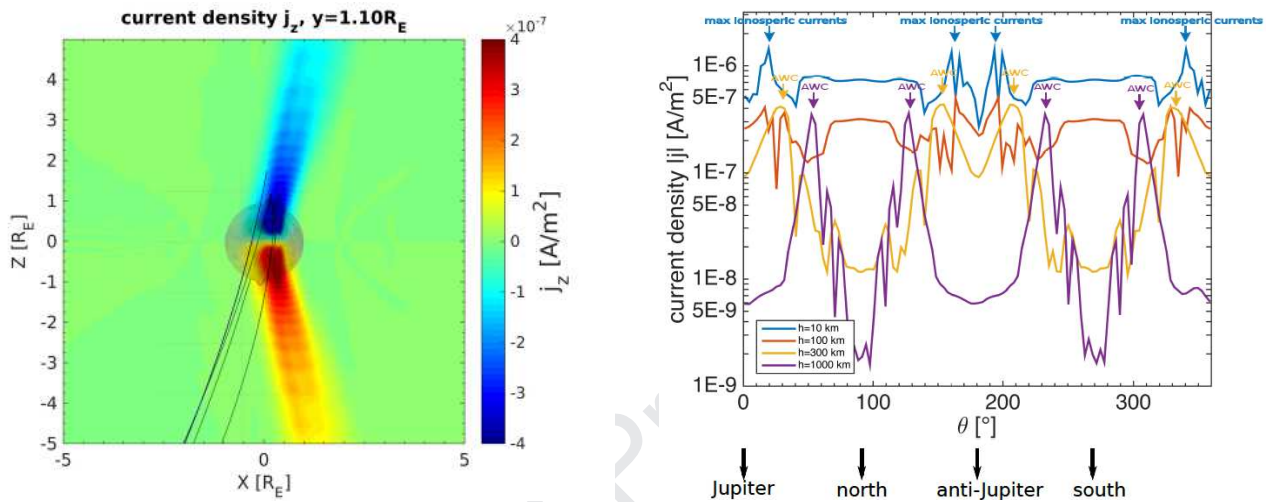


Figure 7: Ionospheric current density (left) in the XZ plane; Ionospheric current density and Alfvén wave currents (AWC) in the northern and southern hemispheres towards and away from Jupiter plotted for various altitudes along circular polar orbits. Adapted from Blöcker et al. (2016).

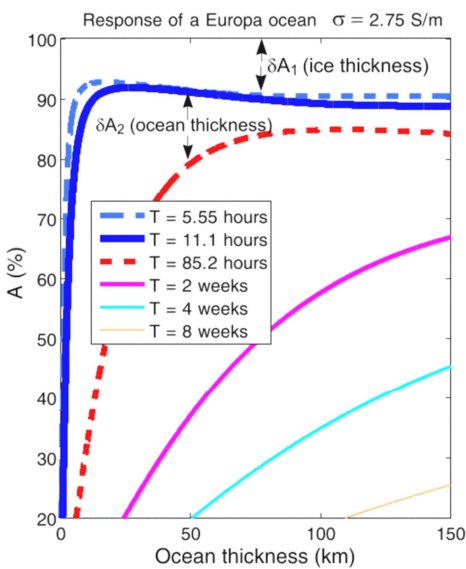


Figure 8: Response (surface induced field at pole/inducing field) of a Europa ocean with conductivity similar to that of the Earth's at six different periods. An ice thickness of 30 km was assumed for results shown in both of these figures. Figure adapted from Khurana et al. (2009)

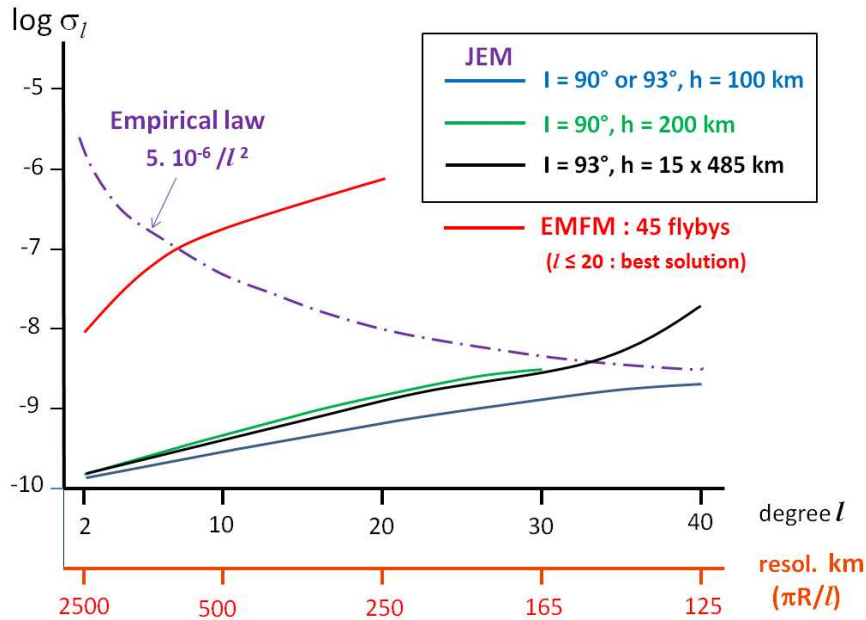


Figure 9: Determination of Europa's gravity field from two possible mission scenarios.

$\sigma_l$  (dimensionless) measures the uncertainty in all harmonic coefficients of degree  $l$ , corresponding to the resolution shown on the second abscissa scale. An empirical law (same shape as for other terrestrial bodies) is shown for comparison.

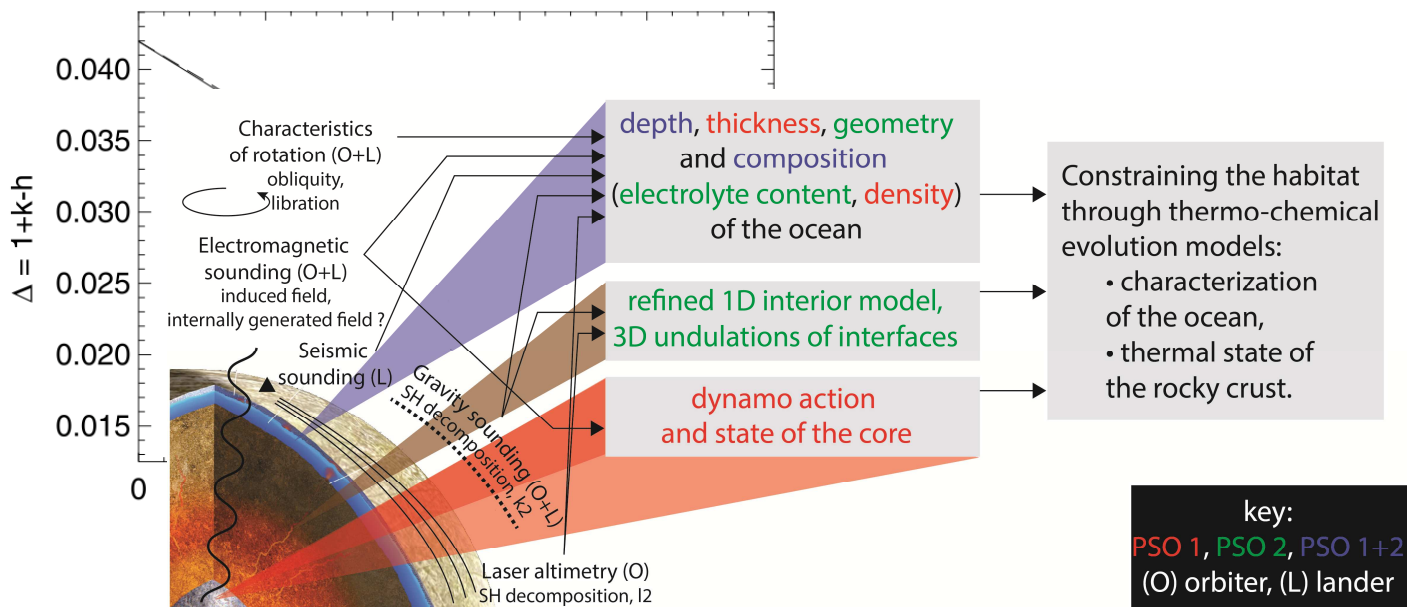


Figure 10: Synergetic orbiter / lander investigation of Europa's response to Jupiter's magnetic and gravitational forcing

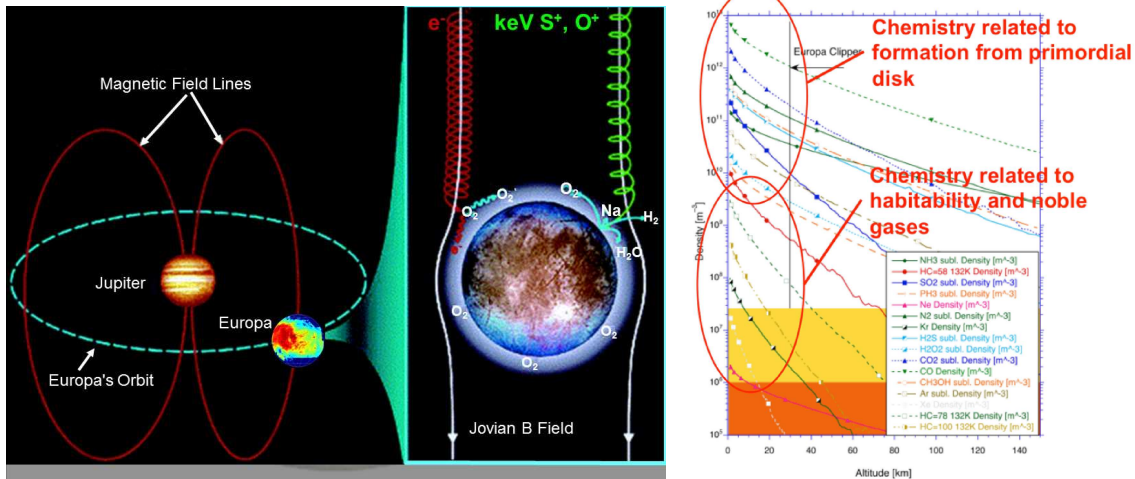


Figure 11: Cartoon of European interaction with Jupiter's magnetosphere showing how the Jovian plasma moving with Jupiter magnetospheric lines induces a trailing/leading asymmetry in the interaction. Neutral species produced by sputtering of Europa's icy surface form Europa's exosphere, which is composed essentially of  $O_2$  and of trace species (left); calculated exospheric density profiles calculated by Shematovich et al. (2005) for species expected to be present based on the formation model (right). "SP" stands for sputtering, and "subl." stands for « released together with sublimation » water. HC are hydrocarbon molecules with the indicated mass

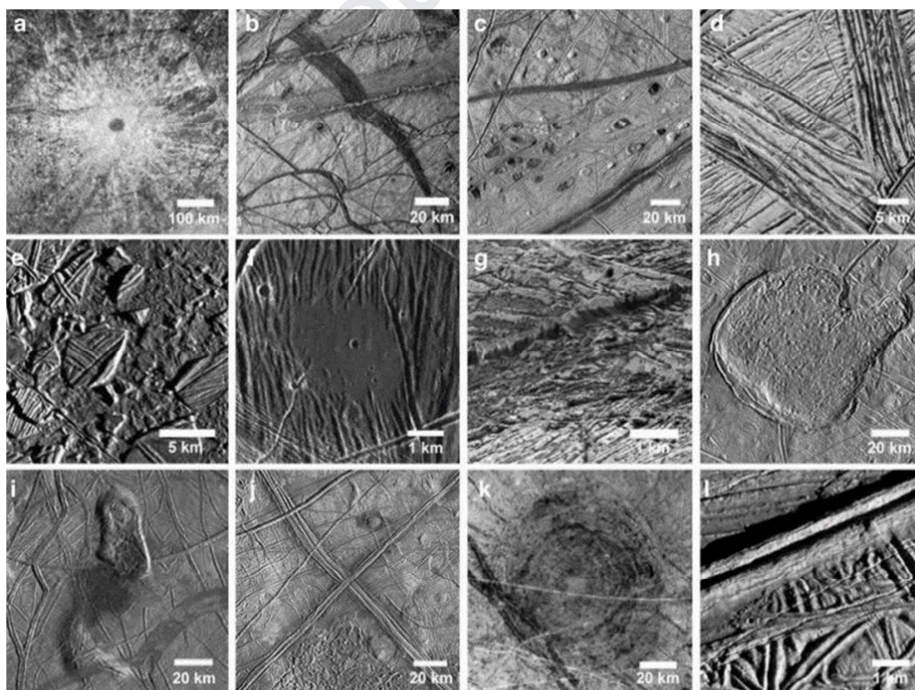


Figure 12: Variety of surface features on Europa: (a) the impact crater Pwyll; (b) pull-apart bands; (c) lenticulae; (d) ridge complexes at high resolution; (e) Conamara Chaos; (f) dark plains material in a



topographic low; (g) very high-resolution image of a cliff, showing evidence of mass wasting; (h) Murias Chaos, a cryovolcanic feature; (i) the Castalia Macula region; (j) double 7 complex ridges; (k) Tyre impact feature; and (l) one of Europa's ubiquitous ridges. (Credit: NASA/JPL/Caltech).

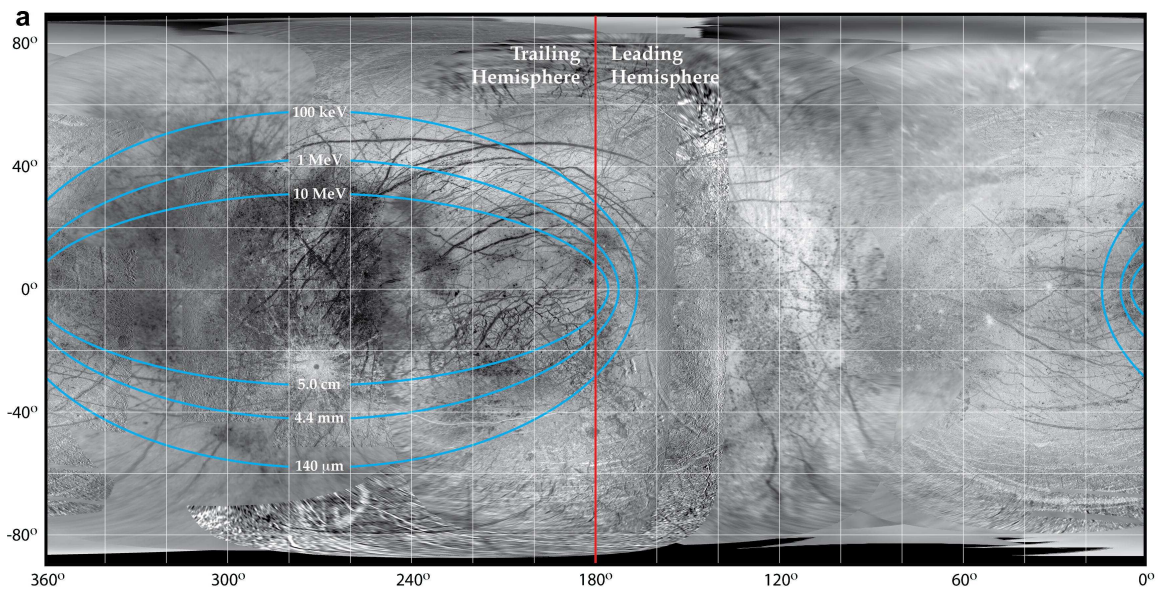


Figure 13: Contour plot of electron bombardment of Europa where energies and penetration depths are indicated from Patterson et al. 2012)

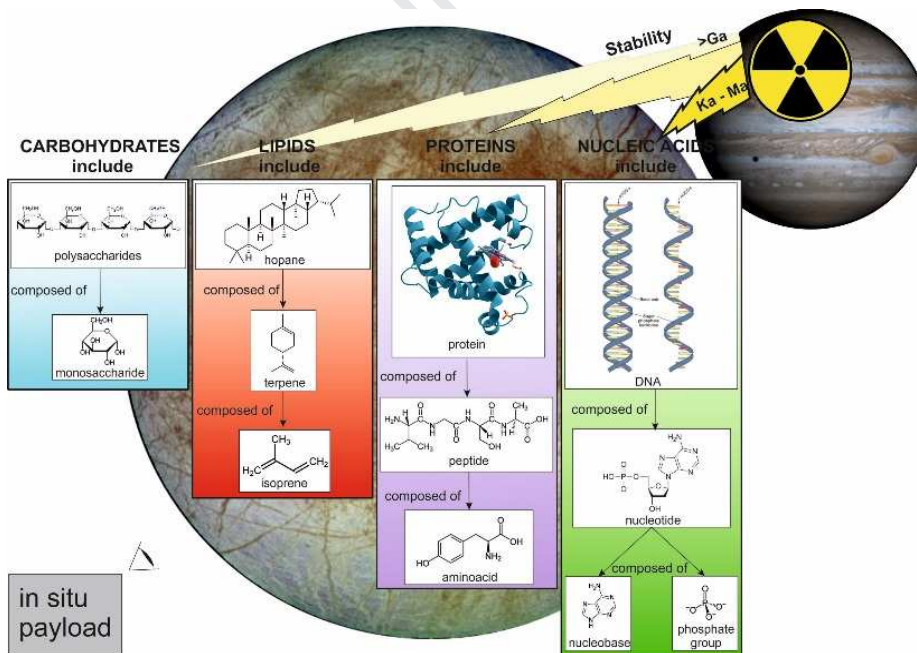


Figure 14: Types of biomolecules, from their monomers to the more complex polymers. Their higher stability under radiation is marked by the lower intensity of the yellow colour of the ray.



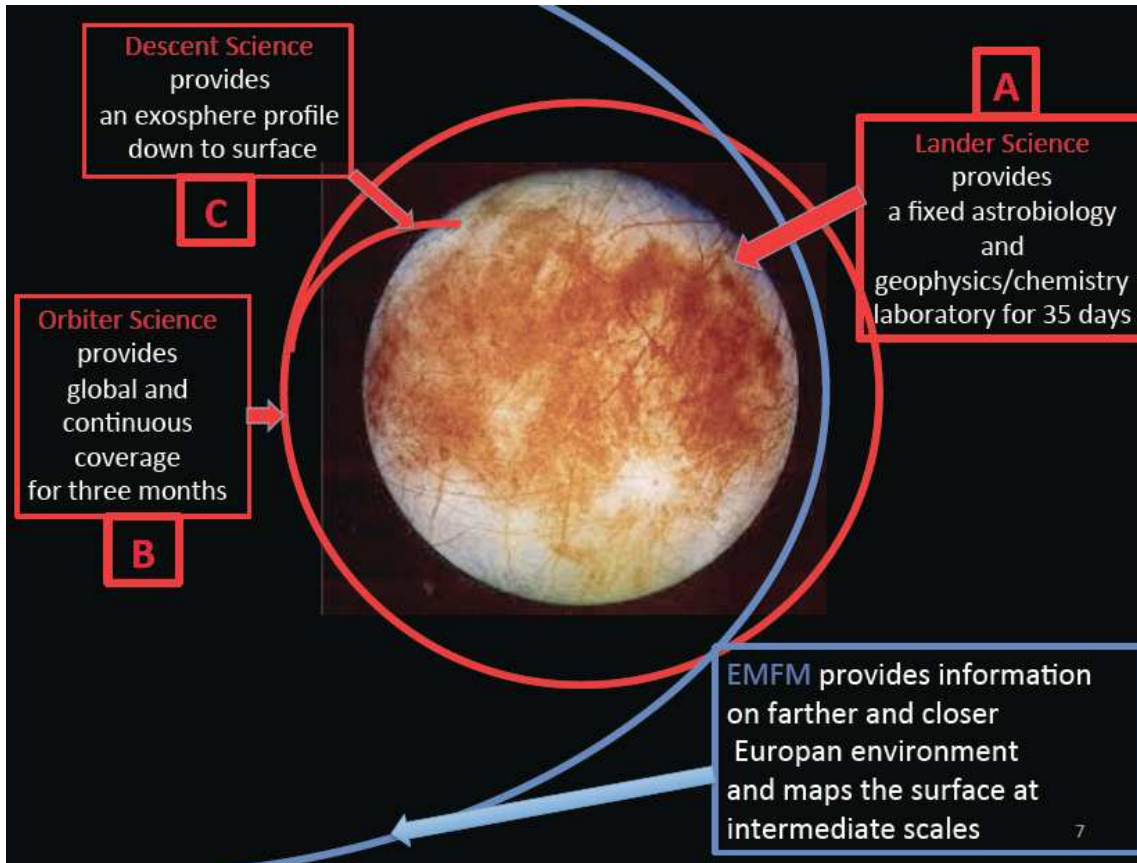


Figure 15: the JEM Observing system, with its two main platforms, will provide three main science sequence, complemented by VLBI astrometry measurements from Earth.

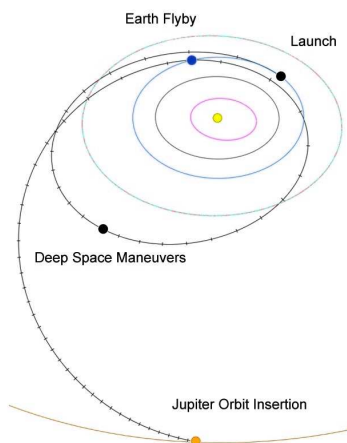


Figure 16: S1 - Interplanetary cruise

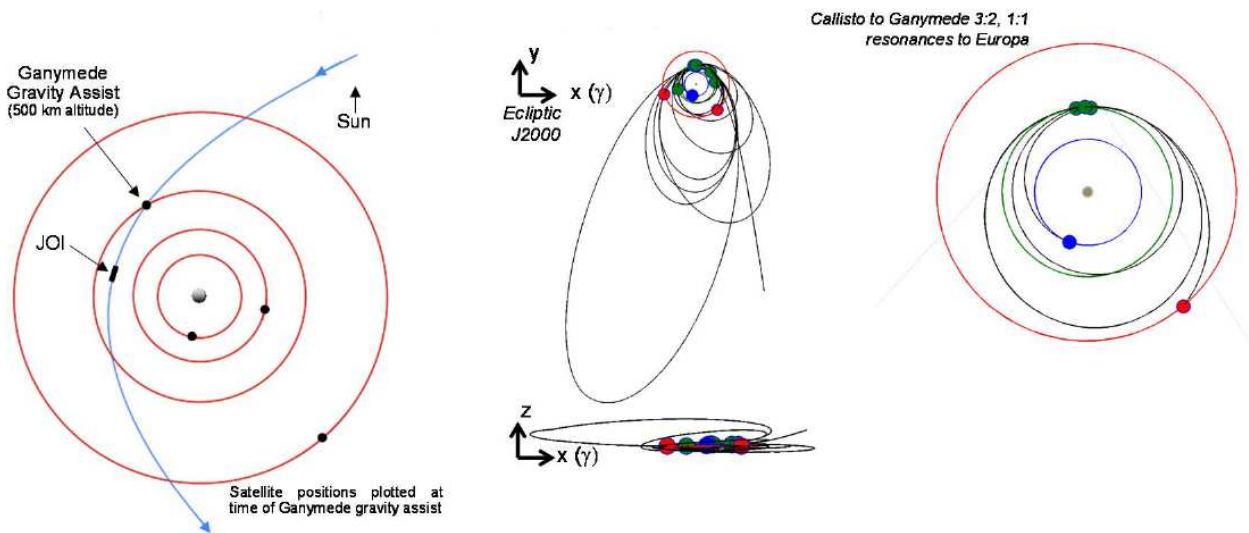


Figure 17: S2 - Jupiter orbit insertion (left) and figure) & S3 - Jovian tour. This tour starts with a series of eccentric orbits whose apoapse and inclination are progressively reduced (center figures, projections in the YX (top) and XZ (bottom) planes, and continues with a set of low-eccentricity orbits in the equatorial plane to progressively approach Europa (blue spot), using its mean motion resonance with Callisto (red spot).

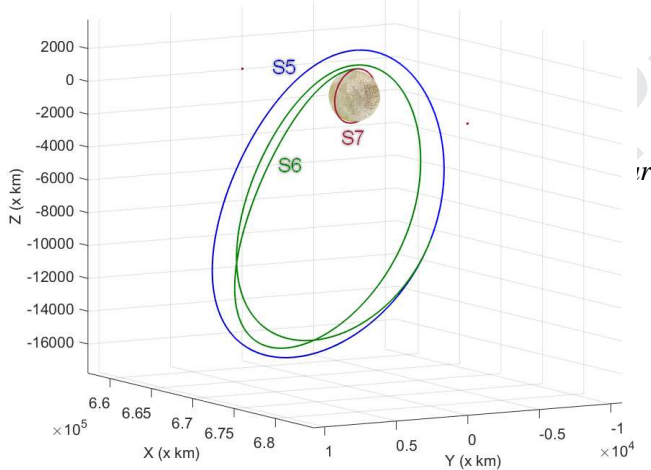


Figure 18: configuration of the Europa science orbits: halo orbit about the L1 Lagrangian point (blue, S5); transfer to Low Europa Orbit (green, S6) and finally low quasi-polar Europa orbit (red, S7).

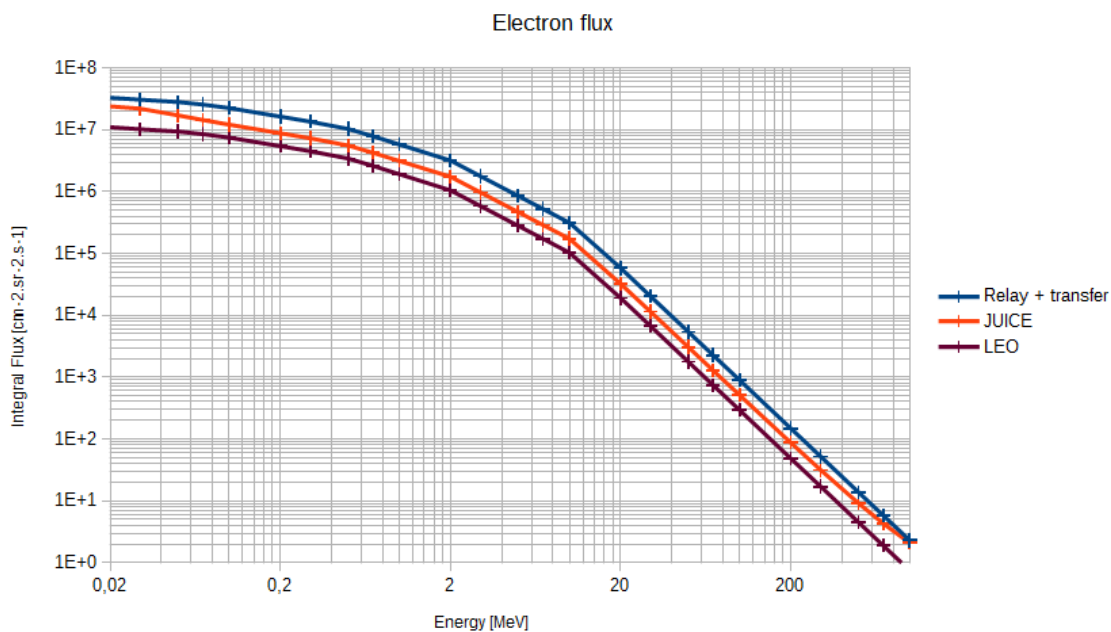


Figure 19: Integral electron flux vs. energy from SPENVIS, displayed for various phases of the JEM and compared to JUICE worst-case.

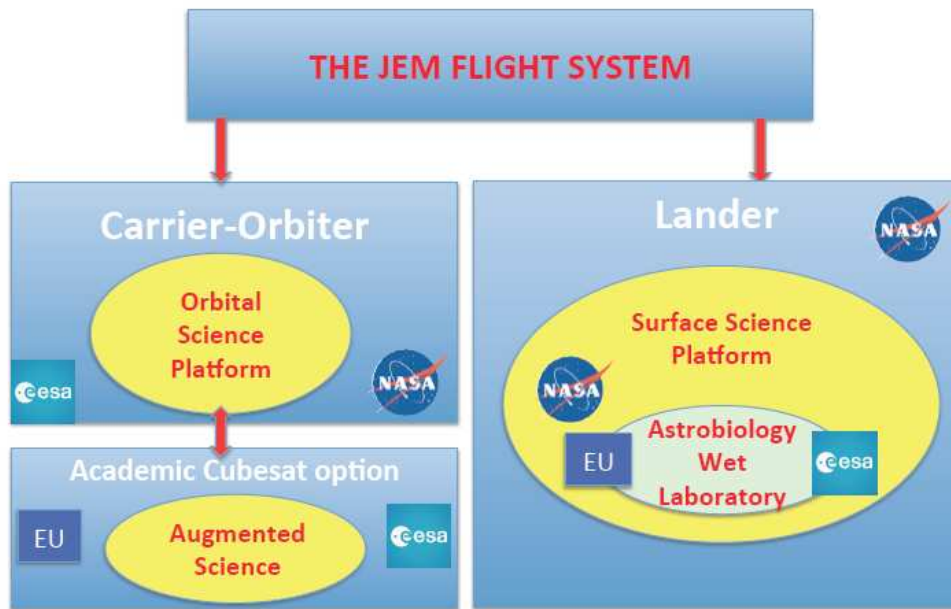


Figure 20: Overall architecture of the proposed JEM flight system, with its different flight elements.

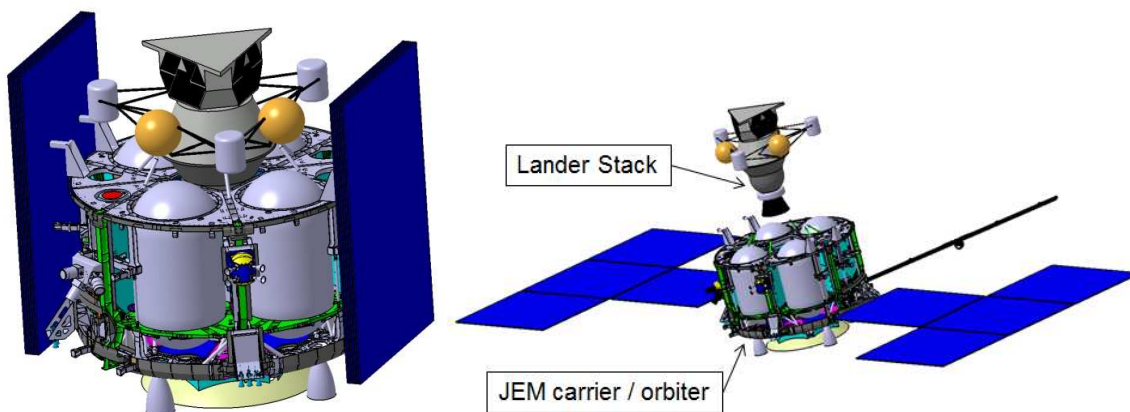


Figure 21: JEM carrier and lander interface

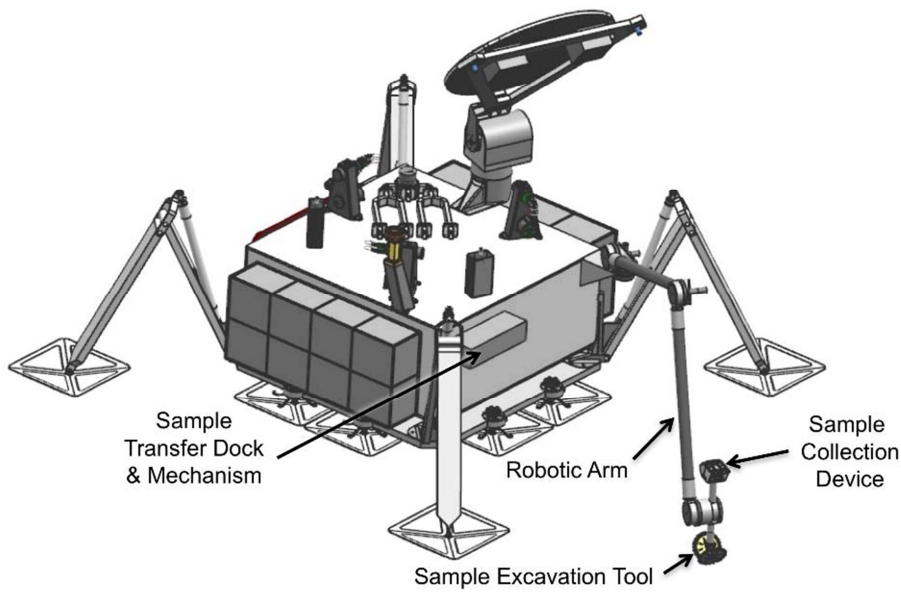


Figure 22: The NASA Europa lander concept presented in the Europa Lander Science Definition Team report (K. Hand et al., 2017).

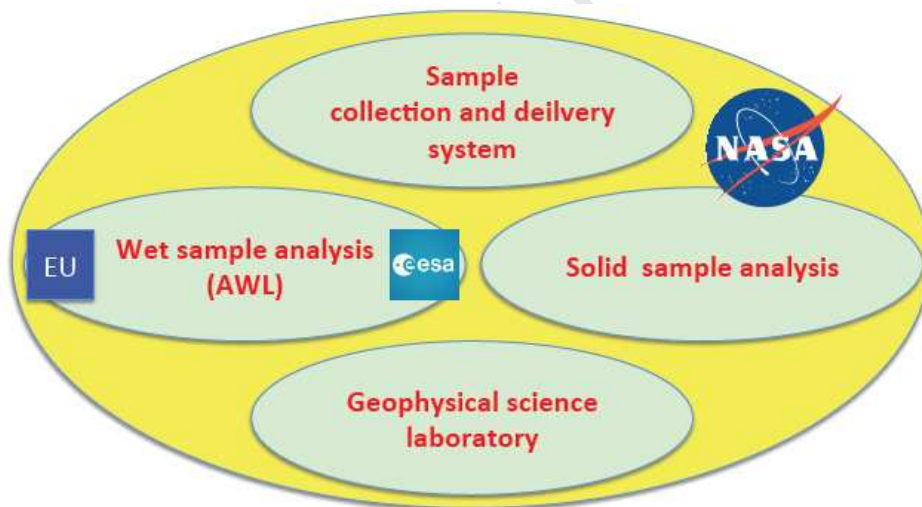


Figure 23: Proposed functional structure of the surface science platform on board the soft lander.

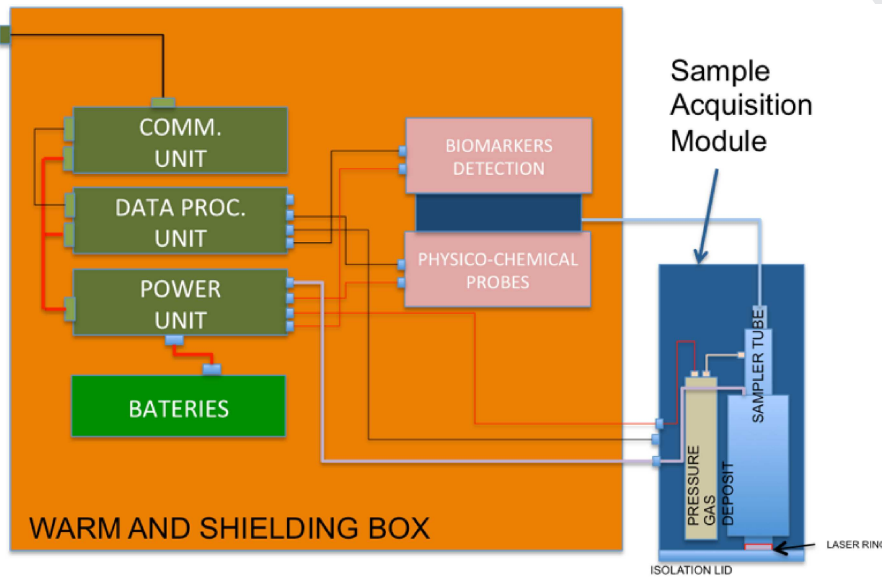
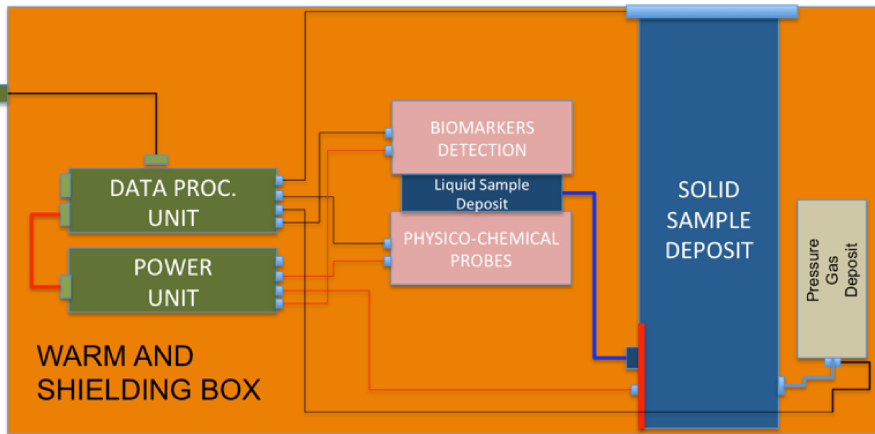
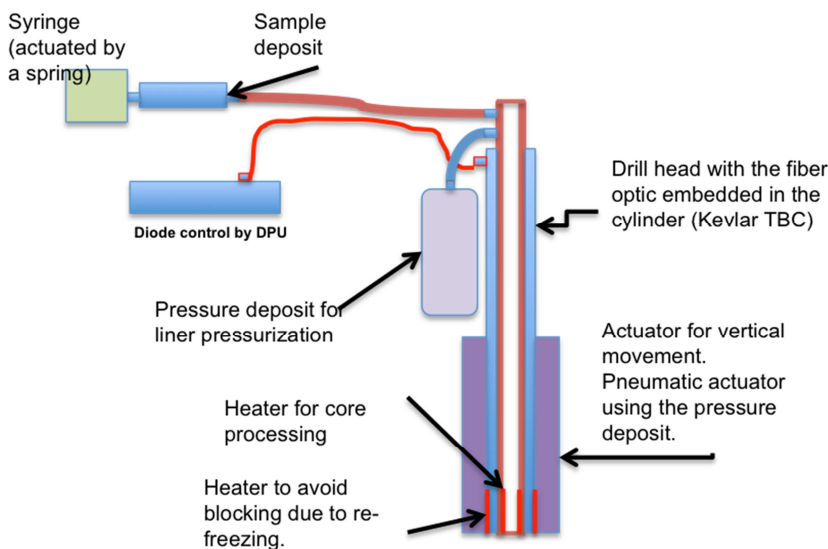


Figure 24: AWL/L (top) Block Diagram in case it is accommodated inside the lander and AWS/S in case it is deployed at the surface



Power estimated 10 watts for 1 hour of drilling TBC. (with pneumatic actuator).



Figure 25: Sample acquisition concept.

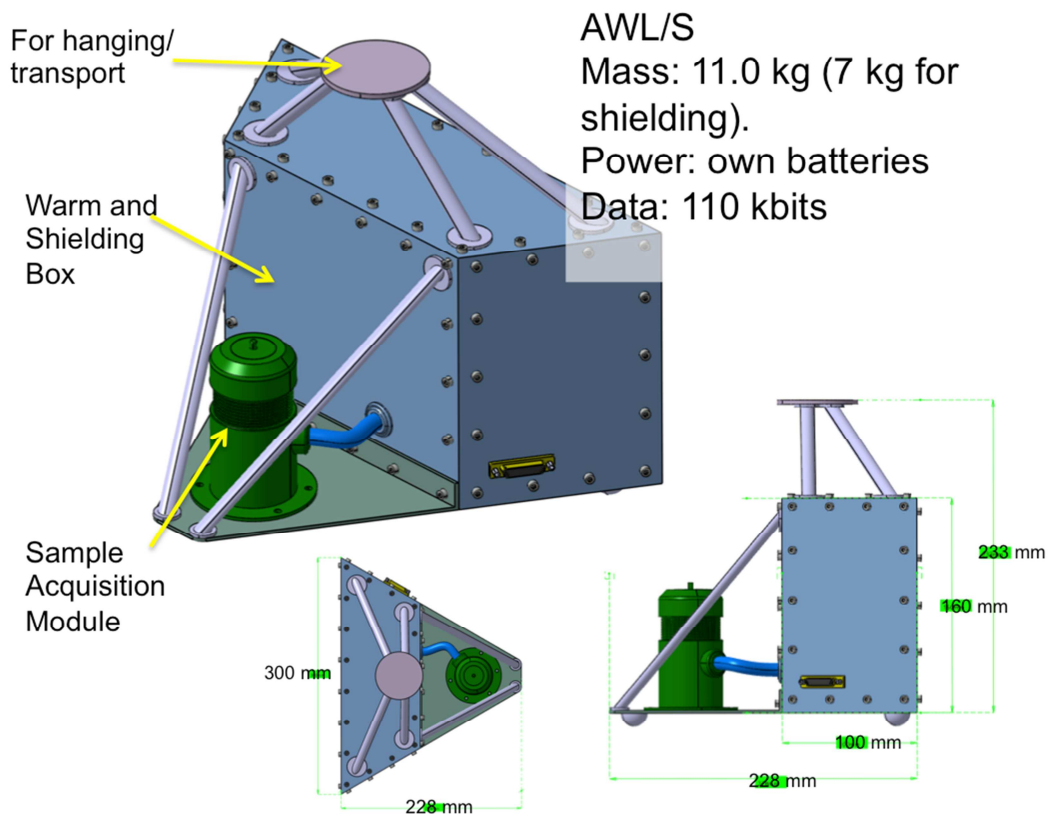


Figure 26: AWL/S mechanical configuration concept. A support structure allows it to be handled by the lander arm. A box protects the electronics, MAP and MPP. The isolation lid, below SAM, has a lateral movement to be open.

## Annex II: JEM orbiter system design

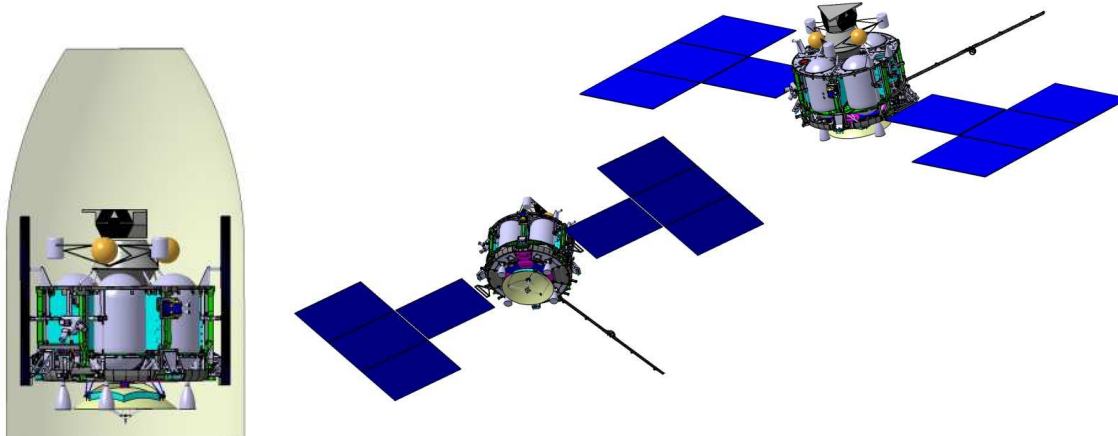


Figure A2.1: Spacecraft configuration (stacked and deployed)

**ANNEX III: Orbitography for the JEM mission**

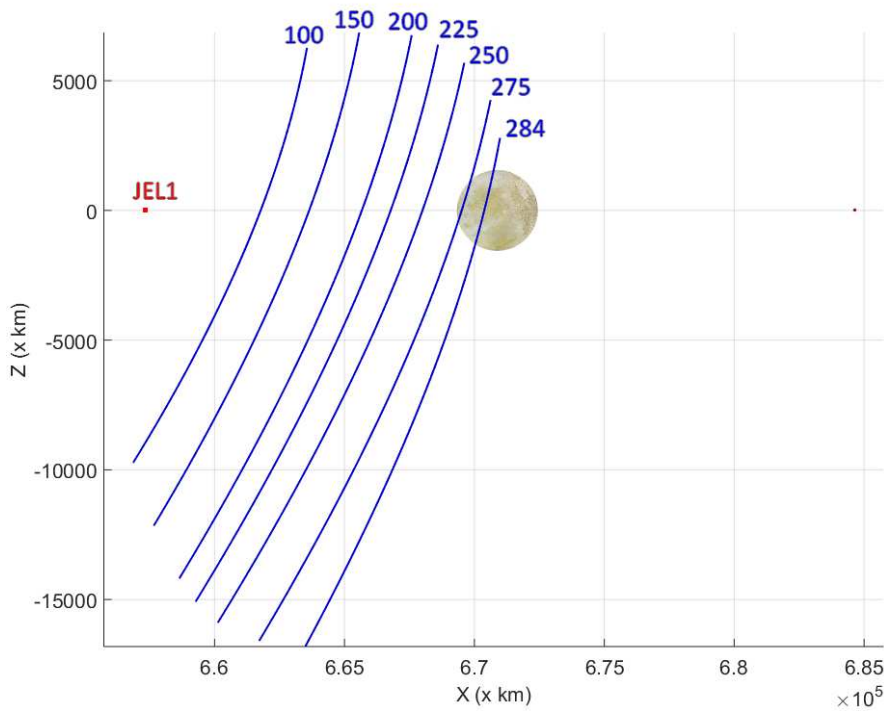


Figure A3.1: A set of JEL1 southern halo orbit in Jupiter-Europa rotating frame

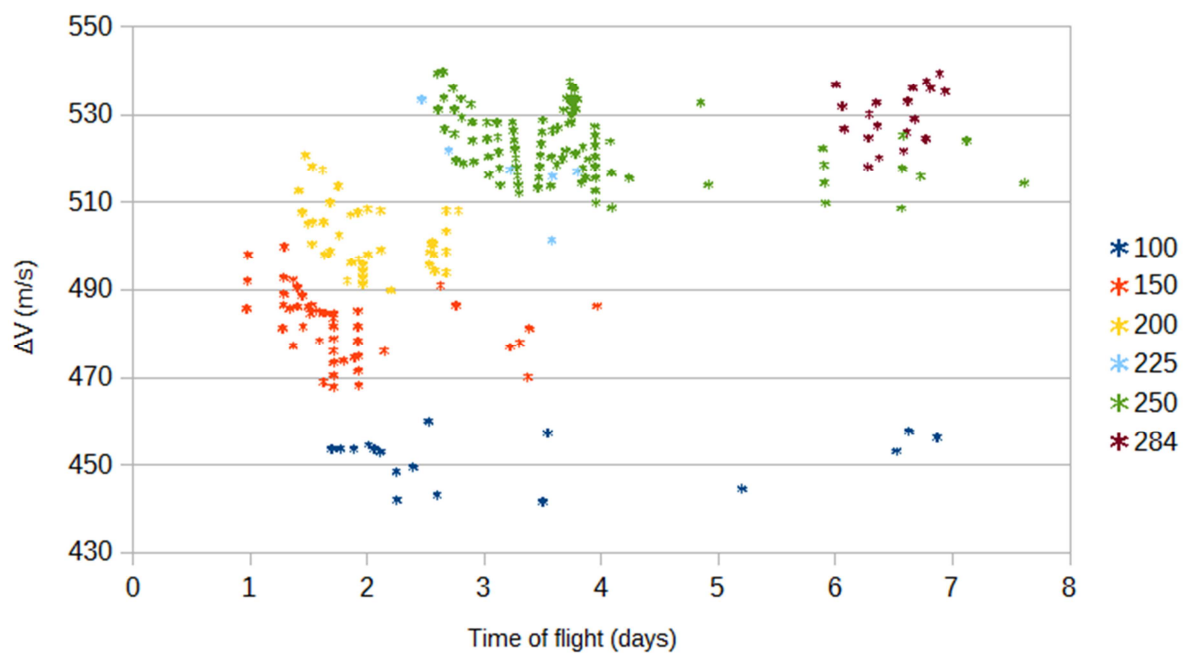


Figure A3.2:  $\Delta V$  vs Time of flight for all the possible transfers of a set of halo orbits

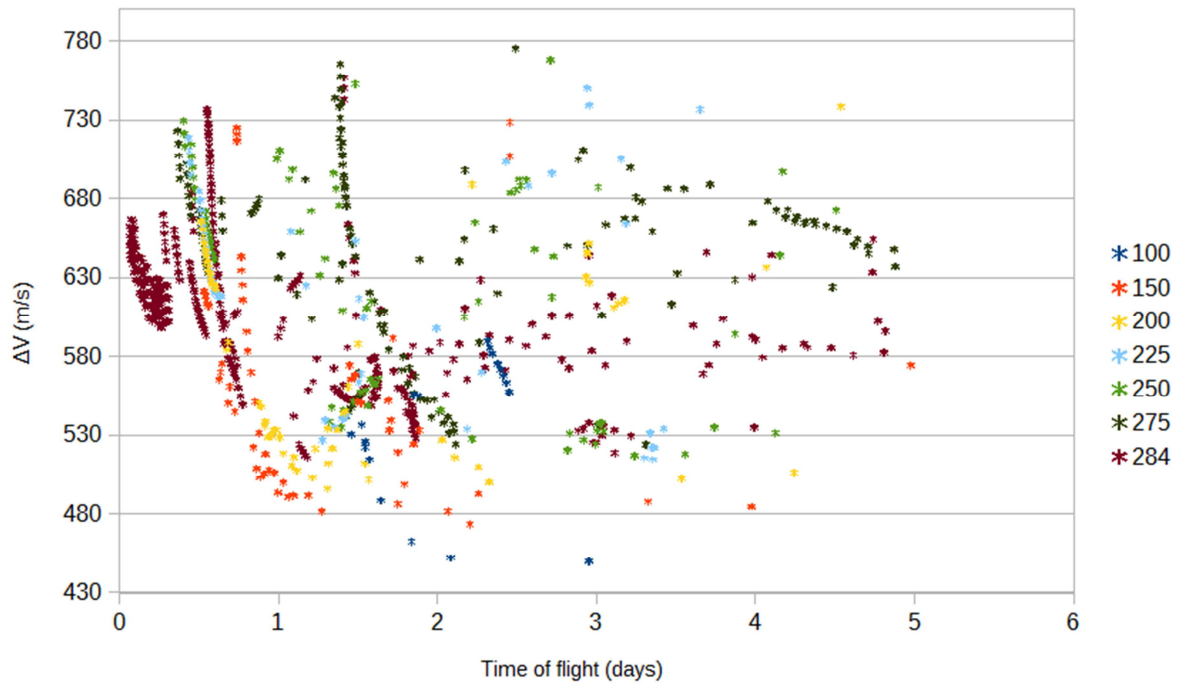
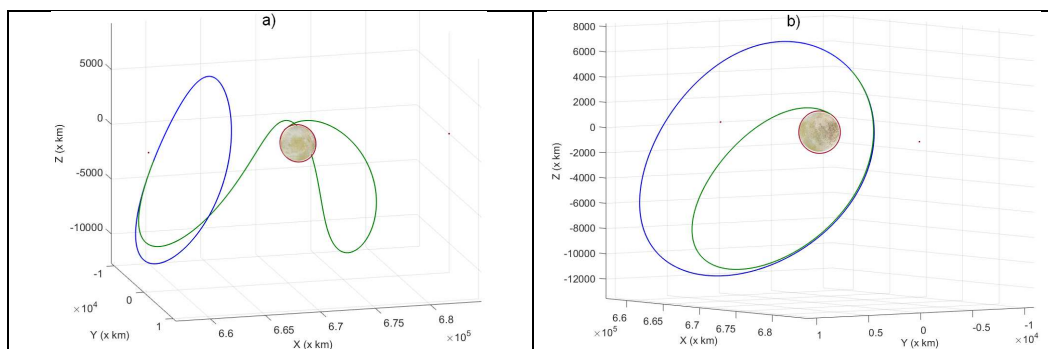


Figure A3.3:  $\Delta V$  vs Time of flight for all the possible transfers with a tangent burn to leave a set of halo orbits





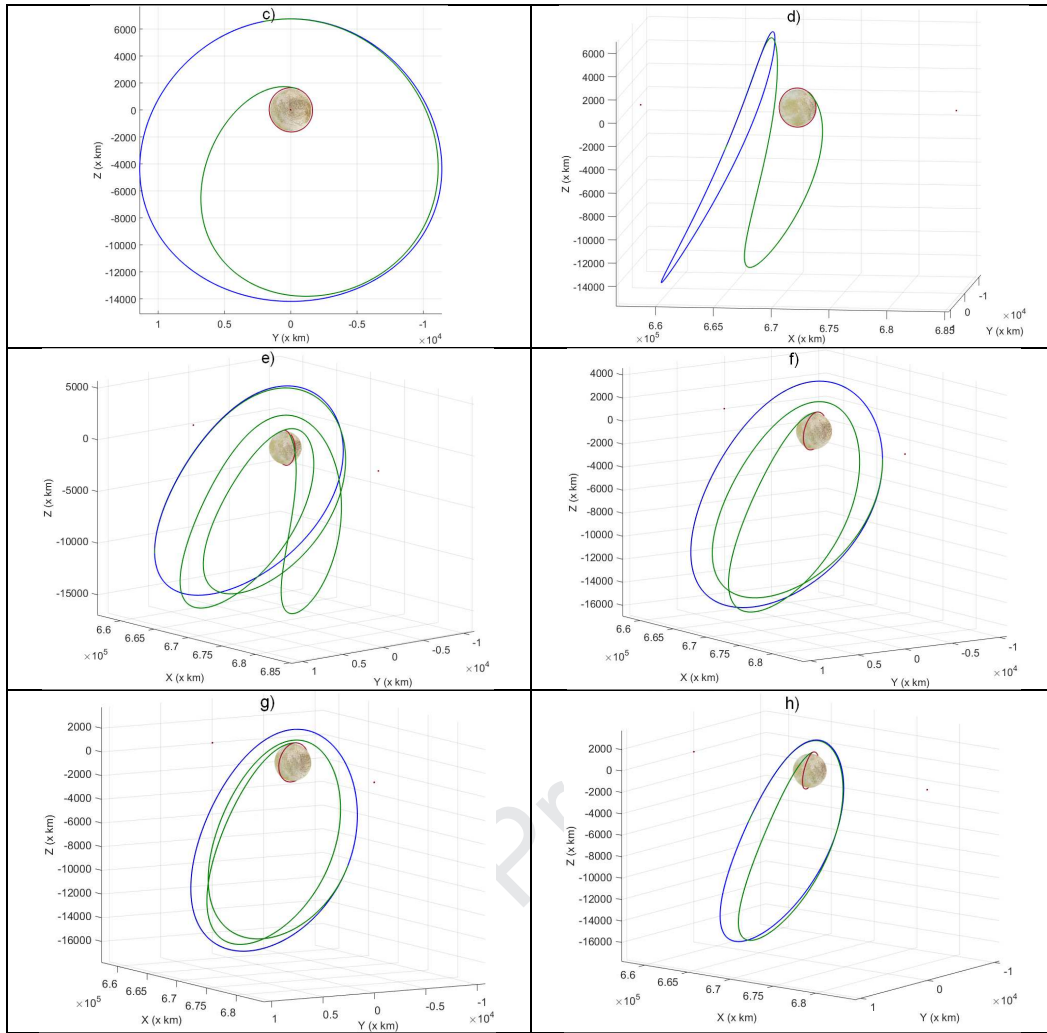


Figure A3.4: Set of transfers using different halo orbits



Figure A4.1: MeerKAT Dish (Left) and Karoo Array Processor Building (Right)

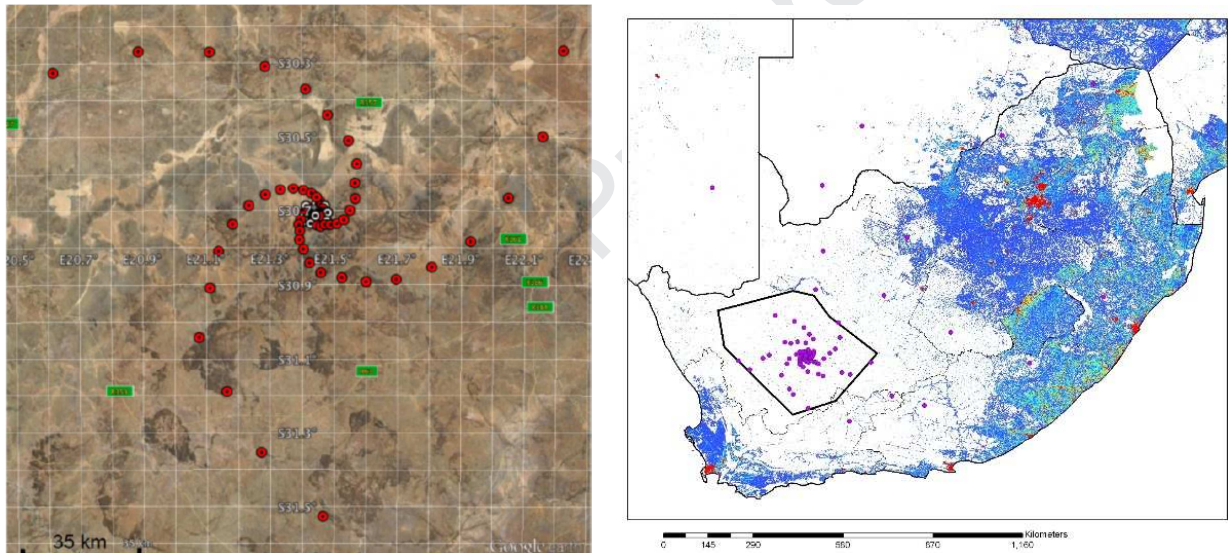


Figure A4.2: SKA1-Mid Array Configuration (Left) and SKA1-Mid Array Location in South Africa (Right, Showing Population Density and an Older Array Config)

## Highlights

In this article we are proposing that ESA collaborates with NASA to design and fly jointly an ambitious and exciting planetary mission, which we call the Joint Europa Mission (JEM), to reach two objectives: perform a *full characterization of Jupiter Moon Europa's habitability* with the capabilities of a Europa orbiter, and *search for bio-signatures in the environment of Europa (surface, subsurface and exosphere)* by the *combination of an orbiter and a lander*. JEM can build on the advanced understanding of this system which the missions preceding JEM will provide: Juno, JUICE and Europa Clipper, and on the Europa lander concept currently designed by NASA (Maize, report to OPAG, 2019).

We propose the following **overarching goals** for our proposed Joint Europa Mission (JEM): **Understand Europa as a complex system responding to Jupiter system forcing, characterize the habitability of its potential biosphere, and search for life at its surface and in its sub-surface and exosphere.**

The JEM observation strategy will combine *three types of scientific measurement sequences*: measurements on a high-latitude, low-altitude European orbit; in-situ measurements to be performed at the surface, using a soft lander; and measurements during the final descent to Europa's surface.

The implementation of these three observation sequences will rest on the combination of *two science platforms*: a *soft lander* to perform all scientific measurements at the surface and sub-surface at a selected landing site, and *an orbiter* to perform the orbital survey and descent sequences.

We describe a *science payload for the lander and orbiter* that will meet our science objectives.

We propose an *innovative distribution of roles for NASA and ESA*; while NASA would provide an SLS launcher, the lander stack and most of the mission operations, ESA would provide the carrier-orbiter-relay platform and a stand-alone astrobiology module for the characterization of life at Europa's surface: *the Astrobiology Wet Laboratory (AWL)*.

Journal Pre-proof

**ANNEX I: Summarized traceability matrix for JEM / OVERARCHING GOAL: Understand Europa as a complex system responding to Jupiter system forcing, characterize the habitability of its potential biosphere, and search for life at its surface**

Priority Science Objectives (PSO)	Carrier-Orbiter		Lander	
	Required measurements	Constraints on mission and platform	Required measurements	Constraints on mission and platform
<b>PSO #1:</b> Determine the global structure of the European magnetic field and plasma environment including potential plume characterization, and the associated response of Europa, including its ocean, to Jupiter System magnetospheric forcing.	Magnetometer Ion Mass Spectrometer/ Electron Mass Spectrometer (Langmuir Probe) Radiation Monitor Ion and Neutral Mass Spectrometer Dust analyzer	-3D Coverage of the European environment including crossing of the Alfvén wings -Low-altitude (100-200 km) near-polar, circular orbit for at least 30 days -Low-altitude crossing of plumes (< 160 km) for orbiter	Magnetometer	Lander lifetime of at least 7 days (2 Europa rotations)
<b>PSO #2:</b> Determine the global structure of the solid body and potential biosphere of Europa, and their response to Jupiter System tidal forcing.	Radio Science Instrument Laser Altimeter		Geophone Laser Reflector	
<b>PSO #3:</b> Understand the exchange and transformation processes at the interface between the ice-shell surface/subsurface and the exosphere/ionosphere including potential plume characterization.	Ion and neutral MS Ion MS + electron Spectrometer Dust Analyzer	-Spatial resolution of few 10's km horizontally and few km in altitude up to 1 Europa radius from the surface; of 100's km horizontally and 10's km in altitude for major species -Full latitudinal and longitudinal coverage at few phase angles with a temporal resolution from one hour to few 10s of hours -Coverage of Europa's exosphere during eclipse		
<b>PSO #4:</b> Understand the exchange processes between the ice-shell surface/subsurface and the aqueous interior environments, focusing on the hydrochemistry and physical state of the ice crust.	Laser altimeter	Altimetry from the orbiter combined with in situ measurements	Imaging camera, Microscope, GCMS, Raman, Geophone Thermogravimeter, Electrochemical sensors, Magnetometer	In situ analysis from the landing site. Sampling and analysis in solid and liquid state
<b>PSO #5:</b> Search for biosignatures at the surface/subsurface.	Ion and neutral MS		GCMS, Raman Microarray immunoassay detector, Imaging camera Microscope Thermogravimeter Geophone Magnetometer	In situ analysis from the landing site. Sampling and analysis in solid and liquid state  Characterize potential plumes if there is some activity

JEM TM	OVERARCHING GOAL				
	Understand Europa as a complex system responding to Jupiter system forcing, characterize the habitability of its potential biosphere, and search for life at its surface				
PSO #	Science Investigation	Required measurement	Instrumentation	Platform	Constraints on platform
1: Determine the global structure of the European magnetic field and plasma environment, and the associated response of Europa, including its ocean and potential plumes, to Jupiter System magnetospheric forcing.	Determine the global structure of magnetic fields, electric currents, and plasma and energetic populations in the European environment	-Energy, flux, angular distributions, direction, and composition of corotating magnetospheric particle populations from 10 eV up to a few MeV with 10s time resolution -Energy, flux, angular distributions, direction, and composition of thermal European exospheric and surface particle populations from <1 eV to 30 keV with 10s time resolution	Magnetometer Ion Mass Spectrometer/ Electron Mass Spectrometer Langmuir Probe Radiation Monitor	Orbiter +Lander	-3D Coverage of the European environment including crossing of the Alfven wings -5-m boom for MAG to be accommodated on orbiter -Small boom for LP to be accommodated on orbiter -Engineering payload for RM to be accommodated on orbiter
	Separate the four contributions to European magnetic fields and current systems	Mass resolved 3D velocity distributions functions (VDFs) of plasma (ions & electrons from <1eV to 30 keV) and pickup ions in Europa's vicinity with 10s time resolution Ion and electron flow direction, speed temperature, number and charge densities (currents), thermal and ram pressure; thermal and pickup ion mass densities; local Alfven and sound speeds with 60s time resolution Electric field vectors, electron and ion density, electron temperature for local conductivity and electrical current determination	Magnetometer Ion Mass Spectrometer/ Electron Mass Spectrometer Langmuir Probe	Orbiter + Lander Orbiter	
	Perform a broad-band magnetic sounding of the European sub-surface ocean and uniquely determine its depth, thickness	Measure three-axis magnetic field components at 8 vectors/s, and a sensitivity of 0.1 nT, near continuously to determine the induction response at multiple frequencies to an accuracy of 0.1 nT.	Magnetometer	Orbiter + Lander	-Low-altitude (100-200 km) near-polar, circular orbit for at least 30 days -Lander lifetime of at least 7 days (2 Europa rotations)
	Determine the composition and flux of plume material to characterize properties of any subsurface water	-Composition, energy spectra, and flux of pick-up ions in plumes Electron energy spectra and density inside and outside Europa's flux tube -Composition of ion and neutral populations in plumes -Composition of dust populations in plumes	Ion Mass Spectrometer/ Electron Mass Spectrometer Ion and Neutral Mass Spectrometer Dust analyzer	Orbiter	Low-altitude crossing of plumes (< 160 km) for orbiter
	2 Determine the global structure of the solid body and potential	Determine the amplitude and phase of the tidal effect on the external gravitational potential of Europa	Perform range-rate measurements with an accuracy ~0.01 mm/s at 60 sec integration time to determine the spacecraft orbital motion to better than 1-meter (rms) over several tidal cycles. Estimate the time-dependent part of the 2nd degree gravitational field of Europa and determine the Love number k2 at the orbital frequency of Europa with an absolute accuracy of better than 0.01 and the phase with a precision below 1 degree Measure topographic differences from globally distributed repeat ranging measurements, to recover spacecraft altitude at crossover	Radio Science Instrument Laser Altimeter	orbiter



		points to 1-meter vertical accuracy by contiguous global ranging to the surface with 10-cm accuracy.			
Characterise the tidal surface displacement as a function of tidal cycle.		Measure topographic differences from globally distributed repeat measurements at varying orbital phase, with better than or equal to 1-meter vertical accuracy, to recover the Love number $h_2$ at the orbital frequency with an absolute accuracy of 0.01 and the phase with a precision below 1 degree by contiguous global ranging to the surface with 10-cm accuracy.	Laser Altimeter Radio Science Instrument radio transponder	Orbiter Lander	quasi-polar orbit, pericenter altitude 200 km or less, tracking for two months  frequent tracking during several orbital cycles from Earth or an orbiter
		Measure spacecraft orbital motion to resolve the position of the spacecraft to better than 1-meter (rms) by performing range-rate measurements with an accuracy $\sim 0.01$ mm/s at 60 sec integration time			
		Perform range-rate measurements with an accuracy $\sim 0.01$ mm/s at 60 sec integration time to determine the changes in the lander position related to tidal surface displacements.			
Determine the tidal surface acceleration		Measure the surface acceleration with an absolute accuracy of 0.01 mGal.	gravimeter	lander	lifetime of at least one tidal cycle (one orbital period). Lander in equatorial region ( $\pm 30^\circ$ ) and near to sub- or anti-Jovian point ( $\pm 50^\circ$ )
Determine the rotation state of Europa		Determine the mean spin pole direction (obliquity) to better than 10 meters from the static external gravitational field and by developing an altimetry-corrected geodetic control network ( $\sim 100$ points) at a resolution better than 100 meter/pixel.	Laser Altimeter, Radio Science Instrument Radio Science Instrument Radio transponder	Orbiter lander	quasi-polar orbit, pericenter altitude 200 km or less, tracking for two months  frequent tracking during several orbital cycles from Earth or an orbiter
		Characterise the forced nutation of the spin pole and determine the amplitude of the forced libration at the orbital period to better than a few meters from variations in the external gravitational field and by developing an altimetry corrected geodetic control network at a resolution better than 10 meter/pixel			
		Perform range-rate measurements with an accuracy $\sim 0.01$ mm/s at 60 sec integration time to determine the position of the lander in time. Determine the obliquity and libration at orbital period to better than a few meters from tracking the lander.			
Determine the orbital characteristics of Europa and its long-term evolution		Determine the position of Europa's center of mass relative to Jupiter during the lifetime of the mission to better than 10 meters, by performing range measurements with an accuracy of 30 cm end-to -end and range-rate measurements with an accuracy $\sim 0.01$ mm/s at 60 sec integration time to determine spacecraft orbit to better than 1-meter (rms) throughout the lifetime of the orbiter.	Radio Science Instrument Radio Science Instrument, Laser Altimeter	orbiter	quasi-polar orbit, pericenter altitude 200 km or less, tracking for two months
		Determine the tidal dissipation in Europa from measurements of the phase of the tidal Love numbers $h_2$ and $k_2$ with a precision below 1 degree.			
Determine locally the depth		Determine the local ice shell thickness from European-diurnal	Seismometer/geoph	lander	Range : 0.1-10 Hz ,

	of Europa's ocean	cycle seismic activity (85.2 h) with an expected power spectral density of -140/-160 dB	one		PSD < -170 dB operating for one month.
	Determine the structure and elastic properties of the ice shell and the possible occurrence of water close to the lander site	Measure European-diurnal cycle seismic activity (85.2 h) with an expected power spectral density of -140/-160 dB	Seismometer/geoph one	lander	Range : 0.1-10 Hz , PSD < -170 dB operating for one month.
	Determine the structure of the crust and deeper interior	Determine the gravity field to degree and order 30 or better by performing range-rate measurements with an accuracy better than 0.01 mm/s at 60 sec integration time.	Radio Science Instrument Laser Altimeter	orbiter	quasi-polar orbit, pericenter altitude 200 km or less, tracking for two months
		Determine the global topography to degree and order 30 or better			
		Measure locally (10s of km) the surface roughness on footprint scale between 1° and 40° (50m) with an accuracy better than 20% (TBC) for different geological terrain type			
Test the hypothesis of hydrostatic equilibrium by measuring the degree 2 coefficients of the gravity field and topography					
Characterize local subsurface thermo-physical properties	Measure the thermal inertia of the shallow subsurface, as well as the roughness and emissivity of the surface.	radiometer	lander	measurements during several diurnal cycles (85.2 hrs)	
3 Understand the exchange and transformation processes at the interface between the ice-shell surface/subsurface and the	Nature of Europa's exosphere today	Composition (major and trace species). -Density of the main neutral exospheric species From few to 108 cm <sup>-3</sup> up to 100 amu with M/ΔM~100 and an energy range of less than few eV -Density of the main ion exospheric species From few 10 <sup>-2</sup> to 104 cm <sup>-3</sup> up to 50 amu with M/ΔM~50, and an energy range from eV to few tens of eV	Ion and neutral MS	orbiter	-Spatial resolution of few tens of km horizontally and few km in altitude from Europa's surface up to 1 Europa radius from the surface -Full latitudinal and longitudinal coverage at few phase angles
		Spatial distribution (relations with magnetosphere, phase angle and surface) and its temporal variability (Jupiter and Europa periods time scales) -Density and energy spatial distributions of the major neutral exospheric species From few cc to 108 cm <sup>-3</sup> up to 50 amu with M/ΔM~30 from eV to few eV with E/ΔE~20% -Density and energy spatial distributions of the major ion exospheric species			-Spatial resolution of few 10's km horizontally and few km in altitude from Europa's surface up to 1 Europa radius from the surface -Full latitudinal and longitudinal coverage at few phase angles with a



		From few 10 <sup>-2</sup> to 10 <sup>4</sup> cm <sup>-3</sup> up to 50 amu with M/ΔM~30 from eV to one keV with E/ΔE~20%			temporal resolution from one hour to few 10s of hours -Coverage of Europa's exosphere during eclipse
	What are the main drivers of exosphere formation? Role of the magnetosphere /dust.	Ion and electron densities - From few 10 <sup>-2</sup> to 10 <sup>4</sup> cm <sup>-3</sup> with M/ΔM~30 from keV to few tens of keV with E/ΔE~20% - Dust density and composition	Ion MS + electron Spectrometer	orbiter	-Spatial resolution of few 10's km horizontally and few km in altitude for trace species; of 100's km horizontally and 10's km in altitude for major species -Full latitudinal and longitudinal coverage at few phase angles with a temporal resolution of one hour
	What are the main drivers of exosphere formation? Role of the Surface /subsurface	Density spatial distributions of the neutral exospheric species From few to 10 <sup>8</sup> cm <sup>-3</sup> up to 100 amu with M/ΔM~100 and an energy range of less than few eV			
	Determine the composition of ejecting compounds from potential plumes	Measure major volatiles and key organic and inorganic compounds and compare with the surrounding exosphere to look for anomalies	Ion and neutral MS Dust analyzer	Orbiter	
4. Understand the exchange processes between the ice-shell surface/subsurface and the aqueous interior environments, focusing on the hydrochemistry and	Detect any geological feature which involves exchange processes between surface/interior at the landing site and determine whether any activity exists today	Correlation between feature topography, morphology and materials Mapping key materials Measure isotopic relationships to determine the age of materials	Imaging camera Geophone GCMS  Laser altimeter	Lander/ orbiter	Altimetry from the orbiter Images from the local site
	Characterize the biosignature preservation potential (BPP) of accessible surface materials at the landing site	Measure the radiation dose and magnetic field intensity that affect the compounds at the landing site	Magnetometer Radiometer	Lander	In situ analysis on landing spot
	Characterize the physical properties at the landing site	Determine the grain size, porosity and mineral crystallinity of the regolith and the fresh materials underneath	Microscope, Imaging camera	Lander	In situ analysis on landing spot
	Characterize the habitability key compounds of the near surface	Identify phase minerals (e.g. salt hydrates, phyllosilicates, clathrate hydrates, oxides), organics, volatiles	Raman spectrometer, GCMS, thermogravimeter	Lander	Near-surface sampling /analysis (solid state)
	Characterize the wet context of exchanging materials	Measure physical chemical parameters of the melt ice: pH, redox, conductivity, ions, volatiles	Electrochemical sensors	Lander	Sampling/analysis in liquid state of the surface/subsurface material

5. Search for biosignatures	Identify general biomarkers	Identify D/L aa, PAHs, Short peptides, Anti-freezing peptides and sugars, EPS from psychrophilic microbes, Cold shock proteins (Concentration <10ppb)	Microarray immunoassay detector	lander	Sampling/analysis in liquid state of the surface/subsurface material.
	Detect and characterize any organic indicator of past or present life	Identify organics, including some monomers of biomolecules (amu TBC, e.g. hydrocarbons, aa) in the near surface and in the potential plumes	GCMS Raman spec. thermogravimeter (only for hydrocarbons) Ion and neutral MS	Lander/orbiter	Near-surface sampling/analysis (solid state) Get face to the potential plumes
	Identify and characterize morphological and textural indicators of life	Identify cellular structures and biogenic fabrics on near-surface minerals	Microscope Raman spectrometer	lander	In situ analysis on landing spot (solid state)
	Detect and characterize any inorganic indicator of past and present life	Measure isotopic ratios, biominerals, decomposition temperature of minerals	GCMS, Raman spectrometer thermogravimeter	lander	Near-surface sampling/analysis (solid state)
	Determine the provenance of sampled material	Isotopic ratios, association with geological features	Imaging camera, GCMS, Raman spectrometer	lander	Near-surface sampling/analysis (solid state)
	Determine if living organisms persist in sampled materials	Measure the release of metabolic products from features in the near surface	GCMS, Raman spectrometer	lander	Near-surface sampling/analysis (solid or liquid)

Journal Pre-proof

**No conflict of interest statement**

The authors declare that they have no known competing financial interests or personal relationships that could have appeared to influence the work reported in this paper.

Journal Pre-proof